

An Optimal Control Approach to Bounding Transport Properties of Thermal Convection

by

Andre N. Souza

A dissertation submitted in partial fulfillment
of the requirements for the degree of
Doctor of Philosophy
(Applied and Interdisciplinary Mathematics)
in the University of Michigan
2016

Doctoral Committee:

Professor Charles R. Doering, Co-Chair
Professor Divakar Viswanath, Co-Chair
Associate Professor Silas D. Alben
Professor Anthony M. Bloch
Professor Daniel B. Forger

©Andre N. Souza

2016

À vovó Tereza e em memória ao vovô Doutor.

Acknowledgments

I would like to thank Dr. Jackson and Dr. Miller for making my transition to the University of Michigan possible. The MLB program was critical to my success. I would like to thank my committee members for taking the time to read and provide feedback on my dissertation. The guidance of Dr. Alben, Dr. Forger, and Dr. Bloch was invaluable throughout the thesis. Dr. Viswanath's extensive computational knowledge and perspective set the foundation for all the numerics. I thank you for all that you have passed on to me. And, of course, Charlie's mentorship throughout my academic career at Michigan leaves a lasting impact on every aspect of how I will conduct research. I could not have imagined a better advisor throughout my years here at Michigan. I thank you for all the patience and kindness (and softball!). My research during graduate school has been generously supported by the US National Science Foundation via award PHY-1205219, augmented with Alliances for Graduate Education and the Professoriate Graduate Research Supplements, and award DMS-1515161. I would also like to thank Dani, Ray, Gary, and Andrea as well as the Ann Arbor Argentine Tango community for all the wonderful memories. Lastly, I would like to thank my parents for their support throughout my life.

TABLE OF CONTENTS

Dedication	ii
Acknowledgments	iii
List of Figures	vi
List of Appendices	viii
Chapter	
1 Introduction	1
1.1 Methods for Obtaining Bounds	2
1.2 Optimal Control	5
1.3 Natural versus Optimal Flows	7
2 Reduced Models	11
2.1 Lorenz	12
2.1.1 Background Analysis	14
2.1.2 Optimal Control Analysis	16
2.1.3 Time Periodic Stirring Protocols	18
2.1.4 Analysis and Bounds on Transport by Arbitrary Stirring	20
2.2 Double Lorenz	24
2.2.1 Background Analysis	26
2.2.2 Optimal Control Analysis	29
2.2.3 Comparison of Steady State to Periodic Solutions	35
3 The Advection-Diffusion Equation	39
3.1 Introduction	39
3.2 Relevant Theorems and Setting Notation	40
3.3 Existence of a Maximizer and Differentiability	43
3.3.1 Existence of the Temperature Field	44
3.3.2 Continuity and Existence of a Maximizer	46
3.3.3 Differentiability	49
3.4 Upper Bound	51
3.5 The Euler-Lagrange Equations	53
3.6 Possible Avenues for Improving the Upper Bound	58
3.6.1 Insights on How to Improve the Upper Bound	59
4 Numerical Discretization and Solutions	65

4.1	Gradient Ascent	66
4.1.1	Gradient Ascent in the Optimal Control System	70
4.1.2	Time Dependent	72
4.1.3	Time Periodic	75
4.1.4	Steady	76
4.1.5	Time Evolution Discretization	78
4.2	Spectral Methods	80
4.2.1	Spectral Integration	81
4.2.2	Kleiser-Schumann Algorithm	89
4.3	Numerical Results	91
5	Discussion	101
	Appendices	104
	Bibliography	133

LIST OF FIGURES

2.1	Long time averaged heat transport for solutions of the Lorenz equations. Dashed line: upper bound on $\langle XY \rangle$ derived by Pétrélis & Pétrélis [1]. Solid line: improved upper bound (2.20) corresponding to the nontrivial fixed points that exist when $r > 1$. Discrete data: direct numerical simulation results for parameter values $\sigma = 10$ and $b = \frac{8}{3}$	16
2.2	The time dependence of optimal $\tau = 2\pi$ periodic stirring protocols for several values of the Péclet number and $b = \frac{8}{3}$. Long dashed line: $Pe = 0.69$; short dashed line: $Pe = 1.71$; dotted line $Pe = 4.50$; solid curve: $Pe = 8.96$	19
2.3	Solid line: absolute upper bound (2.54) on the long time averaged transport vs. Péclet number, corresponding to steady stirring, for parameter value $b = \frac{8}{3}$. Dashed line: transport from numerically computed periodic solution of the optimal Euler-Lagrange equations for period $\tau = 2\pi$ ($\omega = 1$), which is observed to lie strictly below absolute upper bound from the steady solutions of the optimal Euler-Lagrange equations.	20
2.4	The top (black) dashed line is the best known upper bound for the full Rayleigh-Bénard problem from [2]. The solid (green) curve is the background method upper bound on all solutions of the Double Lorenz Equations as well as the transport value for the global optima of the optimal control solution, see §2.2.2. Rayleigh-Nusselt relations for several steady states are also shown. The dotted (red) curve asymptoting to $Nu = 3$ is the steady solution of the first Lorenz system, and the lower dotted (blue) curve is the steady state of the second Lorenz system. The long-dashed (purple) curve is the steady state for the coupled system for $\sigma = 10$. The discrete dots are results from time averages of direct numerical simulations of the Double Lorenz Equations for $\sigma = 10$	30
2.5	Time dependence of optimal 2π (time) periodic stirring protocols for several value of the Péclet number and $k = 1/\sqrt{2}$. Here we show $x_1(t)$. Long dashed (green) line: $Pe=4.2$; short dashed (blue) line: $Pe = 5.4$; dotted (red) line $Pe = 14.1$; and solid (black) curve: $Pe = 35.1$	37
2.6	The top (green) curve is the upper bound on the Nusselt number. Rayleigh-Nusselt relations for several steady states of the Double Lorenz equations are also shown. The long-dashed (purple) purple lines are the coupled steady state solutions for several Prandtl numbers, $\sigma = 0.44$ (bottom), 0.70, 1.42, 5.75 and 10^4 (top), and wavenumber is $k = 1/\sqrt{2}$. The upper dotted (red) curve is the first Lorenz system steady state while the lower dotted (blue) curve is that for the second Lorenz system. The dashed (black) line is the transport for a time-periodic solution to the optimal Double Lorenz system.	38

4.1	Upper bounds to the Nusselt number in 2D Rayleigh-Bénard convection with stress-free boundary conditions. The dashed green line is the rigorous upper bound by Whitehead and Doering [3]. The red dots are numerically computed solutions to the background method problem by Wen et al.[2]. The black line corresponds to numerically computed optimizers of the steady optimal control problem with stress-free boundary conditions.	92
4.2	Optimal stress-free solutions for different enstrophy budgets in the full domain. The black contour lines are the streamlines and the colors represent the temperature field. From left to right, top to bottom the Péclet numbers are 4.0×10^{-1} , 5.0×10^2 , 1.6×10^3 , 3.2×10^3 , 8.0×10^3 , 1.2×10^4 . The best known optimizers consist of a multiplicity of convection cells for a fixed domain size as the enstrophy budget increases.	95
4.3	Optimal no-slip solutions for different enstrophy budgets in the full domain. The black contour lines are the streamlines and the colors represent the temperature field. From left to right, top to bottom the Péclet numbers are 4.0×10^{-1} , 4.0×10^2 , 1.8×10^3 , 5.0×10^3 , 8.0×10^3 , 1.3×10^4 . The best known optimizers consist of a multiplicity of convection cells for a fixed domain size as the enstrophy budget increases.	96
4.4	Optimal stress-free solutions for different enstrophy budgets in a single cell. The black contour lines are the streamlines and the colors represent the temperature field. From left to right, top to bottom the Péclet numbers are 4.0×10^{-1} , 4.0×10^0 , 4.0×10^1 , 4.0×10^2 , 4.0×10^3 , 4.0×10^4 . The domain size in the horizontal x direction shrinks as the Péclet number increases.	97
4.5	Optimal no-slip solutions for different enstrophy budgets in a single cell. The black contour lines are the streamlines and the colors represent the temperature field. From left to right, top to bottom the Péclet numbers are 4.0×10^{-1} , 4.0×10^0 , 4.0×10^1 , 4.0×10^2 , 4.0×10^3 , 4.0×10^4 . The domain size in the horizontal x direction shrinks as the Péclet number increases.	98
4.6	Computed optimal Nusselt number (Nu) and aspect ratio (Γ) as a function of the enstrophy budget (Pe), for stress-free boundary conditions. Top Left: Log-Log plot of Pe vs Nu-1. Bottom Left: The instantaneous slope of the top left plot, Pe vs $d \log(\text{Nu} - 1)/(d \log \text{Pe})$. Top Right: Log-Log plot of Pe vs Γ . Bottom Right: The instantaneous slope of the top right plot, Pe vs $d \log(\Gamma)/(d \log \text{Pe})$. The last instantaneous slope for the bottom left plot is 0.582 and the last instantaneous slope for the bottom right plot is -0.339 . The largest computed value of Pe is 5.65×10^4 corresponding to a μ value of 2.4×10^{-8}	99
4.7	Computed optimal Nusselt number (Nu) and aspect ratio (Γ) as a function of the enstrophy budget (Pe), for no-slip boundary conditions. Top Left: Log-Log plot of Pe vs Nu-1. Bottom Left: The instantaneous slope of the top left plot, Pe vs $d \log(\text{Nu} - 1)/(d \log \text{Pe})$. Top Right: Log-Log plot of Pe vs Γ . Bottom Right: The instantaneous slope of the top right plot, Pe vs $d \log(\Gamma)/(d \log \text{Pe})$. The last instantaneous slope for the bottom left plot is 0.544 and the last instantaneous slope for the bottom right plot is -0.371 . The largest computed value of Pe is 2.5×10^5 corresponding to a μ value of 1.4×10^{-9}	100

LIST OF APPENDICES

A Variations of Boundary Conditions and Domain Size	104
B Compact Sets in Hilbert Spaces	120
C Double Lorenz Properties	123
D Background Bound Details	129

CHAPTER 1

Introduction

In this thesis we examine the transport properties of passive scalars governed by the advection-diffusion equation

$$\partial_t T + \vec{u} \cdot \nabla T = \Delta T, \quad (1.1)$$

driven by incompressible flow fields \vec{u} . The spatial domain of interest is periodic in the horizontal directions and bounded in the vertical. For example in three dimensions the domain is of the form $[0, \Gamma_1] \times [0, \Gamma_2] \times [0, 1]$, with periodicity in the horizontal directions $x \in [0, \Gamma_1]$ and $y \in [0, \Gamma_1]$. The boundary conditions on the $z = 0$ and $z = 1$ boundary are $T = 1$ and $T = 0$ respectively. Furthermore, the flow field \vec{u} does not penetrate through the boundary. This domain and boundary conditions relate to the physical scenario in which a plate is heated from below and cooled from above when interpreting T as temperature.

Our interest is to calculate how much heat is being transported from the bottom of the plate at $z = 0$ to the top of the plate $z = 1$. Writing the advection-diffusion equation (1.1) in conservation law form,

$$\partial_t T + \nabla \cdot (\vec{u}T - \nabla T) = 0, \quad (1.2)$$

lets us easily pick out the heat flux

$$\vec{J} = \vec{u}T - \nabla T. \quad (1.3)$$

The notion of heat transport that we will use is the long time and spatial average of the total heat flux in the vertical direction known as the Nusselt number. The formula for this quantity is

$$\text{Nu} = 1 + \lim_{\tau \rightarrow \infty} \frac{1}{\tau \Gamma_1 \Gamma_2} \int_0^\tau \int_0^{\Gamma_1} \int_0^{\Gamma_2} \int_0^1 wT \, dz \, dy \, dx \, dt, \quad (1.4)$$

where w is the vertical component of velocity.

1.1 Methods for Obtaining Bounds

We will calculate time averages of quantities that depend on the state $s \in S$ of a dynamical system. Let $\overline{\phi(s)}$ denote the long time average average of an observable $\phi : S \rightarrow \mathbb{R}$ given by the formula

$$\overline{\phi} \equiv \limsup_{\tau \rightarrow \infty} \frac{1}{\tau} \int_0^\tau \phi(s(t)) dt. \quad (1.5)$$

Ideally we would like to know the long time average of an observable on a particular attractor of a dynamical system but there is currently no known general method to do so. However there are methods for bounding all solutions [4].

To obtain upper and lower bounds to $\overline{\phi}$ the general approach is as follows: We introduce arbitrary functions of the state, denoted by $g : S \rightarrow \mathbb{R}$ and $h : S \rightarrow \mathbb{R}$, such that

$$\overline{g} = \overline{h} = 0. \quad (1.6)$$

If it is possible to show

$$\phi(s) + g(s) - c \leq 0 \quad (1.7)$$

$$\phi(s) + h(s) - d \geq 0 \quad (1.8)$$

for constants c or d and all values of the state s , then we would have bounds of the form

$$\overline{\phi} = \overline{\phi + g - c + c} \leq c, \quad (1.9)$$

$$\overline{\phi} = \overline{\phi + h - d + d} \geq d. \quad (1.10)$$

All of the rigorous bounds that will be shown in this thesis follow this general approach.

One philosophy behind choosing a bounding function (g or h) for state variables that are bounded ($\|s\| < \infty$ for some norm $\|\cdot\|$) is to pick a differentiable function V and choose g or h to be $\dot{s} \cdot \nabla V = \dot{V}$ where the dot denotes a derivative with respect to time. The bounding potential V is bounded either due to the boundedness of V itself or due to the state being bounded for all times. For a fixed initial condition $|V(s)| \leq M$ for all time.

This choice satisfies (1.6) since

$$|\overline{\dot{s} \cdot \nabla V}| = |\overline{\dot{V}}| = \left| \limsup_{\tau \rightarrow \infty} \frac{V(s(\tau)) - V(s(0))}{\tau} \right| \leq \limsup_{\tau \rightarrow \infty} \frac{2M}{\tau} = 0. \quad (1.11)$$

We mention that for potentials V that only depend on a finite number of states, such as ODE's or a finite selection of modes for a PDE, it is possible to formulate the problem of choosing an upper bound and a potential V as a semi-definite program [5, 6] if one limits the choice V to be a sum of squares polynomial; however, our interest is in developing approaches that work for PDE's and a great simplification is obtained if one chooses V to be a quadratic function (or functional) of the state variables.

For example, consider the dynamical system governed by the evolution equation

$$\dot{s} = s(1 - s^2) \quad (1.12)$$

and the observable $\phi(s) = s^2$. A lower bound for this observable is zero and it is sharp since it is saturated by the (unstable) steady state solution $s = 0$. The trajectories of this dynamical system are bounded thus a choice of potential $V(s) = 0.5s^2$ and $c = 1$ yields

$$\overline{\phi(s)} = \overline{\phi(s) + \dot{V}(s) - 1 + 1} = \overline{s^2 + s^2(1 - s^2) - 1 + 1} \quad (1.13)$$

$$= \overline{-(s^2 - 1)^2 + 1} \leq 1. \quad (1.14)$$

Thus we have an upper bound of 1 for the long time average of the observable $\phi(s) = s^2$. This bound is sharp since it is saturated by the steady state solutions $s = \pm 1$.

A more complicated example of this approach may be applied to the Boussinesq approximation of the Navier-Stokes equations. In modern dimensionless form the equations are

$$\frac{1}{\text{Pr}} (\partial_t \vec{u} + \vec{u} \cdot \nabla \vec{u}) = \Delta \vec{u} - \nabla p + \text{Ra} T \hat{e}_3 \quad (1.15)$$

$$\nabla \cdot \vec{u} = 0 \quad (1.16)$$

$$\partial_t T + \vec{u} \cdot \nabla T = \Delta T, \quad (1.17)$$

where $\vec{u} = (u_1, u_2, u_3)$, $\vec{u}(x, y, z, t)$ and $T(x, y, z, t)$ are periodic in $x \in [0, \Gamma_1]$ and $y \in [0, \Gamma_2]$. The velocity field \vec{u} satisfies homogeneous (no-slip) boundary conditions on $z = 0$ and $z = 1$ and the temperature field is $T = 1$ at $z = 0$ and $T = 0$ at $z = 1$. The parameter $\text{Ra} \in (0, \infty)$ is the Rayleigh number and the parameter $\text{Pr} \in (0, \infty)$ is the Prandtl number. The convective heat flux in the vertical direction is given by wT and the conductive heat

flux is $-\partial_z T$, hence the Nusselt number is $\langle wT - \partial_z T \rangle = 1 + \langle wT \rangle$ where the angle brackets denote the spatial and long time averages

$$\langle f \rangle = \lim_{\tau \rightarrow \infty} \frac{1}{\tau \Gamma_1 \Gamma_2} \int_0^\tau \int_0^{\Gamma_1} \int_0^{\Gamma_2} \int_0^1 f \, dz \, dy \, dx \, dt. \quad (1.18)$$

It is straightforward to deduce $\text{Nu} = \langle \nabla T \cdot \nabla T \rangle$ from the equations of motion and prescribed boundary conditions. A choice of functional

$$V[\vec{u}, T] = \frac{1}{2\Gamma_1 \Gamma_2} \int_0^{\Gamma_1} \int_0^{\Gamma_2} \int_0^1 \left(\frac{1}{\sigma \text{Ra}} \vec{u} \cdot \vec{u} + \theta^2 \right) dz \, dy \, dx \, dt \quad (1.19)$$

where $\theta = T - \tau(z)$,

$$\tau(z) = \begin{cases} 1 - \left(\frac{1}{\delta} - 1\right) z & \text{for } 0 \leq z < \delta \\ z & \text{for } \delta \leq z \leq 1 - \delta \\ \left(\frac{1}{\delta} - 1\right) (1 - z) & \text{for } 1 - \delta < z \leq 1 \end{cases} \quad (1.20)$$

and $\delta = 4\text{Ra}^{1/2}$ yields

$$\text{Nu} = \left\langle \frac{1}{2} (1 + u_3 T) + \frac{1}{2} \nabla T \cdot \nabla T + \partial_t V \right\rangle = \frac{1}{2} + \frac{1}{2} \int_0^1 (\tau')^2 dz - \mathcal{Q}[\vec{u}, T] \quad (1.21)$$

where

$$\mathcal{Q}[\vec{u}, T] = \left\langle \frac{1}{2\text{Ra}} \nabla \vec{u} : \nabla \vec{u} + [\tau' - 1] u_3 \theta + \frac{1}{2} \nabla \theta \cdot \nabla \theta \right\rangle, \quad (1.22)$$

and $\nabla \vec{u} : \nabla \vec{u}$ is $\partial_j u_k \partial_j u_k$ with repeated indices summed. Constantin and Doering [4] showed that the quadratic functional \mathcal{Q} is positive semi-definite, hence we have an upper bound

$$\text{Nu} \leq \frac{1}{4} \text{Ra}^{1/2} - 1, \quad (1.23)$$

for $\text{Ra} \geq 64$.

It is possible to lower the prefactor using a different functional, and the $\text{Nu} \sim \text{Ra}^{1/2}$ scaling seems to be higher than most observed scalings in numerical experiments which are closer to $\text{Nu} \sim \text{Ra}^{1/3}$. It is perhaps possible to incorporate a more complicated functional in order to lower the scaling, but thus far this has only been possible for two dimensional flows with stress-free boundary conditions [3].

At this point it may seem rather mysterious how to choose a proper bounding potential V . The background method of Constantin and Doering [4] provides a framework in which one can learn how to build the pieces for V . In Chapter 2 we show how to construct V for the Lorenz and Double Lorenz system and their optimal control counterparts using the background method. In Chapter 3 we repeat the Doering and Constantin calculation for the optimal control analog to the Rayleigh-Bénard problem. This method for obtaining bounds does not give any hint as to what flow fields could maximize transport nor do we know if the bounds are sharp.

1.2 Optimal Control

The optimal control approach to bounding an observable of interest is a refinement of the previous method. The general idea is to replace one of the equations of the dynamical system with a bulk constraint while fully enforcing the others. Suppose that a dynamical system state variable can be split into two parts $s = (u, \theta)$ where, for a given initial condition, θ is uniquely determined by u . We will think of u as the “control” and θ as the “state variable” governed by the evolution equations

$$\dot{u} = f(u, \theta) \tag{1.24}$$

$$\dot{\theta} = g(u, \theta). \tag{1.25}$$

For a given observable $\phi(u, \theta)$ we would like to find an upper bounds to long time averages of ϕ , subject to the equations of state. Furthermore we suppose that the long time average of the square norm of the control is finite, that is

$$\limsup_{T \rightarrow \infty} \frac{1}{T} \int_0^T \|u\|^2 dt = \overline{\|u\|^2} < \infty \tag{1.26}$$

where $\|\cdot\|$ is a norm on u . The norms that we will work with will come from a Hilbert space of some kind hence the squaring of the norm. The “natural” problem is to maximize the observable in the long time limit

$$\sup_{u_0, \theta_0} \overline{\phi(u, \theta)} \tag{1.27}$$

subject to

$$\dot{u} = f(u, \theta) \tag{1.28}$$

$$\dot{\theta} = g(u, \theta) \tag{1.29}$$

where u_0 and θ_0 are initial conditions for the u and θ equations. In contrast the optimal control problem is

$$\sup_u \overline{\phi(u, \theta)} \quad (1.30)$$

subject to

$$\|u\|^2 = \text{Pe}^2 \quad (1.31)$$

$$\dot{\theta} = g(u, \theta) \quad (1.32)$$

where $\text{Pe} \in (0, \infty)$ is a constant. In order to not waste time on particular initial conditions we further make the supposition that the value of the observable becomes independent of initial conditions in the long time limit. Hence we may fix an initial condition as opposed to optimizing over all possible initial conditions.

We would like to know the functional relation between $\overline{\phi(u, \theta)}$ and Pe . Suppose that we solve the natural problem (1.27) and denote the solution by v . By our assumption $\|v\|^2 = \text{Pe}^2 < \infty$ for a number Pe . Now consider the solution to the optimal problem (1.30) with the same value of Pe and denote the solution by u . The optimal control problem contains the “natural” problem as a subset of possible choices for u , hence

$$\overline{\phi(v, \theta_v)} \leq \overline{\phi(u, \theta_u)}. \quad (1.33)$$

where θ_v is the state solution associated with the natural problem and θ_u is the state solution associated with the optimal problem. In the work considered here we expect a power law relation between the observable ϕ and the budget $\|u\|^2$ in the limit of small Pe as well as in the limit of large Pe .

Under suitable assumptions we may formulate this problem as one of finding the critical points of the augmented action

$$\mathcal{A}[u] = \overline{\phi(u, \theta) + \varphi(\dot{\theta} - g(u, \theta)) + \frac{1}{2}\mu(\text{Pe}^2 - \|u\|^2)} \quad (1.34)$$

leading to the Euler-Lagrange equations

$$\dot{\theta} = g(u, \theta) \quad (1.35)$$

$$\dot{\varphi} = -\nabla_{\theta}g(u, \theta) + \nabla_{\theta}\phi(u, \theta) \quad (1.36)$$

$$\frac{\mu}{2}\nabla_u\|u\|^2 = \nabla_u\phi(u, \theta) - \varphi\nabla_u g(u, \theta) \quad (1.37)$$

$$\|u\|^2 = \text{Pe}^2. \quad (1.38)$$

The first equation is known as the state equation, the second equation as the adjoint equation, and the third equation as the optimality condition. The hope is that the optimality condition (1.37) is easier to analyze than the evolution equation for u (1.24). In the section that follows we will discuss some specific cases of this approach as applied to Rayleigh-Bénard convection and related truncated models.

1.3 Natural versus Optimal Flows

With regards to Rayleigh-Bénard convection we maximize the long time and spatial average of the vertical heat flux in the domain $[0, \Gamma_1] \times [0, \Gamma_2] \times [0, 1]$. Thus the the “natural” problem is to consider

$$\sup_{\vec{u}_0, T_0} \langle wT \rangle \quad (1.39)$$

subject to

$$\frac{1}{\text{Pr}} (\partial_t \vec{u} + \vec{u} \cdot \nabla \vec{u}) = \Delta \vec{u} - \nabla p + \text{Ra}T \hat{e}_3, \quad (1.40)$$

$$\nabla \cdot \vec{u} = 0 \quad (1.41)$$

$$\partial_t T + \vec{u} \cdot \nabla T = \Delta T. \quad (1.42)$$

where $\vec{u} = (u, v, w) = (u_1, u_2, u_3)$, $\vec{u}(x, y, z, t)$ and $T(x, y, z, t)$ are periodic in $x \in [0, \Gamma_1]$ and $y \in [0, \Gamma_2]$. Again the angle brackets $\langle \cdot \rangle$ denote the long-time and spatial average, see (1.18). The vertical velocity field w satisfies homogeneous boundary conditions on $z = 0$ and $z = 1$ and the temperature field is $T = 1$ at $z = 0$ and $T = 0$ at $z = 1$. The horizontal velocities will either satisfy no slip boundary conditions (meaning that they are zero on the $z = 0$ and $z = 1$ boundaries) or stress-free (meaning $\partial_x u = \partial_y v = 0$ on the boundaries). The optimal problem is

$$\sup_{\vec{u}} \langle wT \rangle \quad (1.43)$$

subject to

$$\partial_t T + \vec{u} \cdot \nabla T = \Delta T \quad (1.44)$$

$$\langle \nabla \vec{u} : \nabla \vec{u} \rangle = \text{Pe}^2 \quad (1.45)$$

$$\nabla \cdot \vec{u} = 0, \quad (1.46)$$

where the velocity field and temperature fields satisfy the same boundary conditions as the natural problem. As mentioned in the previous section the upper bound to (1.39) is lower

than the upper bound to (1.43) for flows that satisfy $\langle \nabla \vec{u} : \nabla \vec{u} \rangle = \text{Pe}^2$.

Upper bounds to heat transport in Rayleigh-Bénard convection are not reported in terms of $\langle \nabla \vec{u} : \nabla \vec{u} \rangle = \text{Pe}^2$, but rather the parameter Ra that appears in the momentum equation (1.40). We may use the integral balance relation $\text{Pe}^2 = \text{Ra}(\text{Nu} - 1)$ derived from (1.40) to convert upper bounds from (1.43) to upper bounds in terms of Ra . For example, if $(\text{Nu} - 1)_{\text{optimal}} \leq c\text{Pe}^\beta$ where $0 < \beta < 2$ and $0 < c$ then

$$(\text{Nu} - 1)_{\text{natural}} \leq (\text{Nu} - 1)_{\text{optimal}} \leq c\text{Pe}^\beta \quad (1.47)$$

\Rightarrow

$$\frac{\text{Pe}^2}{\text{Ra}} \leq c\text{Pe}^\beta \quad (1.48)$$

\Rightarrow

$$\text{Pe} \leq c^{\frac{1}{2-\beta}} \text{Ra}^{\frac{1}{2-\beta}} \quad (1.49)$$

\Rightarrow

$$(\text{Nu} - 1)_{\text{natural}} \leq c^{\frac{2}{2-\beta}} \text{Ra}^{\frac{\beta}{2-\beta}}. \quad (1.50)$$

Recall that the optimal transport and the natural transport are being compared at the same Pe value.

In Chapter 3 we formulate the optimal control problem (1.43) rigorously for steady flows, discuss time-dependent implications, and deduce rigorous upper bounds to the problem. In Chapter 4 we present algorithms for solving the Euler-Lagrange equations associated with (1.43) as well as present numerical solutions for two dimensional flows steady-flows.

The full optimization problem (1.43) is difficult and thus we look at reduced models in Chapter 2 to develop intuition. The first reduced model that we analyze are the famous Lorenz equations

$$\dot{X} = -\sigma X + \sigma Y \quad (1.51)$$

$$\dot{Y} = rX - Y - XZ \quad (1.52)$$

$$\dot{Z} = XY - bZ, \quad (1.53)$$

where b, σ, r are parameters. The analogous quantity to the Nusselt number in this context

is \overline{XY} . The natural problem is

$$\sup_{X_0, Y_0, Z_0} \overline{XY} \quad (1.54)$$

subject to

$$\dot{X} = -\sigma X + \sigma Y \quad (1.55)$$

$$\dot{Y} = rX - Y - XZ \quad (1.56)$$

$$\dot{Z} = XY - bZ, \quad (1.57)$$

and the optimal problem is

$$\sup_X \overline{XY} \quad (1.58)$$

subject to

$$\dot{Y} = rX - Y - XZ \quad (1.59)$$

$$\dot{Z} = XY - bZ \quad (1.60)$$

$$\overline{X^2} = \text{Pe}^2. \quad (1.61)$$

In §2.1 we find the sharp upper bounds to both problems.

The next reduced model that we look at in Chapter 2 is the Double Lorenz equations

$$\dot{x}_1 = -\sigma x_1 + \sigma r_1 y_1 + (c_1 w_1 - d_1 w_2) x_2 \quad (1.62)$$

$$\dot{y}_1 = -y_1 + x_1 - x_1 z_1 + \frac{1}{2}(w_1 - w_2) y_2 \quad (1.63)$$

$$\dot{z}_1 = -b_1 z_1 + x_1 y_1 \quad (1.64)$$

$$\dot{x}_2 = -\sigma a x_2 + \sigma a r_2 y_2 - a(c_2 w_1 - d_2 w_2) x_1 \quad (1.65)$$

$$\dot{y}_2 = -a y_2 + a x_2 - a x_2 z_2 - 2(w_1 - w_2) y_1 \quad (1.66)$$

$$\dot{z}_2 = -b_2 a z_2 + a x_2 y_2 \quad (1.67)$$

$$\dot{w}_1 = -\sigma \frac{1}{4} b_1 w_1 - \frac{3}{8} a x_1 x_2 \quad (1.68)$$

$$\dot{w}_2 = -\sigma \frac{9}{4} b_1 w_2 + \frac{3}{8} a x_1 x_2, \quad (1.69)$$

where $(\sigma, r_1, r_2, a, b_1, b_2, c_1, d_1)$ are parameters. Here we have

$$\text{Nu} = 1 + \frac{1 + k^2}{2} \left(\overline{x_1 y_1 + \frac{a}{4} x_2 y_2} \right), \quad (1.70)$$

$$\text{Pe}^2 = \frac{1}{2} \frac{(1 + k^2)^4}{k^2} x_1^2 + \frac{1}{8} \frac{(4 + k^2)^4}{k^2} x_2^2 + 2 \frac{(1 + k^2)^2}{k^2} w_1^2 + 18 \frac{(1 + k^2)^2}{k^2} w_2^2, \quad (1.71)$$

where k is another parameter. We form analogous “natural” and “optimal” problems for this system in §2.2. There we find sharp upper bounds to the optimal control problem and compare it to the known solutions of the “natural” problem.

CHAPTER 2

Reduced Models

Modal truncations of partial differential equations have a long history of modeling the essential physics and producing interesting mathematics. Low dimensional dynamical systems approximations can provide insights into the full partial differential equations of motion, and they can serve as a simplified setting in which to test analytical and numerical techniques. In the context of fluid mechanics, certain distinguished truncations, e.g., those respecting energy and/or enstrophy conservation in the inviscid limit, are of particular interest [7]. Finite dimensional dynamical systems are naturally derived as Galerkin truncations of the Boussinesq equations, but only a subset of such truncations preserve certain physical features of the full system. The modal truncations of Rayleigh-Bénard convection with stress-free boundaries that we will look at in this chapter include the celebrated Lorenz equations [8] as well as the Double Lorenz equations [9], an eight-mode extension of Lorenz.

We examine these modal truncations as models for both understanding the background method of §1.1 and the optimal control method of §1.2 in the context of Rayleigh-Bénard convection. In §2.1 we perform these two distinct analyses for the Lorenz equations. The background method and the optimal control method produce the same bound and correspond to an exact solution of the original equations of motion as well as the optimal transport equations. We mirror this procedure for the Double Lorenz equations in §2.2. In contrast to what was found for the Lorenz equations, it appears that the optimal transport bounds are not saturated by solutions of the original equations of motion; however bounds from the background method and the optimal control method coincide.

Although reduced models continue to be the focus of much modern theoretical [10, 11, 12], computational [13], and experimental [14] research it is widely appreciated that they do not inform us quantitatively about high Rayleigh number turbulent convection, the primary motivation for this investigation. But evaluation of the accuracy of rigorous bounds on heat transport in Rayleigh-Bénard convection remains an important open problem for

both physics and mathematics, and studies of simplified systems like this help us to assess the strength of available analytical tools.

The results presented in this chapter appeared in [15] and [16] for the Lorenz and Double Lorenz equations, respectively.

2.1 Lorenz

Few mathematical models have had as profound an influence on the development of non-linear science over the last half century as the Lorenz equations [8]

$$\dot{X} = -\sigma X + \sigma Y \quad (2.1)$$

$$\dot{Y} = rX - Y - XZ \quad (2.2)$$

$$\dot{Z} = XY - bZ. \quad (2.3)$$

This system arises as a severe modal truncation of Rayleigh's 1916 model of two-dimensional buoyancy-driven flow between parallel isothermal plates with stress-free boundaries [17].

In stream function vorticity representation Rayleigh's model takes the form,

$$\dot{\omega} + J(\psi, \omega) = \sigma \Delta \omega + \sigma \text{Ra} \theta_x \quad (2.4)$$

$$\dot{\theta} + J(\psi, \theta) = \Delta \theta + \psi_x \quad (2.5)$$

where the $J(\alpha, \beta) = \alpha_x \beta_y - \alpha_y \beta_x$, $\omega(x, y, t) = \Delta \psi(x, y, t)$ is the vorticity associated with stream function ψ , and $\theta(x, y, t)$ is the deviation of temperature from the steady linear conduction profile. The boundary conditions are $\psi = \psi_{yy} = \theta = 0$ at $y = 0$ and $y = 1$ with everything L -periodic in x .

Lorenz's variables are modal amplitudes in the Galerkin truncation approximation

$$\begin{aligned} \psi(x, y, t) &= \frac{\sqrt{2}}{\pi} \left(\frac{k^2 + \pi^2}{k} \right) X(t) \sin kx \sin \pi y \\ \theta(x, y, t) &= \frac{\sqrt{2}}{\pi r} Y(t) \cos kx \sin \pi y - Z(t) \frac{1}{\pi r} \sin 2\pi y \end{aligned} \quad (2.6)$$

where the 'reduced' Rayleigh number $r = Ra/Ra_c$, the domain-shape parameter $b = \frac{4\pi^2}{k^2 + \pi^2}$, and time is rescaled. Solutions of Rayleigh's continuum model are reasonably well approximated by Lorenz's truncation only near the primary bifurcation, i.e., for $r = \mathcal{O}(1)$, but the differential equations are nevertheless of theoretical (and historical) interest even for $r \gg 1$ due to the appearance of chaos in the solutions.

The bulk heat transport is measured by the Nusselt number Nu , the ratio of the sum of the total (conductive plus convective) heat flux to the flow-independent conductive flux. The convective heat flux is proportional to the correlation between the vertical velocity ψ_x and the temperature θ , which reduces to $\text{Nu} - 1 = \frac{k^2 + \pi^2}{2\pi^2 r} \langle XY \rangle$ for Lorenz's variables where $\langle \cdot \rangle$ indicates the infinite time average (when the infinite time limit of long-but-finite time averages exist). The Nusselt number is a key indicator of the nonlinear response of the system to the driving whose strength is measured by the Rayleigh number (Ra or r). The classical linear and nonlinear stability results for both Rayleigh's and Lorenz's models are that the pure conduction state with $\text{Nu} = 1$, respectively $\psi = 0 = \theta$ and $X = Y = Z = 0$, is absolutely stable for $\text{Ra} < \text{Ra}_c \equiv r < 1$ and linearly unstable for $\text{Ra} > \text{Ra}_c \equiv r > 1$.

The study of rigorous bounds on Nu for solutions of the Lorenz equations has received less attention with the notable exceptions of Malkus [18], Knobloch [19], and Foias *et al* [20] who found that the steady state maximizes transport among statistically steady solutions and for invariant measures, and Pétrélis & Pétrélis [1] who proved that $\langle XY \rangle \leq b \frac{(r + \sigma - \sqrt{\sigma})^2}{r + \sigma}$ for any solution. We examine two alternative approaches to establish the improved estimate $\langle XY \rangle \leq b(r - 1)$, uniformly in σ for $r > 1$, when the long-time limit exists. In case long-time averages do not converge, our result is that the limit supremum of finite-time averages satisfies the bound. Most significantly this upper bound is *sharp*: it is saturated by the exact steady solutions $(X_s, Y_s, Z_s) = (\pm \sqrt{b(r - 1)}, \pm \sqrt{b(r - 1)}, r - 1)$.

In the next section we employ the background method, originally contrived for estimating bulk averaged transport in solutions of the Navier-Stokes and related equations [4], to prove this upper bound. The subsequent section uses an optimal control strategy for upper bound analysis: we relax the momentum equation (2.1) and treat $X(t)$ as a control variable constrained only by $\langle X^2 \rangle = \text{Pe}^2$ to drive the temperature variables via (2.2) and (2.3). We prove in this setting that $\langle XY \rangle \leq r b \text{Pe}^2 / (b + \text{Pe}^2)$. Then auxiliary relation $\text{Pe}^2 = \langle XY \rangle$, from the neglected equation (2.1), can then be used to connect the optimal transport with solutions of the Lorenz equations, yielding the same bound as obtained from the background analysis. This shows that no time-dependent stirring protocol, whether it solves the first Lorenz equation (2.1) or not, transports more than the steady flow. We also show, in a certain precise sense, that the steady stirring strategy is the *unique* maximizer.

2.1.1 Background Analysis

We are interested in the $r > 1$ parameter regime. It is convenient to rewrite the Lorenz equations as

$$\dot{x} = -\sigma x + \sigma r y \quad (2.7)$$

$$\dot{y} = x - y - x z \quad (2.8)$$

$$\dot{z} = x y - b z, \quad (2.9)$$

where $X = x$, $Y = r y$ and $Z = r z$ and the Nusselt number in terms of the correlation of $x(t)$ and $y(t)$ is $\text{Nu} = 1 + \frac{k^2 + \pi^2}{2\pi^2} \langle xy \rangle$. (Note: do not confuse these lower case x and y variables with the spatial coordinates in Rayleigh's model discussed in the introduction.)

It is well known that, after possible initial transients, solutions of the Lorenz equations are uniformly bounded in time [21, 22, 23, 24, 25, 26]. For example

$$\frac{1}{2} \frac{d}{dt} \left[\frac{1}{r^2} x^2 + y^2 + \left(z - 1 - \frac{\sigma}{r} \right)^2 \right] = -\frac{\sigma}{r^2} x^2 - y^2 - b z^2 + b \left(1 + \frac{\sigma}{r} \right) z \quad (2.10)$$

so that

$$\overline{\lim}_{t \rightarrow \infty} \left[\frac{1}{r^2} x^2 + y^2 + \left(z - 1 - \frac{\sigma}{r} \right)^2 \right] \leq \begin{cases} \left(1 + \frac{\sigma}{r} \right)^2 & \text{if } \min\{1, \sigma, \frac{b}{2}\} = \frac{b}{2} \\ \frac{b^2 \left(1 + \frac{\sigma}{r} \right)^2}{4(b-1)} & \text{if } \min\{1, \sigma, \frac{b}{2}\} = 1 \\ \frac{b^2 \left(1 + \frac{\sigma}{r} \right)^2}{4\sigma(b-\sigma)} & \text{if } \min\{1, \sigma, \frac{b}{2}\} = \sigma. \end{cases} \quad (2.11)$$

Thus for differentiable functions $F : R^3 \rightarrow R$, long time averages of time derivatives satisfy

$$\langle \dot{F}(x, y, z) \rangle_T \equiv T^{-1} \int_0^T \left[\frac{d}{dt} F(x(t), y(t), z(t)) \right] dt = \mathcal{O}(T^{-1}) \text{ as } T \rightarrow \infty. \quad (2.12)$$

Hence, averaging time derivatives of $\frac{1}{2}x^2$, $\frac{1}{2}(y^2 + z^2)$, and $-z$ we deduce the balances

$$0 = -\langle x^2 \rangle_T + r \langle xy \rangle_T + \mathcal{O}(T^{-1}) \quad (2.13)$$

$$0 = -\langle y^2 \rangle_T - b \langle z^2 \rangle_T + \langle xy \rangle_T + \mathcal{O}(T^{-1}) \quad (2.14)$$

$$0 = -\langle xy \rangle_T + b \langle z \rangle_T + \mathcal{O}(T^{-1}). \quad (2.15)$$

Now write $z(t) = z_0 + \zeta(t)$ where, anticipating the result, we choose the time-independent ‘‘background’’ component $z_0 = \frac{r-1}{r}$. One may choose to decompose the x and y variables as well, but insight from the full Rayleigh–Bénard problem suggests that this is unneces-

sary. Indeed we expect that the long time averages of the x and y variables for chaotic solutions average out to zero, thus there is nothing to be gained by separating it into such components. On the other hand we expect z to have a non-zero average value for $r > 1$. Looking at the modal amplitude that the z variable comes from provides additional insight. It is purely a function of the vertical direction (unlike the other Lorenz modes) and thus it is the only one affected by the background decomposition of full PDE, see §3.4.

Substituting $z(t) = z_0 + \varsigma(t)$ into (2.14) and (2.15) yields

$$0 = -\langle y^2 \rangle_T - b\langle \varsigma^2 \rangle_T - 2bz_0\langle \varsigma \rangle_T - bz_0^2 + \langle xy \rangle_T + \mathcal{O}(T^{-1}) \quad (2.16)$$

$$0 = bz_0 + b\langle \varsigma \rangle_T - \langle xy \rangle_T + \mathcal{O}(T^{-1}). \quad (2.17)$$

Then the combination (2.16) + $2z_0 \times$ (2.17) is

$$0 = -\langle y^2 \rangle_T - b\langle \varsigma^2 \rangle_T + bz_0^2 + (1 - 2z_0)\langle xy \rangle_T + \mathcal{O}(T^{-1}) \quad (2.18)$$

so that, adding zero cleverly disguised as $\frac{1}{r} \times (2.13) + r \times (2.18)$ to $(r - 1)\langle xy \rangle_T$, we have

$$\begin{aligned} (r - 1)\langle xy \rangle_T &= rbz_0^2 - \langle (\frac{x}{\sqrt{r}} - \sqrt{r}y)^2 + rb\varsigma^2 \rangle_T + \mathcal{O}(T^{-1}) \\ &\leq rbz_0^2 + \mathcal{O}(T^{-1}) = b\frac{(r - 1)^2}{r} + \mathcal{O}(T^{-1}). \end{aligned} \quad (2.19)$$

This, in turn, implies

$$\overline{\lim}_{T \rightarrow \infty} \langle XY \rangle_T = \overline{\lim}_{T \rightarrow \infty} r\langle xy \rangle_T \leq b(r - 1) = X_s Y_s. \quad (2.20)$$

Therefore, when the long time limit exists, $\langle XY \rangle = \lim_{T \rightarrow \infty} \langle XY \rangle_T \leq b(r - 1)$ as advertised.

As a corollary it is interesting to note that the proof also shows that any sustained time dependence in the solutions, whether periodic or chaotic, strictly lowers the transport. Indeed, (2.1) and the penultimate expression in (2.19) imply

$$\langle XY \rangle_T \leq b(r - 1) - \frac{1}{\sigma^2(r - 1)} \langle \dot{X}^2 \rangle_T + \mathcal{O}(T^{-1}) \quad (2.21)$$

so that $\langle XY \rangle$ is *strictly* less than $X_s Y_s$ when $\langle \dot{X}^2 \rangle \neq 0$.

This is illustrated in Figure 2.1 where we plot the upper limit realized by the non-trivial steady state solutions along with measurements of $\langle XY \rangle$ from direct numerical solutions of the Lorenz equations. For these particular parameter values ($\sigma = 10$ and $b = \frac{8}{3}$) the non-zero fixed points are stable for $1 < r \leq \frac{470}{19} = 24.73 \dots$ [8] while chaotic and periodic

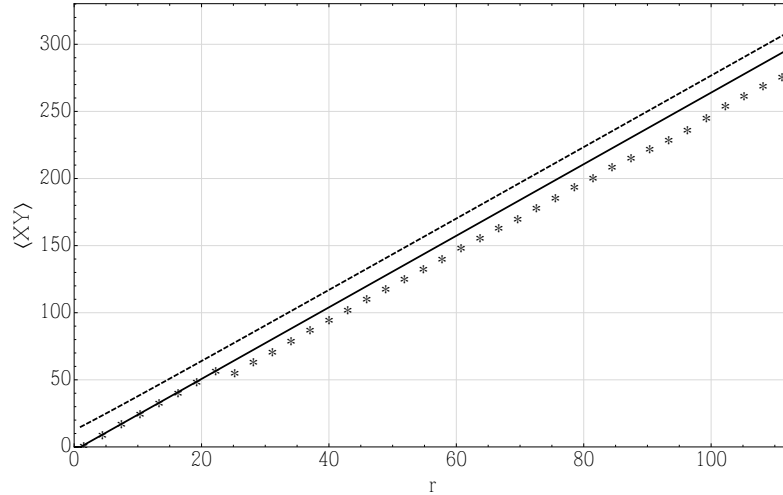


Figure 2.1: Long time averaged heat transport for solutions of the Lorenz equations. Dashed line: upper bound on $\langle XY \rangle$ derived by Pétrélis & Pétrélis [1]. Solid line: improved upper bound (2.20) corresponding to the nontrivial fixed points that exist when $r > 1$. Discrete data: direct numerical simulation results for parameter values $\sigma = 10$ and $b = \frac{8}{3}$.

solutions—that necessarily transporting less heat—are robustly realized for higher r .

2.1.2 Optimal Control Analysis

The same upper bound results from an alternative analysis and yields insight into the dynamics of optimal transport in the Lorenz equations. The idea is to consider the flow as a control variable driving the temperature field via the advection-diffusion equation and ask: What is the maximal transport that can be realized among all flows subject to a suitable intensity constraint? The relevant constraint for Rayleigh’s model is the value of the space-time averaged enstrophy (the mean squared vorticity $\langle \omega^2 \rangle$, where $\langle \cdot \rangle$ includes the spatial average in this context) the magnitude of which becomes a parameter in the control problem. By revisiting the neglected momentum equation we connect the flow intensity parameter with the transport and the original parameter(s): for Rayleigh’s model the connection is established by multiplying (2.4) by ψ and averaging over space and time to see that $\langle \omega^2 \rangle = \text{Ra} \langle \psi_x \theta \rangle = \text{Ra}(\text{Nu} - 1)$.

For the Lorenz equations we neglect dynamical equation (2.1) and treat $X(t)$ as a control variable in (2.2) and (2.3) for $Y(t)$ and $Z(t)$. The amplitude of X is subject to the constraint $\langle X^2 \rangle = \text{Pe}^2 < \infty$ where the Péclet number Pe parameterizes the strength of the stirring. We seek to determine the optimal $X(t)$ that maximize the convective trans-

port proportional to the correlation $\langle XY \rangle$. Afterwards, to connect the Péclet number to the Rayleigh-Bénard problem, we impose the relation $\text{Pe}^2 = \frac{2\pi^2 r}{k^2 + \pi^2} (\text{Nu} - 1)$ satisfied by natural buoyancy driven flow. The bound on Nu is also a bound for solutions of the full Lorenz system since we maximize over a larger class of functions $X(t)$ than just those generated by (2.1).

To carry this out it is again convenient to rewrite (2.2) and (2.3) as the inhomogeneous and (generally) non-autonomous linear dynamical system

$$\frac{d}{dt} \begin{pmatrix} y \\ z \end{pmatrix} = \begin{pmatrix} -1 & -x \\ x & -b \end{pmatrix} \begin{pmatrix} y \\ z \end{pmatrix} + \begin{pmatrix} x \\ 0 \end{pmatrix} \quad (2.22)$$

where $y(t) = Y(t)/r$, $z(t) = Z(t)/r$, and $x(t) = X(t)$ is now a locally square integrable function of time subject only to the mean constraint $\langle x^2 \rangle = \text{Pe}^2$ (strictly speaking we require $\langle x^2 \rangle_T = \text{Pe}^2 + o(1)$ as $T \rightarrow \infty$). The optimal control problem is a constrained optimization problem: we seek to determine the maximum possible value, over all admissible functions $x(t)$, of the long-time average $\langle xy \rangle$ where $y(t)$ and $z(t)$ solve (2.22).

According to the calculus of variations the mother functional that we differentiate to derive the Euler-Lagrange equations satisfied by the optimizers is

$$\mathcal{F} = \left\langle xy - \eta(\dot{y} - x + y + xz) + \zeta(\dot{z} - xy + bz) - \frac{\mu}{2}(x^2 - \text{Pe}^2) \right\rangle \quad (2.23)$$

where $\eta(t)$ and $\zeta(t)$ are Lagrange multipliers enforcing (2.22) and the real variable μ is the Lagrange multiplier enforcing the intensity constraint. Ignoring initial (and final) conditions for the moment, the Euler-Lagrange equations obtained by setting $\delta\mathcal{F}/\delta y$, $\delta\mathcal{F}/\delta z$, and $\delta\mathcal{F}/\delta u$ to zero are, respectively,

$$\frac{d}{dt} \begin{pmatrix} \eta \\ \zeta \end{pmatrix} = \begin{pmatrix} 1 & x \\ -x & b \end{pmatrix} \begin{pmatrix} \eta \\ \zeta \end{pmatrix} - \begin{pmatrix} x \\ 0 \end{pmatrix} \quad (2.24)$$

and

$$\mu x(t) = y(t)(1 - \zeta(t)) + \eta(t)(1 - z(t)) \quad (2.25)$$

that prescribes the optimal stirring strategy $x(t)$ in terms of the dynamical variables and the Lagrange multipliers. Note that for a given control $x(t)$ the linear inhomogeneous system (2.24) for the ‘adjoint’ functions η and ζ is precisely the time reversed dynamics of (2.22).¹

¹If we were interested in maximizing the time average of $x(t)y(t)$ over a finite time interval $(0, T)$ given initial conditions $y(0)$ and $z(0)$, the adjoint dynamics in (2.24) would come equipped with homogeneous final conditions $\eta(T) = 0 = \zeta(T)$, following from the integration by parts involved with evaluating the functional

Operationally one chooses a value of μ , solves the four dimensional nonlinear system consisting of (2.22) and (2.24) coupled together by (2.25), and then evaluates both the sought-after extreme value of $\langle xy \rangle$ the original parameter of the problem, the Péclet number Pe .

The time independent solution of the optimal control problem is

$$x_s = \pm \text{Pe}, \quad y_s = \eta_s = \pm \frac{b \text{Pe}}{\text{Pe}^2 + b}, \quad z_s = \zeta_s = \frac{\text{Pe}^2}{\text{Pe}^2 + b} \quad (2.26)$$

yielding an extreme transport value

$$x_s y_s = \frac{b \text{Pe}^2}{\text{Pe}^2 + b}. \quad (2.27)$$

The Lagrange multiplier $\mu = 2b^2/(\text{Pe}^2 + b)^2 \in (0, 2]$ for these solutions. Recalling that the Nusselt number in terms of the correlation of $x(t)$ and $y(t)$ is $\text{Nu} = 1 + \frac{k^2 + \pi^2}{2\pi^2} \langle xy \rangle$ and, from the abandoned ‘momentum’ Lorenz equation (2.1) the reduced Rayleigh number r is related to Pe and Nu via $\text{Pe}^2 = \frac{2\pi^2 r}{k^2 + \pi^2} (\text{Nu} - 1)$, we may eliminate the Péclet number and express this steady stirring extreme transport

$$x_s y_s = b \left(1 - \frac{1}{r}\right) \iff X_s Y_s = r x_s y_s = b(r - 1), \quad (2.28)$$

precisely the same upper bound to transport from the previous section.

In the two following subsections we will first display and discuss numerically computed time-periodic solutions of the optimal Euler-Lagrange equations, and then prove (a) that the steady solution of the Euler-Lagrange equations realizes the absolute upper bound and (b) that any non-constant time-periodic control transports strictly less. This establishes the fact that steady stirring is the *unique* global maximizer among the infinitely many time-periodic solutions of the Euler-Lagrange equations.

2.1.3 Time Periodic Stirring Protocols

We numerically constructed some time-periodic solutions of the optimal control problem defined by (2.22), (2.24), and (2.25) by computationally continuing analytical time-periodic solutions from the linearized problem at small Pe into the strongly nonlinear regime. In the derivatives, suitable to specify the time-reversed evolution.

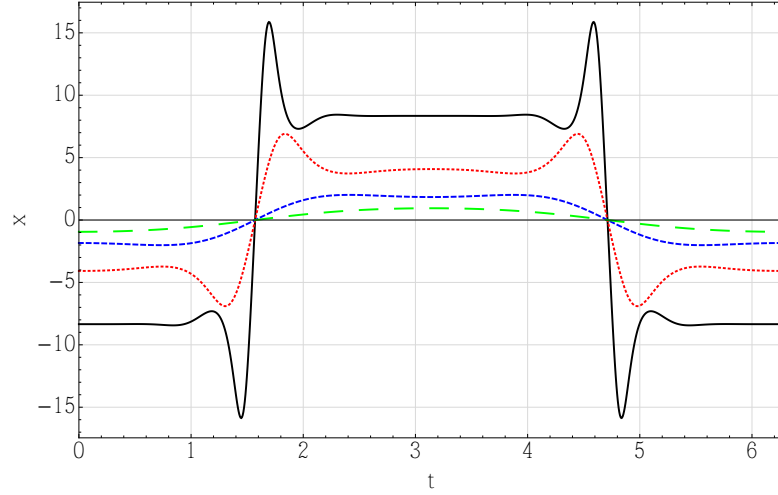


Figure 2.2: The time dependence of optimal $\tau = 2\pi$ periodic stirring protocols for several values of the Péclet number and $b = \frac{8}{3}$. Long dashed line: $\text{Pe} = 0.69$; short dashed line: $\text{Pe} = 1.71$; dotted line $\text{Pe} = 4.50$; solid curve: $\text{Pe} = 8.96$.

limit $\text{Pe} \rightarrow 0$ the linearized Euler-Lagrange equations are

$$\dot{y} = -y + x \quad (2.29)$$

$$\dot{z} = -bz \quad (2.30)$$

$$\dot{\eta} = \eta - x \quad (2.31)$$

$$\dot{\zeta} = b\zeta \quad (2.32)$$

$$\mu x = y + \eta. \quad (2.33)$$

Let $\tau = \frac{2\pi}{\omega}$ denote the period of the sought-after solutions. Then $z(t) = 0 = \zeta(t)$ and, requiring without loss of generality that $y(t) = \eta(\tau - t)$ to set the phase,

$$y(t) = \frac{\sqrt{2}\text{Pe}}{1 + \omega^2} (\cos \omega t + \omega \sin \omega t) \quad (2.34)$$

$$\eta(t) = \frac{\sqrt{2}\text{Pe}}{1 + \omega^2} (\cos \omega t - \omega \sin \omega t) \quad (2.35)$$

where the Lagrange multiplier $\mu = \frac{2}{1 + \omega^2}$, the optimal control is $x(t) = \sqrt{2}\text{Pe} \cos \omega t$, and the transport is $\langle xy \rangle = \text{Pe}^2 / (1 + \omega^2)$. To computationally search for τ -periodic solutions of (2.22), (2.24), and (2.25) we first truncate the Fourier series expansion of the full non-linear system and solve the resulting system of algebraic equations via Newton's method continuing from small values of Pe using the linearized solutions as the initial guess.

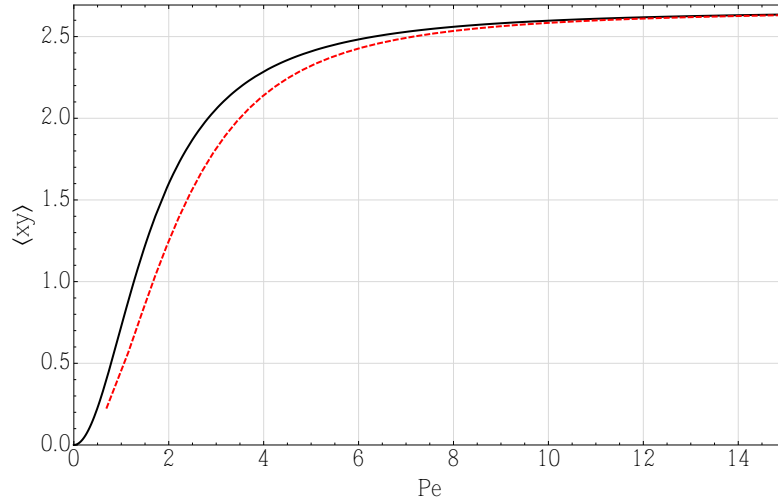


Figure 2.3: Solid line: absolute upper bound (2.54) on the long time averaged transport vs. Péclet number, corresponding to steady stirring, for parameter value $b = \frac{1}{\omega} \rightarrow \infty$. Dashed line: transport from numerically computed periodic solution of the optimal Euler-Lagrange equations for period $\tau = 2\pi$ ($\omega = 1$), which is observed to lie strictly below absolute upper bound from the steady solutions of the optimal Euler-Lagrange equations.

Figure 2.2 displays $\tau = 2\pi$ periodic solutions for the control $x(t)$ for several values of the the Péclet number. For $Pe > \mathcal{O}(1)$ it is evident that $x(t)$ is ‘attempting’ to take on the steady stirring value $x_s = Pe$ but is frustrated, forced to switch by the mandated periodic behavior.

Figure 2.3 is a plot of the absolute upper bound for the transport, $b Pe^2 / (b + Pe^2)$, and the transport from numerically computed periodic solutions of the optimal Euler-Lagrange equations for period $\tau = 2\pi$. The time dependent solution produces strictly less transport than steady stirring of the same averaged intensity, as was the case for all periods that we sampled. This suggests that steady stirring is actually the *unique* global optimizer—at least among time-periodic stirring protocols—and in the next subsection we show that this is so.

2.1.4 Analysis and Bounds on Transport by Arbitrary Stirring

Given a general stirring protocol $x(t)$ defined over a semi-infinite interval—without loss of generality $(0, \infty)$ —it is evident that in the long run $y(t)$ and $z(t)$, and hence also the largest possible long time averaged transport $\overline{\lim}_{T \rightarrow \infty} \langle xy \rangle_T$, become independent of the initial data $y(0)$ and $z(0)$. Indeed, if both $y(t)$ and $z(t)$ and $\tilde{y}(t)$ and $\tilde{z}(t)$ satisfy (2.22) with the same $x(t)$ albeit with different initial conditions, then the differences $\Delta y = y - \tilde{y}$ and $\Delta z = z - \tilde{z}$

satisfy the homogeneous linear system

$$\frac{d}{dt} \begin{pmatrix} \Delta y \\ \Delta z \end{pmatrix} = \begin{pmatrix} -1 & -x \\ x & -b \end{pmatrix} \begin{pmatrix} \Delta y \\ \Delta z \end{pmatrix} \quad (2.36)$$

so that

$$\frac{d}{dt} \frac{1}{2} ((\Delta y)^2 + (\Delta z)^2) = -(\Delta y)^2 - b(\Delta z)^2 \quad (2.37)$$

ensuring that the difference $|\Delta y(t)| \leq c e^{-\alpha t}$ for some finite nonnegative c depending on $\Delta y(0)$ and $\Delta z(0)$ and $\alpha = \min\{1, b\} > 0$. Then the Cauchy-Schwarz inequality guarantees

$$|\langle x \Delta y \rangle_T| \leq \langle x^2 \rangle_T^{1/2} \left(T^{-1} \int_0^T [\Delta y(t)]^2 dt \right)^{1/2} \quad (2.38)$$

$$\leq (\text{Pe} + o(1)) \times \frac{c}{\sqrt{2\alpha T}} \xrightarrow{T \rightarrow \infty} 0. \quad (2.39)$$

That being said, we do not know how to solve the Euler-Lagrange equations, or how to prove the existence of solutions in the most general setting. We also do not know that the $T \rightarrow \infty$ limit of $\langle xy \rangle_T$ exists for locally square integrable $x(t)$ for which the $T \rightarrow \infty$ limit of $\langle x^2 \rangle_T$ does exist.

Nevertheless we can be certain that $\langle xy \rangle_T$ is bounded uniformly as $T \rightarrow \infty$ so that the limit supremum is finite and it always makes sense to seek an upper estimate applicable for all possible values of the long time average. To see this observe that $y(t)$ and $z(t)$ are bounded uniformly in time, independent of the stirring function $x(t)$ [23]. Indeed,

$$\frac{d}{dt} \frac{1}{2} (y^2 + (z-1)^2) = -y^2 - bz^2 + bz \quad (2.40)$$

implying

$$\overline{\lim}_{t \rightarrow \infty} [y^2 + (z-1)^2] \leq \begin{cases} 1 & \text{if } 0 < b \leq 2 \\ \frac{b^2}{4(b-1)} & \text{if } b \geq 2. \end{cases} \quad (2.41)$$

Cauchy-Schwarz thus guarantees

$$\overline{\lim}_{T \rightarrow \infty} \langle xy \rangle_T \leq \text{Pe} \times \begin{cases} 1 & \text{if } 0 < b \leq 2 \\ \frac{b}{2\sqrt{b-1}} & \text{if } b \geq 2. \end{cases} \quad (2.42)$$

But a much lower *a priori* estimate on the transport, one that is uniform in Pe as $\text{Pe} \rightarrow$

∞ , is also easily established:

$$\frac{d}{dt} \frac{1}{2} (y^2 + z^2) = -y^2 - bz^2 + xy \quad (2.43)$$

so that

$$\langle xy \rangle_T = \langle y^2 + bz^2 \rangle_T + \frac{y(T)^2 + bz(T)^2 - y(0)^2 - bz(0)^2}{2T}. \quad (2.44)$$

In view of the Pe-independent time asymptotic limits on $|y|$ and $|z|$ in (2.41), we conclude that $\langle xy \rangle_T$ posses a Pe-independent upper bound.

To determine the absolute—and, as will be seen, sharp—upper limit start with the differential equation for $z(t)$ in (2.22) to infer

$$\langle xy \rangle_T = b\langle z \rangle_T + \mathcal{O}(T^{-1}). \quad (2.45)$$

Then, as in the background analysis, let $z(t) = z_0 + \varsigma(t)$, rewrite (2.44) and $2z_0 \times$ (2.45) as

$$0 = -\langle y^2 + b\varsigma^2 \rangle_T - 2bz_0\langle \varsigma \rangle_T - bz_0^2 + \langle xy \rangle_T + \mathcal{O}(T^{-1}) \quad (2.46)$$

$$0 = -2z_0\langle xy \rangle_T + 2bz_0^2 + 2bz_0\langle \varsigma \rangle_T + \mathcal{O}(T^{-1}) \quad (2.47)$$

and recall that because the infinite time average $\langle x^2 \rangle$ exists,

$$0 = 1 - \frac{1}{\text{Pe}^2} \langle x^2 \rangle_T + o(1). \quad (2.48)$$

Define

$$a = \frac{b \text{Pe}}{b + \text{Pe}^2} \quad (2.49)$$

and add 0 in the form of (2.46) + (2.47) + $a^2 \times$ (2.48) to $\langle xy \rangle_T$ to deduce

$$\langle xy \rangle_T = bz_0^2 + a^2 - \left\langle \frac{a^2}{\text{Pe}^2} x^2 + y^2 - 2(1 - z_0)xy + b\varsigma^2 \right\rangle_T + o(1). \quad (2.50)$$

The quadratic form on the right hand side above is non-negative when

$$\frac{a^2}{\text{Pe}^2} - (1 - z_0)^2 \geq 0. \quad (2.51)$$

which is guaranteed by the choice

$$z_0 = \frac{\text{Pe}^2}{b + \text{Pe}^2}. \quad (2.52)$$

Then

$$\langle xy \rangle_T \leq bz_0^2 + a^2 + o(1) = \frac{b\text{Pe}^2}{b + \text{Pe}^2} + o(1). \quad (2.53)$$

and we have proven the global upper bound

$$\overline{\lim}_{T \rightarrow \infty} \langle xy \rangle_T \leq \frac{b\text{Pe}^2}{b + \text{Pe}^2}. \quad (2.54)$$

Therefore, when the long time limit exists, transport by any protocol $x(t)$ satisfies $\langle xy \rangle \leq b\text{Pe}^2/(b + \text{Pe}^2)$. This corresponds precisely to the extreme value (2.27) obtained from the steady solution (2.26) of the Euler-Lagrange equations for the optimal control problem. Then, utilizing the relation $\text{Pe}^2 = r\langle xy \rangle$ to reintroduce the reduced Rayleigh number r , we conclude that $\langle xy \rangle \leq b(1 - \frac{1}{r})$ even when $x(t)$ does not satisfy the first Lorenz equation.

The analysis above is also sufficient to show that steady control is the unique global optimizer among the class of periodic protocols. To see this, first note that when $x(t) = x_\tau(t)$ is τ -periodic both $y(t)$ and $z(t)$ converge to unique τ -periodic functions $y_\tau(t)$ and $z_\tau(t)$.² This means that the long time average of any continuous function of x , y , and z exists and is equal to the average of the function of $x_\tau(t)$, $y_\tau(t)$, and $z_\tau(t)$ over just one period. In the periodic case (2.50) with the choice (2.52) averaged over a period becomes an equality:

$$\langle x_\tau y_\tau \rangle_\tau = \frac{b\text{Pe}^2}{b + \text{Pe}^2} - \left\langle \frac{a}{\text{Pe}} \left(\sqrt{\frac{b}{b + \text{Pe}^2}} x_\tau - \sqrt{\frac{b + \text{Pe}^2}{b}} y_\tau \right)^2 + b\zeta_\tau^2 \right\rangle_\tau. \quad (2.55)$$

Thus $\langle x_\tau y_\tau \rangle_\tau = \frac{b\text{Pe}^2}{b + \text{Pe}^2}$ if and only if

$$x_\tau(t) = \frac{b + \text{Pe}^2}{b} y_\tau(t) \quad \text{and} \quad \zeta_\tau \equiv 0 \Leftrightarrow z_\tau(t) = z_0 = \text{Pe}^2/(b + \text{Pe}^2) = \text{constant}. \quad (2.56)$$

But then the differential equation for $y_\tau(t)$ is

$$\dot{y}_\tau = -y_\tau - x_\tau z_\tau + x_\tau = -y_\tau - \frac{b + \text{Pe}^2}{b} \times y_\tau \times \frac{\text{Pe}^2}{b + \text{Pe}^2} + \frac{b + \text{Pe}^2}{b} y_\tau \equiv 0 \quad (2.57)$$

so $y_\tau(t) = \text{constant}$ as well. Thus it is proved that the *only* periodic solutions saturating the

²Indeed, the differences $\Delta y(t) = y(t + \tau) - y(t)$ and $\Delta z(t) = z(t + \tau) - z(t)$ satisfy the homogeneous system (2.36) when $x(t) = x_\tau(t)$ is τ -periodic, so both $|\Delta y(t)|$ and $|\Delta z(t)|$ converge to zero uniformly (and exponentially) as $t \rightarrow \infty$. This is sufficient to guarantee the existence of a unique periodic solution to the linear inhomogeneous system of differential equations with periodic coefficients defining y_τ and z_τ .

upper bounds are the constant solutions.

We do not know how to state or prove more general claims about the uniqueness of the steady optimal stirring strategy. One obstruction is the fact that any transiently time-dependent function $x(t)$ that converge to $x_s = \text{Pe}$ as $t \rightarrow \infty$ will produce precisely the same time asymptotic mean transport as $x(t) = x_s$. Moreover, at this stage we do not know how to rule out the existence of optimal protocols that fluctuate non-periodically forever, i.e., $x(t)$ which are not periodic but do *not* converge as $t \rightarrow \infty$, even though the long time average of $\langle x^2 \rangle_T$ does converge to Pe^2 as $T \rightarrow \infty$.

2.2 Double Lorenz

The eight-ODE model of Gluhovsky *et al* [9] is a generalization of the Lorenz equations and an extension of the seven-ODE model of Thiffeault. It includes an extra shear mode to conserve enstrophy as well as energy in the dissipationless limit and captures more details of the bifurcation structure of Rayleigh’s model near onset [27].

In order to correspond to [16] we change the domain of Rayleigh’s model in the vertical direction from $[0, 1]$ to $[0, \pi]$ so that the horizontal domain is now $[0, A\pi]$ where A is the aspect ratio. The version of Rayleigh’s model in stream function vorticity representation that we will be using here is of the form,

$$\partial_t \Delta \psi - J(\psi, \Delta \psi) = \sigma \Delta^2 \psi + \text{Ra} \sigma \partial_x \theta \quad (2.58)$$

$$\partial_t \theta - J(\psi, \theta) = \Delta \theta + \partial_x \psi \quad (2.59)$$

where $\psi(x, z, t)$ is the stream function and $\theta(x, z, t)$ is the deviation of the temperature from the linear profile of the conduction state. The Jacobian is $J(f, g) = \partial_x f \partial_z g - \partial_x g \partial_z f$. In this formulation on this domain Ra is the “traditional” Rayleigh number divided by π^4 so that the onset of convection for $A = 2\sqrt{2}$ occurs at the minimum critical value $\text{Ra}_c = \frac{27}{4}$. The minus sign in front of the Jacobian is different from the one in §2.1 because of the change of vertical coordinate y to z and hence a redefinition of the stream function.

We use angle brackets $\langle \cdot \rangle$ to denote the spatio-temporal average

$$\langle f \rangle = \lim_{T \rightarrow \infty} \int_0^T \frac{dt}{T} \int_0^{A\pi} \frac{dx}{A\pi} \int_0^\pi \frac{dz}{\pi} f(x, z, t), \quad (2.60)$$

assuming that the long time limit exists. The nondimensional measure of heat transport is

the Nusselt number

$$\text{Nu} = 1 + \langle \theta \partial_x \psi \rangle, \quad (2.61)$$

and the flow intensity is indicated by the Péclet number Pe which for our purposes is the root mean square vorticity (i.e., the square root of the enstrophy, which is itself proportional to the bulk viscous energy dissipation rate):

$$\text{Pe} = \langle (\Delta \psi)^2 \rangle^{1/2}. \quad (2.62)$$

The Péclet and Nusselt number are related by

$$\text{Pe}^2 = \text{Ra}(\text{Nu} - 1), \quad (2.63)$$

derived by multiplying (2.58) by ψ and taking the spatio-temporal average employing suitable integrations by parts utilizing the boundary conditions.

The Double Lorenz equations [9] emerge from the Galerkin truncation

$$\begin{aligned} \psi(x, z, t) \approx & 2 \frac{1+k^2}{\sqrt{2}k} x_1(t) \sin(kx) \sin(z) + \frac{4+k^2}{\sqrt{2}k} x_2(t) \cos(kx) \sin(2z) \\ & + 2 \frac{1+k^2}{k} w_1(t) \sin(z) + \frac{2}{3} \frac{1+k^2}{k} w_2(t) \sin(3z) \end{aligned} \quad (2.64)$$

$$\begin{aligned} \theta(x, z, t) \approx & \frac{2}{\sqrt{2}} y_1(t) \cos(kx) \sin(z) + z_1(t) \sin(2z) \\ & - \frac{1}{\sqrt{2}} y_2(t) \sin(kx) \sin(2z) + \frac{1}{2} z_2(t) \sin(4z), \end{aligned} \quad (2.65)$$

where $k = 2/A$. Rescaling time $t \mapsto (1+k^2)^{-1}t$ leads to the ordinary differential equations

for the modal amplitudes

$$\dot{x}_1 = -\sigma x_1 + \sigma r_1 y_1 + (c_1 w_1 - d_1 w_2) x_2 \quad (2.66)$$

$$\dot{y}_1 = -y_1 + x_1 - x_1 z_1 + \frac{1}{2}(w_1 - w_2) y_2 \quad (2.67)$$

$$\dot{z}_1 = -b_1 z_1 + x_1 y_1 \quad (2.68)$$

$$\dot{x}_2 = -\sigma a x_2 + \sigma a r_2 y_2 - a(c_2 w_1 - d_2 w_2) x_1 \quad (2.69)$$

$$\dot{y}_2 = -a y_2 + a x_2 - a x_2 z_2 - 2(w_1 - w_2) y_1 \quad (2.70)$$

$$\dot{z}_2 = -b_2 a z_2 + a x_2 y_2 \quad (2.71)$$

$$\dot{w}_1 = -\sigma \frac{1}{4} b_1 w_1 - \frac{3}{8} a x_1 x_2 \quad (2.72)$$

$$\dot{w}_2 = -\sigma \frac{9}{4} b_1 w_2 + \frac{3}{8} a x_1 x_2 \quad (2.73)$$

where the r_i (for $i = 1, 2$) are related to the Rayleigh number and a rational function of k , and a and b_i, c_i, d_i , (also for $i = 1, 2$) are parameters that depend on k . The explicit expressions are tabulated in Appendix C.1. The (x_1, y_1, z_1) variables are precisely the familiar (albeit rescaled) Lorenz variables which, in this system, are coupled to a second set of Lorenz-like variables (x_2, y_2, z_2) by the shear flow modal amplitudes w_1 and w_2 .

The Nusselt and Péclet numbers for the Double Lorenz equations are obtained by inserting (2.64) and (2.65) into (2.61) and (2.62):

$$\text{Nu} = 1 + \frac{1 + k^2}{2} \left(\langle x_1 y_1 \rangle + \frac{a}{4} \langle x_2 y_2 \rangle \right), \quad (2.74)$$

$$\text{Pe}^2 = \frac{1}{2} \frac{(1 + k^2)^4}{k^2} \langle x_1^2 \rangle + \frac{1}{8} \frac{(4 + k^2)^4}{k^2} \langle x_2^2 \rangle + 2 \frac{(1 + k^2)^2}{k^2} \langle w_1^2 \rangle + 18 \frac{(1 + k^2)^2}{k^2} \langle w_2^2 \rangle. \quad (2.75)$$

The goal is to bound Nu as a function of Ra or Pe. Relation (2.63), which also holds for the truncated system, is used to convert between Ra and Pe.

The origin of the eight-dimensional phase space, i.e., $x_1 = x_2 = w_1 = w_2 = y_1 = y_2 = z_1 = z_2 = 0$, corresponds to the no-flow (Pe = 0) conduction solution with Nu = 1. This state is absolutely stable when $r_1 \leq 1$ so we are generally interested in the $r_1 > 1$ regime, i.e., $\text{Ra} > \text{Ra}_c(k^2) = (1 + k^2)^3 / k^2$.

2.2.1 Background Analysis

We will now use the background method to derive an upper bound to transport values in the Double Lorenz equations. Decompose the temperature variables as $z_i(t) = z_i^0 + \varsigma_i(t)$ where z_i^0 are “background” values to be chosen later. The uniform-in-time boundedness of

all the dynamical variables [9] (see Appendix C) implies

$$0 = \left\langle \frac{d}{dt} \left(y_1^2 + \varsigma_1^2 - 2z_1^0 \varsigma_1 + \frac{1}{4} (y_2^2 + \varsigma_1^2 - 2z_2^0 \varsigma_2) \right) \right\rangle. \quad (2.76)$$

(As in §2.1 we could take finite time averages for $t \in [0, T]$ throughout the subsequent calculations, leading to $\mathcal{O}(T^{-1})$ corrections to the formulae as $T \rightarrow \infty$, but the end result is a bound on the limit supremum, so for simplicity of exposition we forgo the demonstration.) The equations of motion for the temperature variables equation inserted into (2.76) reveal

$$0 = -\langle y_1^2 \rangle - b_1 \langle \varsigma_1^2 \rangle + (1 - 2z_1^0) \langle x_1 y_1 \rangle + b_1 (z_1^0)^2 - \frac{a}{4} \langle y_2^2 \rangle - \frac{a}{4} b_2 \langle \varsigma_2^2 \rangle + \frac{a}{4} (1 - 2z_2^0) \langle x_2 y_2 \rangle + \frac{a}{4} b_2 (z_2^0)^2. \quad (2.77)$$

We emphasize that the derivation of (2.77) relies only on the temperature equations. Then (2.63) in the form $0 = \frac{2}{1+k^2} (-\text{Pe}^2/\text{Ra} + \text{Nu} - 1)$ yields

$$0 = - \left(\frac{1}{r_1} \langle x_1^2 \rangle + \frac{a}{4} \frac{1}{r_2} \langle x_2^2 \rangle + \frac{1}{r_3} \langle w_1^2 \rangle + \frac{1}{r_4} \langle w_2^2 \rangle \right) + \langle x_1 y_1 \rangle + \frac{a}{4} \langle x_2 y_2 \rangle \quad (2.78)$$

where r_i (for $i = 1, 2, 3, 4$) are proportional to Ra and a rational function of k ; see C.1. Adding (2.77) and (2.78) produces the expression

$$0 = -\langle y_1^2 \rangle - b_1 \langle \varsigma_1^2 \rangle - \frac{a}{4} \langle y_2^2 \rangle - \frac{a}{4} b_2 \langle \varsigma_2^2 \rangle + 2(1 - z_1^0) \langle x_1 y_1 \rangle + b_1 (z_1^0)^2 - \frac{1}{r_1} \langle x_1^2 \rangle + 2 \frac{a}{4} (1 - z_2^0) \langle x_2 y_2 \rangle + \frac{a}{4} b_2 (z_2^0)^2 - \frac{a}{4} \frac{1}{r_2} \langle x_2^2 \rangle - \frac{1}{r_3} \langle x_3^2 \rangle - \frac{1}{r_4} \langle x_4^2 \rangle. \quad (2.79)$$

Now introduce “balance parameter” α and add zero in the form $\alpha \times (2.79)$ to the right hand side of

$$\langle x_1 y_1 \rangle + \frac{a}{4} \langle x_2 y_2 \rangle = \frac{1}{r_1} \langle x_1^2 \rangle + \frac{a}{4} \frac{1}{r_2} \langle x_2^2 \rangle + \frac{1}{r_3} \langle w_1^2 \rangle + \frac{1}{r_4} \langle w_2^2 \rangle \quad (2.80)$$

to see that

$$\begin{aligned} \langle x_1 y_1 \rangle + \frac{a}{4} \langle x_2 y_2 \rangle &= \left\langle \begin{bmatrix} x_1 & y_1 \end{bmatrix} \begin{bmatrix} \frac{1}{r_1}(1-\alpha) & \alpha(1-z_1^0) \\ \alpha(1-z_1^0) & -\alpha \end{bmatrix} \begin{bmatrix} x_1 \\ y_1 \end{bmatrix} \right\rangle + b_1 \alpha (z_1^0)^2 \\ &+ \frac{a}{4} \left\langle \begin{bmatrix} x_2 & y_2 \end{bmatrix} \begin{bmatrix} \frac{1}{r_2}(1-\alpha) & \alpha(1-z_2^0) \\ \alpha(1-z_2^0) & -\alpha \end{bmatrix} \begin{bmatrix} x_2 \\ y_2 \end{bmatrix} \right\rangle + \frac{a}{4} b_2 \alpha (z_2^0)^2 \\ &- \alpha b_1 \langle \varsigma_1^2 \rangle - \alpha \frac{a}{4} b_2 \langle \varsigma_2^2 \rangle + \left(\frac{1-\alpha}{r_3} \right) \langle w_1^2 \rangle + \left(\frac{1-\alpha}{r_4} \right) \langle w_2^2 \rangle. \end{aligned} \quad (2.81)$$

The essence of the background method is the observation that *if* we can choose $\alpha \in [1, \infty)$ and z_1^0 and z_2^0 so that the matrices in (2.81) are negative semi-definite, then we have produced an upper bound on $\frac{2}{1+k^2}(\text{Nu} - 1)$ of the form

$$\langle x_1 y_1 \rangle + \frac{a}{4} \langle x_2 y_2 \rangle \leq b_1 \alpha (z_1^0)^2 + \frac{a}{4} b_2 \alpha (z_2^0)^2. \quad (2.82)$$

For example choosing $z_1^0 = 0 = z_2^0$, it is easy to check that both matrices are negative semi-definite when $r_1 \leq (\alpha - 1)/\alpha$. Thus $\text{Nu} = 1$ is the upper bound for $\text{Ra} \leq (\alpha - 1)(1 + k^2)^3/\alpha k^2$ for any $\alpha \in [1, \infty)$. Taking the limit $\alpha \rightarrow \infty$, this shows that the $\text{Nu} = 1$ conduction state is absolutely stable for all $\text{Ra} < \text{Ra}_c(k^2) \equiv (1 + k^2)^3/k^2$.

To deduce bounds for higher Rayleigh numbers ($r_1 > 1$), let $\alpha = \frac{z_1^0 + z_2^0}{(z_1^0)^2 + (z_2^0)^2}$; we will soon choose $z_1^0 \in (0, 1)$ and $z_2^0 \in [0, 1)$ so that $\alpha \in (1, \infty)$. Introduce

$$\rho_1 = \frac{(1 + k^2)^3}{k^2} \quad \text{and} \quad \rho_2 = \frac{(4 + k^2)^3}{k^2} \quad (2.83)$$

so that $r_i = \text{Ra}/\rho_i$ for $i = 1, 2$ and let the background variables be

$$z_1^0 = \left(1 - \frac{\rho_1}{\text{Ra}}\right) \quad \text{and} \quad z_2^0 = 0. \quad (2.84)$$

Then the matrices in (2.81) are both negative semi-definite for $\rho_1 < \text{Ra} \leq \sqrt{\rho_1 \rho_2}$.

For $\text{Ra} > \sqrt{\rho_1 \rho_2}$ choose

$$z_1^0 = \sqrt{\rho_1} \frac{-\rho_1 + 2\text{Ra} \sqrt{\frac{\rho_2}{\rho_1}} - \rho_2 + \sqrt{(\rho_1 + \rho_2)^2 + 4\text{Ra}(\text{Ra} - 2\sqrt{\rho_1 \rho_2})}}{2\text{Ra}(\sqrt{\rho_1} + \sqrt{\rho_2})}, \quad (2.85)$$

$$z_2^0 = \sqrt{\frac{\rho_2}{\rho_1}} (z_1^0 - 1) + 1. \quad (2.86)$$

In Appendix C.3 we show how to derive this background, $z_1^0, z_2^0 \in (0, 1)$, and the matrices are negative semi-definite when $\text{Ra} > \sqrt{\rho_1 \rho_2}$. Combining the results, the upper bounds are

$$\text{Nu} \leq \begin{cases} 1 & \text{for } \text{Ra} \in [0, \rho_1) \\ 1 + 2 \left(1 - \frac{\rho_1}{\text{Ra}}\right) & \text{for } \text{Ra} \in [\rho_1, \sqrt{\rho_1 \rho_2}) \\ 1 + 2 \left(1 - \frac{\rho_1}{\text{Ra}}\right) + \frac{\rho_1 - \rho_2 + \sqrt{(\rho_2 - \rho_1)^2 + 4(\text{Ra} - \sqrt{\rho_1 \rho_2})^2}}{\text{Ra}} & \text{for } \text{Ra} \in [\sqrt{\rho_1 \rho_2}, \infty). \end{cases} \quad (2.87)$$

Figure 2.4 is a plot of the bound, the steady state solutions, and results of some direct numerical simulations (dns) of the Double Lorenz Equations with aspect ratio $A = 2\sqrt{2}$ and Prandtl number $\sigma = 10$. For additional information the best known numerically com-

puted upper bound (the black dashed line) for the PDE is included in the figure as well [2]. The dns data is generated using a finite time sample of a signal that is integrated for a long enough time interval to eliminate transients. It is computed using three different definitions of the Nusselt number (which are equivalent in the long time average) and are within one percent of one another for the finite time samples of the figure. Indeed, the Nusselt number has all of the following representations,

$$\text{Nu} = 1 + \frac{1 + k^2}{2} \langle x_1 y_1 + \frac{a}{4} x_2 y_2 \rangle, \quad (2.88)$$

$$\text{Nu} = 1 + \text{Pe}^2 / \text{Ra} = 1 + \left(\frac{1}{r_1} \langle x_1^2 \rangle + \frac{a}{4} \frac{1}{r_2} \langle x_2^2 \rangle + \frac{1}{r_3} \langle w_1^2 \rangle + \frac{1}{r_4} \langle w_2^2 \rangle \right) \frac{1 + k^2}{2}, \quad (2.89)$$

$$\text{Nu} = 1 + 2 \langle z_1 + z_2 \rangle. \quad (2.90)$$

The absolute upper bound is sharp—saturated by the nontrivial steady state—until $\text{Ra} = 81\sqrt{3}/4 \approx 35$ (i.e., $\sqrt{\rho_1 \rho_2}$ for this aspect ratio) but not apparently so at higher Rayleigh numbers. The steady states appear to be stable until around $\text{Ra} \approx 140$ at which point the solutions become time-dependent. The second drop in the numerically computed Nusselt number at around $\text{Ra} \approx 290$ comes from a transition to seemingly periodic solutions. For this truncated system the Nusselt number bound asymptotes to $\text{Nu} = 5$ as can be seen from (2.87) by taking the limit $\text{Ra} \rightarrow \infty$.

As will be shown in the next section, the upper bound cannot be lowered by including more information from the equations of motion for the temperature variables. This does not preclude the possibility of lowering the bound by incorporating additional constraints via the velocity equations x_1, x_2, w_1 and w_2 . In the background method the only place the velocity variables came into the background analysis is via the $\text{Pe}^2 = \text{Ra} (\text{Nu} - 1)$ relation.

2.2.2 Optimal Control Analysis

We now provide a complementary analysis to bound heat transport in the Double Lorenz system. Instead of subjecting the velocity variables x_i, w_i to a momentum equation, we fix the total intensity of all the variables, the Péclet number (2.75), and attempt to deduce the optimal stirring strategy. Said differently, we treat the velocity field variables x_i and w_i for $i = 1, 2$ as control variables subject to the finite Péclet number condition. A global upper bound to this optimal control problem is an upper bound to heat transport in the Double Lorenz equations with Ra defined by (2.63). This formulation has the additional benefit of explicitly producing flows for which the upper bound is achieved, something that is lacking in the background method.

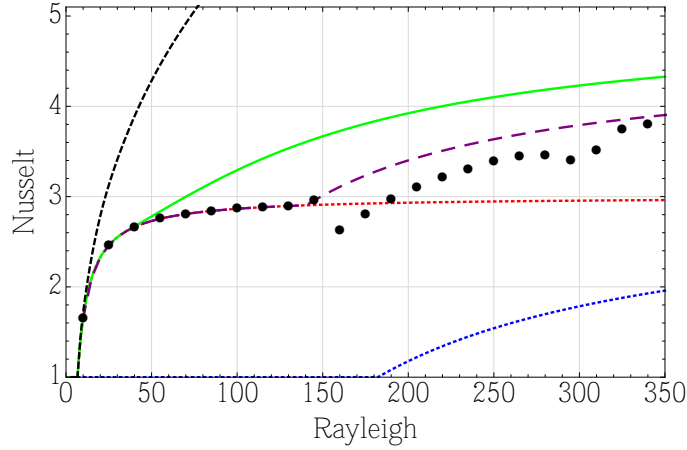


Figure 2.4: The top (black) dashed line is the best known upper bound for the full Rayleigh-Bénard problem from [2]. The solid (green) curve is the background method upper bound on all solutions of the Double Lorenz Equations as well as the transport value for the global optima of the optimal control solution, see §2.2.2. Rayleigh-Nusselt relations for several steady states are also shown. The dotted (red) curve asymptoting to $\text{Nu} = 3$ is the steady solution of the first Lorenz system, and the lower dotted (blue) curve is the steady state of the second Lorenz system. The long-dashed (purple) curve is the steady state for the coupled system for $\sigma = 10$. The discrete dots are results from time averages of direct numerical simulations of the Double Lorenz Equations for $\sigma = 10$.

The optimal control problem is to maximize $\langle x_1 y_1 + \frac{a}{4} x_2 y_2 \rangle \equiv \frac{2}{1+k^2} (\text{Nu} - 1)$ subject to

$$\dot{y}_1 = -y_1 + x_1 - x_1 z_1 + \frac{1}{2}(w_1 - w_2)y_2 \quad (2.91)$$

$$\dot{z}_1 = -b_1 z_1 + x_1 y_1 \quad (2.92)$$

$$\dot{y}_2 = -a y_2 + a x_2 - a x_2 z_2 - 2(w_1 - w_2)y_1 \quad (2.93)$$

$$\dot{z}_2 = -b_2 a z_2 + a x_2 y_2 \quad (2.94)$$

$$\text{Pe}^2 = \left\langle 2 \frac{\rho_1}{b_1} x_1^2 + 2 \frac{\rho_2}{b_2} x_2^2 + \frac{\rho_1 b_1}{2} (w_1^2 + 9w_2^2) \right\rangle, \quad (2.95)$$

where the expression for Péclet has been rewritten using the definitions of ρ_1, ρ_2, b_1 , and b_2 in preparation for subsequent calculations (see Appendix C.1 for the definitions of the

constants). Equivalently, the functional to be extremized is

$$\begin{aligned}
\mathcal{F} = & \left\langle \left(x_1 y_1 + \frac{a}{4} x_2 y_2 \right) + v_1 \left(-y_1 + x_1 - x_1 z_1 + \frac{1}{2} (w_1 - w_2) y_2 - \dot{y}_1 \right) \right. \\
& - \zeta_1 (-b_1 z_1 + x_1 y_1 - \dot{z}_1) \\
& + \frac{1}{4} v_2 (-a y_2 + a x_2 - a x_2 z_2 - 2(w_1 - w_2) y_1 - \dot{y}_2) \\
& - \frac{1}{4} \zeta_2 (-b_2 a z_2 + a x_2 y_2 - \dot{z}_2) \\
& \left. + \frac{\mu}{2} \left(\text{Pe}^2 - \left[2 \frac{\rho_1}{b_1} x_1^2 + 2 \frac{\rho_2}{b_2} x_2^2 + \frac{\rho_1 b_1}{2} (w_1^2 + 9w_2^2) \right] \right) \right\rangle \quad (2.96)
\end{aligned}$$

where the Lagrange multipliers (a.k.a. adjoint variables) $v_i(t)$ and $\zeta_i(t)$ for $i = 1, 2$ enforce the temperature equations and μ enforces the finite Peclet number condition. The Euler-Lagrange equations for the extreme values are the temperature and adjoint variable differential equations

$$\dot{y}_1 = -y_1 + x_1 - x_1 z_1 + \frac{1}{2} (w_1 - w_2) y_2 \quad (2.97)$$

$$\dot{z}_1 = -b_1 z_1 + x_1 y_1 \quad (2.98)$$

$$\dot{v}_1 = v_1 - x_1 + x_1 \zeta_1 + \frac{1}{2} (w_1 - w_2) v_2 \quad (2.99)$$

$$\dot{\zeta}_1 = b_1 \zeta_1 - x_1 v_1 \quad (2.100)$$

$$\dot{y}_2 = -a y_2 + a x_2 - a x_2 z_2 - 2(w_1 - w_2) y_1 \quad (2.101)$$

$$\dot{z}_2 = -b_2 a z_2 + a x_2 y_2 \quad (2.102)$$

$$\dot{v}_2 = a v_2 - a x_2 + a x_2 \zeta_2 - 2(w_1 - w_2) v_1 \quad (2.103)$$

$$\dot{\zeta}_2 = b_2 \zeta_2 - x_2 v_2 \quad (2.104)$$

and the optimal stirring conditions

$$x_1 = \frac{1}{2\mu} \frac{b_1}{\rho_1} (v_1(1 - z_1) + y_1(1 - \zeta_1)) \quad (2.105)$$

$$x_2 = \frac{1}{2\mu} \frac{b_1}{\rho_2} (v_2(1 - z_2) + y_2(1 - \zeta_2)) \quad (2.106)$$

$$w_1 = \frac{1}{\mu} \frac{1}{\rho_1 b_1} (v_1 y_2 - v_2 y_1) \quad (2.107)$$

$$w_2 = -\frac{9}{\mu} \frac{1}{\rho_1 b_1} (v_1 y_2 - v_2 y_1) \quad (2.108)$$

$$\text{Pe}^2 = \left\langle 2 \frac{\rho_1}{b_1} x_1^2 + 2 \frac{\rho_2}{b_2} x_2^2 + \frac{\rho_1 b_1}{2} (w_1^2 + 9w_2^2) \right\rangle. \quad (2.109)$$

The identity $\frac{a}{4}b_2 = b_1$ was used in deriving the expression for x_2 , a helpful simplification for later calculations. We refer to this entire system as the Optimal Double Lorenz equations, and in the following analysis we prove that the global optimum upper bound on the Nusselt number is realized by a steady solution.

Some of the steady solutions to the Optimal Double Lorenz equations for $\sqrt{\frac{1}{\mu} \frac{b_1}{\rho_2}} - 1 \geq 0$ are

$$y_i = v_i = b_i \frac{x_i}{b_i + (x_i)^2} \quad (2.110)$$

$$z_i = \zeta_i = \frac{(x_i)^2}{b_i + (x_i)^2} \quad (2.111)$$

$$(x_i)^2 = b_i \left(\sqrt{\frac{b_1}{\rho_i \mu}} - 1 \right) \quad (2.112)$$

$$w_i = 0 \quad (2.113)$$

$$\text{Pe}^2 = 2\sqrt{\frac{b_1}{\mu}} (\sqrt{\rho_1} + \sqrt{\rho_2}) - 2\rho_1 - 2\rho_2 \quad (2.114)$$

for $i = 1, 2$. If $\sqrt{\frac{1}{\mu} \frac{b_1}{\rho_2}} - 1 \leq 0$ and $\sqrt{\frac{1}{\mu} \frac{b_1}{\rho_1}} - 1 \geq 0$ then $0 = x_2 = y_2 = z_2 = \zeta_2 = v_2$, equations (2.110) through (2.113) remain the same for $i = 1$, and $\text{Pe}^2 = 2 \left(\sqrt{\frac{\rho_1 b_1}{\mu}} - \rho_1 \right)$. Lastly, if $\sqrt{\frac{1}{\mu} \frac{b_1}{\rho_1}} - 1 \leq 0$ then the only solution to the equations is zero. Eliminating μ in favor of Pe , reveals two exceptional Péclet regimes $0 \leq \text{Pe}^2 \leq 2(\sqrt{\rho_1 \rho_2} - \rho_1)$ and $\text{Pe}^2 > 2(\sqrt{\rho_1 \rho_2} - \rho_1)$. Of particular interest are the steady state solutions for z_1 and z_2 rewritten in terms of Péclet in the different regimes,

$$z_1 = \begin{cases} \frac{\text{Pe}^2}{\text{Pe}^2 + 2\rho_1} & \text{for } \text{Pe}^2 \in [0, 2(\sqrt{\rho_1 \rho_2} - \rho_1)] \\ \frac{\text{Pe}^2 + 2(\rho_2 - \sqrt{\rho_1 \rho_2})}{\text{Pe}^2 + 2(\rho_1 + \rho_2)} & \text{for } \text{Pe}^2 \in [2(\sqrt{\rho_1 \rho_2} - \rho_1), \infty), \end{cases} \quad (2.115)$$

$$z_2 = \begin{cases} 0 & \text{for } \text{Pe}^2 \in [0, 2(\sqrt{\rho_1 \rho_2} - \rho_1)] \\ \frac{\text{Pe}^2 + 2(\rho_1 - \sqrt{\rho_1 \rho_2})}{\text{Pe}^2 + 2(\rho_1 + \rho_2)} & \text{for } \text{Pe}^2 \in [2(\sqrt{\rho_1 \rho_2} - \rho_1), \infty). \end{cases} \quad (2.116)$$

Note that $\text{Nu} = 1 + 2(z_1 + z_2)$ so the corresponding transport values are

$$\text{Nu} = \begin{cases} 1 + 2\frac{\text{Pe}^2}{\text{Pe}^2 + 2\rho_1} & \text{for } \text{Pe}^2 \in [0, 2(\sqrt{\rho_1 \rho_2} - \rho_1)] \\ 1 + 4\frac{\text{Pe}^2 + (\sqrt{\rho_2} - \sqrt{\rho_1})^2}{\text{Pe}^2 + 2(\rho_1 + \rho_2)} & \text{for } \text{Pe}^2 \in [2(\sqrt{\rho_1 \rho_2} - \rho_1), \infty). \end{cases} \quad (2.117)$$

Using (2.63) to re-express (2.117) in terms of Ra we recover (2.87). That is, these steady

states correspond precisely to the background bound.

We now show that the Nusselt number for any solution of the Optimal Double Lorenz equations is bounded from above by particular steady solutions. To do so we employ the background method yet again. The equations of motion for the momentum variables (x_i, w_i) for $i = 1, 2$ are no longer available, but we still have the evolution equations for the temperature variables y_i and z_i (for $i = 1, 2$) to work with, and the same background-type decomposition $z_i = \varsigma_i + z_i^0$ can be used.

Only the temperature equations were used to derive (2.77), so it still holds for the Optimal Double Lorenz system. Adding $\langle x_1 y_1 \rangle + \frac{a}{4} \langle x_2 y_2 \rangle$ to both sides of (2.77), and then adding zero in the form

$$0 = \alpha^2 \left(1 - \frac{\langle 2\frac{\rho_1}{b_1} x_1^2 + 2\frac{\rho_2}{b_2} x_2^2 + \frac{\rho_1 b_1}{2} (w_1^2 + 9w_2^2) \rangle}{\text{Pe}^2} \right) \quad (2.118)$$

(where $\alpha^2 \geq 0$) to the right hand side of (2.77), it is evident that

$$\begin{aligned} \langle x_1 y_1 \rangle + \frac{a}{4} \langle x_2 y_2 \rangle &= \alpha^2 + b_1 (z_1^0)^2 - \left\langle \begin{bmatrix} x_1 & y_1 \end{bmatrix} \begin{bmatrix} \frac{2\rho_1}{b_1 \text{Pe}^2} \alpha^2 & z_1^0 - 1 \\ z_1^0 - 1 & 1 \end{bmatrix} \begin{bmatrix} x_1 \\ y_1 \end{bmatrix} \right\rangle \\ &\quad - b_1 \langle \varsigma_1^2 \rangle - \frac{\alpha^2 \rho_1 b_1}{\text{Pe}^2} \frac{1}{2} \langle w_1^2 \rangle + \frac{a}{4} b_2 (z_2^0)^2 \\ &\quad - \frac{a}{4} \left\langle \begin{bmatrix} x_2 & y_2 \end{bmatrix} \begin{bmatrix} \frac{2\rho_2}{b_1 \text{Pe}^2} \alpha^2 & z_2^0 - 1 \\ z_2^0 - 1 & 1 \end{bmatrix} \begin{bmatrix} x_2 \\ y_2 \end{bmatrix} \right\rangle \\ &\quad - \frac{a}{4} b_2 \langle \varsigma_2^2 \rangle - \frac{\alpha^2 9\rho_1 b_1}{\text{Pe}^2} \frac{1}{2} \langle w_2^2 \rangle. \end{aligned} \quad (2.119)$$

The relation $\frac{a}{4} b_2 = b_1$ was used to rewrite the top left corner of the second matrix.

We must now choose the background and constant α^2 . Let

$$\alpha^2 = b_1 (z_1^0 (1 - z_1^0) + z_2^0 (1 - z_2^0)). \quad (2.120)$$

For the $\text{Pe}^2 \leq 2(\sqrt{\rho_1 \rho_2} - \rho_1)$ regime pick the steady states

$$z_1^0 = \frac{\text{Pe}^2}{\text{Pe}^2 + 2\rho_1} \quad \text{and} \quad z_2^0 = 0 \quad (2.121)$$

and confirm that the second matrix in (2.119) is positive definite. Also, the relation

$$\frac{2\rho_1}{b_1} \frac{\alpha^2}{\text{Pe}^2} = (1 - z_1^0)^2 \quad (2.122)$$

holds allowing us to rewrite (2.119) in the $\text{Pe}^2 \leq 2(\sqrt{\rho_1\rho_2} - \rho_1)$ regime as

$$\begin{aligned} \langle x_1 y_1 \rangle + \frac{a}{4} \langle x_2 y_2 \rangle &= b_1 \frac{\text{Pe}^2}{\text{Pe}^2 + 2\rho_1} - \langle (x_1(z_1^0 - 1) + y_1)^2 \rangle - b_1 \langle \zeta_1^2 \rangle \\ &\quad - \frac{a}{4} \langle (x_2 - y_2)^2 \rangle - \frac{a}{4} \left(\frac{4\rho_1\rho_2}{(\text{Pe}^2 + 2\rho_1)^2} - 1 \right) \langle x_2^2 \rangle - \frac{a}{4} b_2 \langle \zeta_2^2 \rangle \\ &\quad - \frac{\alpha^2}{\text{Pe}^2} \frac{\rho_1 b_1}{2} (\langle w_1^2 \rangle + 9\langle w_2^2 \rangle). \end{aligned} \quad (2.123)$$

This expression implies that $b_1 \frac{\text{Pe}^2}{\text{Pe}^2 + 2\rho_1}$ is an upper bound since all the subsequent terms are negative. An examination of (2.117) reveals a correspondence to a steady state Nusselt number.

For the $\text{Pe}^2 > 2(\sqrt{\rho_1\rho_2} - \rho_1)$ regime we again pick steady state solutions for z_i for the backgrounds, namely,

$$z_1^0 = \frac{\text{Pe}^2 + 2(\rho_2 - \sqrt{\rho_1\rho_2})}{\text{Pe}^2 + 2(\rho_1 + \rho_2)} \quad \text{and} \quad z_2^0 = \frac{\text{Pe}^2 + 2(\rho_1 - \sqrt{\rho_1\rho_2})}{\text{Pe}^2 + 2(\rho_1 + \rho_2)}. \quad (2.124)$$

Observe that

$$1 - z_1^0 = 2 \frac{\rho_1 + \sqrt{\rho_1\rho_2}}{\text{Pe}^2 + 2(\rho_1 + \rho_2)} = 2\sqrt{\rho_1} \frac{\sqrt{\rho_1} + \sqrt{\rho_2}}{\text{Pe}^2 + 2(\rho_1 + \rho_2)}, \quad (2.125)$$

$$1 - z_2^0 = 2 \frac{\rho_2 + \sqrt{\rho_1\rho_2}}{\text{Pe}^2 + 2(\rho_1 + \rho_2)} = 2\sqrt{\rho_2} \frac{\sqrt{\rho_1} + \sqrt{\rho_2}}{\text{Pe}^2 + 2(\rho_1 + \rho_2)}, \quad (2.126)$$

$$\alpha^2 = b_1 2 \frac{\text{Pe}^2 (\sqrt{\rho_1} + \sqrt{\rho_2})^2}{(\text{Pe}^2 + 2(\rho_1 + \rho_2))^2}, \quad (2.127)$$

hence the top left corners of the matrices in (2.119) are simplified to

$$\frac{2\rho_1}{b_1} \frac{\alpha^2}{\text{Pe}^2} = 4\rho_1 \frac{(\sqrt{\rho_1} + \sqrt{\rho_2})^2}{(\text{Pe}^2 + 2(\rho_1 + \rho_2))^2} = (1 - z_1^0)^2, \quad (2.128)$$

$$\frac{2\rho_2}{b_1} \frac{\alpha^2}{\text{Pe}^2} = 4\rho_2 \frac{(\sqrt{\rho_1} + \sqrt{\rho_2})^2}{(\text{Pe}^2 + 2(\rho_1 + \rho_2))^2} = (1 - z_2^0)^2. \quad (2.129)$$

With these facts in place rewrite (2.119) as

$$\begin{aligned} \langle x_1 y_1 \rangle + \frac{a}{4} \langle x_2 y_2 \rangle &= 2b_1 \frac{\text{Pe}^2 + (\sqrt{\rho_2} - \sqrt{\rho_1})^2}{\text{Pe}^2 + 2(\rho_1 + \rho_2)} - \langle (x_1(z_1^0 - 1) + y_1)^2 \rangle - b_1 \langle \zeta_1^2 \rangle \\ &\quad - \frac{a}{4} \langle (x_2(z_2^0 - 1) + y_2)^2 \rangle - \frac{a}{4} b_2 \langle \zeta_2^2 \rangle - \frac{\alpha^2}{\text{Pe}^2} \frac{\rho_1 b_1}{2} (\langle w_1^2 \rangle + 9\langle w_2^2 \rangle). \end{aligned} \quad (2.130)$$

All the terms following $2b_1 \frac{\text{Pe}^2 + (\sqrt{\rho_2} - \sqrt{\rho_1})^2}{\text{Pe}^2 + 2(\rho_1 + \rho_2)}$ are negative and again we have a correspondence to a steady state Nusselt number in (2.117). This establishes that the absolute maximum value is realized by the optimal steady state stirring, i.e., for any extremum of \mathcal{F} we have

$$\text{Nu} \leq \begin{cases} 1 + 2 \frac{\text{Pe}^2}{\text{Pe}^2 + 2\rho_1} & \text{for } \text{Pe}^2 \in [0, 2(\sqrt{\rho_1\rho_2} - \rho_1)], \\ 1 + 4 \frac{\text{Pe}^2 + (\sqrt{\rho_2} - \sqrt{\rho_1})^2}{\text{Pe}^2 + 2(\rho_1 + \rho_2)} & \text{for } \text{Pe}^2 \in [2(\sqrt{\rho_1\rho_2} - \rho_1), \infty). \end{cases} \quad (2.131)$$

The inability of both the background method and the optimal control problem to produce demonstrably sharp upper bounds with respect to the Double Lorenz equations past $\text{Ra} = \sqrt{\rho_1\rho_2}$ deserves some comment. It is possible that unstable time-dependent solutions to the Double Lorenz system saturate the upper bound, but we do not expect this to be the case. In the double Lorenz model the only way to activate both Lorenz modes at the same time ((x_i, y_i, z_i) for $i = 1, 2$) and hence have enhanced heat transport is to also have non-zero shear modes (w_i for $i = 1, 2$). That is to say if $w_1 = 0$ or $w_2 = 0$ then the equations of motion imply that either the first Lorenz mode is zero or the second. These shear modes do not contribute to heat transport and thus, as far as the optimal control problem or the background method are concerned, are ineffectual. The optimal control problem may choose to ignore these modes and achieve the same Nusselt number at a reduced Péclet cost. It seems that the only ways to lower the bound is to either incorporate a shear mode constraint (or an advective constraint) into the optimal control formulation or perhaps a more judicious combination of moments from the equations of motion in the background method. The advective term of the velocity equations in the PDE is notoriously difficult to deal with and the goal of the optimal control formulation is precisely to bypass this barrier. Thus for the optimal control problem considered here incorporating additional constraints on the velocity variables breaks correspondence to the original PDE optimal control problem.

2.2.3 Comparison of Steady State to Periodic Solutions

Equations (2.123) and (2.130) show that the only periodic solutions that saturate the upper bound are the steady. Indeed, in the $\text{Pe}^2 \leq 2(\sqrt{\rho_1\rho_2} - \rho_1)$ regime if equality holds in (2.131) then it must be the case that $w_i = \zeta_i = 0$ for $i = 1, 2$, $x_1(1 - z_1) = y_1$, $x_2 = y_2$. This means that z_i is constant; it is equal to the background. Using the y_i equations and the relations $x_1(1 - z_1) = y_1$ and $x_2 = y_2$, we can conclude that $\dot{y}_i = 0$ and that $x_2 = y_2 = z_2 = 0$. Similar reasoning leads to the same conclusion about the optimizer for $\text{Pe}^2 \geq 2(\sqrt{\rho_1\rho_2} - \rho_1)$.

It is interesting to examine why the periodic solutions do worse than the steady state. We have computed time-dependent periodic solutions to the Optimal Double Lorenz sys-

tem using standard methods: a Fourier Galerkin truncation, Newton-Kantorovich iteration, and numerical continuation, the same method that was used for the Lorenz problem. In Figure 2.5 we show the solutions for $x_1(t)$ for several different Péclet number. As the Péclet number is increased the solutions begin to develop sharp transition regions from positive/negative steady states. That is, it appears that the controls “want” to remain steady, but are unable to do so due to the branch that they were numerically continued from.

This is exactly analogous to what happens in the optimal control version of the Lorenz system §2.1, where the transition between steady states control values is even simpler, absent some of the “ringing” that is seen in Figure 2.5. The forced transitions in the time-dependent, albeit locally optimal, control have a cost in terms of the transport: it is definitely below the transport that is achieved by steady flow variables. This is seen in Figure 2.6 where the green curve (corresponding to optimal steady solutions) are above the dashed curve (corresponding to time-dependent periodic solutions). In addition to the optimal steady and locally optimal periodic solutions, Figure 2.6 includes some steady states of the Double Lorenz equations at a selection of Prandtl numbers. We see that the optimal steady solutions are sharp upper bounds until a transition occurs to the “second set” of optimal solutions. It is interesting to see that the time-periodic optimal solution is closer to the steady solutions and direct numerical simulations of the Double Lorenz equations. Whether or not time-dependent periodic optimal solutions correspond to an upper bound of time-dependent dynamical quantities is not known, hence this observation may just be a coincidence.

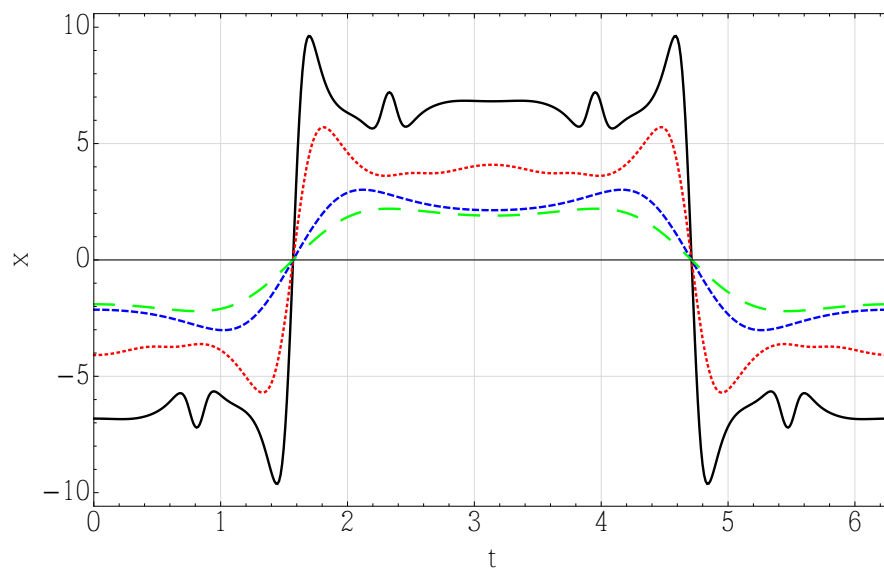


Figure 2.5: Time dependence of optimal 2π (time) periodic stirring protocols for several value of the Péclet number and $k = 1/\sqrt{2}$. Here we show $x_1(t)$. Long dashed (green) line: $Pe=4.2$; short dashed (blue) line: $Pe = 5.4$; dotted (red) line $Pe = 14.1$; and solid (black) curve: $Pe = 35.1$

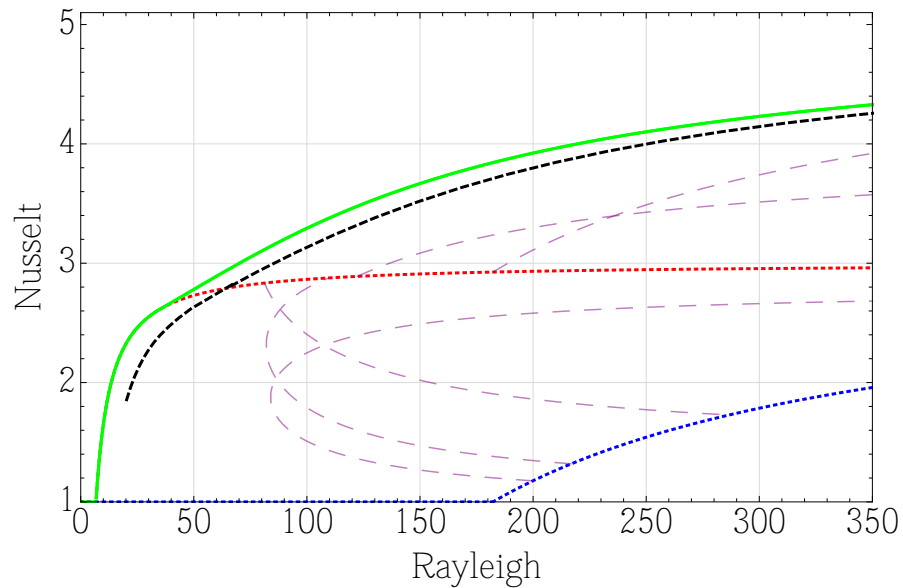


Figure 2.6: The top (green) curve is the upper bound on the Nusselt number. Rayleigh-Nusselt relations for several steady states of the Double Lorenz equations are also shown. The long-dashed (purple) purple lines are the coupled steady state solutions for several Prandtl numbers, $\sigma = 0.44$ (bottom), 0.70, 1.42, 5.75 and 10^4 (top), and wavenumber is $k = 1/\sqrt{2}$. The upper dotted (red) curve is the first Lorenz system steady state while the lower dotted (blue) curve is that for the second Lorenz system. The dashed (black) line is the transport for a time-periodic solution to the optimal Double Lorenz system.

CHAPTER 3

The Advection-Diffusion Equation

3.1 Introduction

In this chapter we will discuss the well-posedness of the steady state maximization problem

$$\text{Maximize } \langle wT \rangle \quad (3.1)$$

subject to

$$\vec{u} \cdot \nabla T = \Delta T \quad (3.2)$$

$$\langle \nabla \vec{u} : \nabla \vec{u} \rangle \leq \text{Pe}^2 \quad (3.3)$$

$$\nabla \cdot \vec{u} = 0 \quad (3.4)$$

with relevant boundary/integral conditions in a bounded domain with a well-behaved boundary as well as properties of the first-order optimality conditions. Here we have decomposed the vector \vec{u} into three components $\vec{u} = (u, v, w) = (u_1, u_2, u_3)$ and w is the velocity in the vertical direction whereas (u, v) are the components in the horizontal direction. The notation $\langle \cdot \rangle$ denotes an average over the domain Ω (we restrict attention to steady flows) and $\nabla \vec{u} : \nabla \vec{u} = \partial_j u_k \partial_j u_k = |\nabla \vec{u}|^2$.

To verify that this optimization problem is well-posed we first review well-known theorems and then apply it to the optimization problem. We show that the steady optimization problem admits a maximizer and obtain an upper bound by using the background method in §3.4. After demonstrating that the functional $\langle wT \rangle$ is differentiable we utilize the Euler-Lagrange equations (first-order optimality conditions) to find conditions for the “best” domain size as well as the optimal boundary conditions for the horizontal velocity fields. We also deduce that the maximizer must occur when $\langle \nabla \vec{u} : \nabla \vec{u} \rangle = \text{Pe}^2$ in §3.5.

In §3.6 we look at additional properties of the Euler-Lagrange equations, formulate a related optimal control problem, and examine a particular incompressible flow field that achieves a scaling $\text{Nu} \lesssim \text{Pe}^{1/2}$. In light of the discussion in this section we see that we must

both enforce incompressibility and the advection-diffusion equation in order to understand the true scaling.

3.2 Relevant Theorems and Setting Notation

Let us set notation:

- Let $\alpha = (\alpha_1, \alpha_2, \dots, \alpha_n)$ where $\alpha_i \in \mathbb{N} \cup \{0\}$ for $i = 1, \dots, n$ which we will call a multi-index. We use $|\alpha| = \sum_{i=1}^n \alpha_i$ and $\sum_{|\alpha|=\beta}$ denotes the sum over all multi-indices α such that the sum adds up to β . The notation D^α is shorthand for $\frac{\partial^{|\alpha|}}{\partial x_{\alpha_1} \dots \partial x_{\alpha_n}} f$ where the partial derivatives are interpreted in the weak sense. For example, for $n = 2$ we have that $\sum_{|\alpha|=1} D^\alpha f = \frac{\partial f}{\partial x_1} + \frac{\partial f}{\partial x_2}$.
- $L^p(\Omega)$ the space of Lebesgue measurable functions f such that $\int_\Omega |f|^p < \infty$. We will usually drop the specification of the domain (Ω) and write L^p and $\|f\|_p \equiv (\int_\Omega |f|^p)^{1/p}$.
- $W^{1,p}(\Omega)$ Sobolev space, the space of Lebesgue measurable functions $f \in L^p$ such that $D^\alpha f \in L^p$ for each α such that $|\alpha| = 1$. We will usually drop the specification of the domain and write $W^{1,p}$. Furthermore we use the notation $\|f\|_{W^{1,p}} = \|f\|_p + \sum_{|\alpha|=1} \|D^\alpha f\|_p$.
- $H^1 = W^{1,2}$. We will also impose conditions on f such that $\|f\|_{H^1}$ and $\sqrt{\sum_{|\alpha|=1} \|D^\alpha f\|_2^2}$ are equivalent norms.
- H^{-1} is the dual of H^1 .
- V the set of vectors \vec{u} such that $\nabla \cdot \vec{u} = 0$ and $\vec{u} \in H^1$.

All the spaces mentioned above are complete. Furthermore we will overload notation when it comes to scalar and vector functions as well as boundary conditions. For example, denote the components of \vec{u} by u_j , we interpret $\vec{u} \in H^1$ to mean $\int_\Omega \partial_i u_j \partial_i u_j < \infty$ and that \vec{u} has boundary conditions (or integral constraints) such that $(\int_\Omega \partial_i u_j \partial_i u_j)^{1/2}$ defines a norm. Recall that equivalent metrics induce the same topology. Standard references for Lebesgue and Sobolev spaces include Folland's analysis text [28] and Evan's PDE text [29]. For spaces relevant to fluid mechanics (those of incompressible flow fields) see [30].

All the inequalities that we use to prove continuity and differentiability of 3.1 are standard, the most important of which are as follows.

Hölder's Inequality. Let Ω be an open subset of \mathbb{R}^n and $p_i \geq 1$ for $i = 1, \dots, n$ be numbers whose reciprocal add up to one,

$$\sum_{i=1}^n \frac{1}{p_i} = 1. \quad (3.5)$$

For all $f_i \in L^{p_i}(\Omega)$ we have that the product is in $L^1(\Omega)$,

$$\left\| \prod_{i=1}^n f_i \right\|_1 \leq \prod_{i=1}^n \|f_i\|_{p_i}. \quad (3.6)$$

L^p Inclusions. Let Ω be a subset of \mathbb{R}^n with finite Lebesgue measure, i.e. $\mu(\Omega) < \infty$; then

$$\|f\|_p \leq \mu(\Omega)^{\frac{q-p}{pq}} \|f\|_q \quad (3.7)$$

$$(3.8)$$

for $p < q$.

Sobolev Embedding Theorem. Let Ω be a bounded open subset of \mathbb{R}^n with Lipschitz boundary. Let $1 \leq p < n$, and $f \in W^{1,p}(\Omega)$, then

$$\|f\|_q \leq C \|f\|_{W^{1,p}} \quad (3.9)$$

where $q = \frac{np}{n-p}$ and C depends on p, n and Ω , but not on the function f .

Although in the functional setting it is not the case that a bounded sequence has a convergent sequence in the strong topology, we do have convergence in the weak topology by the Banach-Alaoglu theorem for Hilbert spaces.

Banach-Alaoglu Theorem. Every bounded sequence in a Hilbert space has a weakly convergent subsequence.

To show that a maximizer exists we make use of the compactness of the $W^{1,p}$ ball in less regular topologies via Rellich's theorem.

Rellich-Kondrachov Theorem. Let Ω be an open bounded subset of \mathbb{R}^n with Lipschitz boundary. Suppose that $1 \leq p < n$. Then $W^{1,p}(\Omega)$ is compactly embedded in $L^q(\Omega)$ where

$$1 \leq q < \frac{np}{n-p}. \quad (3.10)$$

This theorem states that weak convergence of a sequence in $W^{1,p}(\Omega)$ implies strong convergence in $L^q(\Omega)$. Furthermore it says that the $W^{1,p}(\Omega)$ closed ball B , meaning

$$B = \{u \in W^{1,p} : \|u\|_{W^{1,p}} \leq 1\} \quad (3.11)$$

is a compact set in $L^q(\Omega)$. Once we have shown that our functional is continuous with respect to the L^3 topology on \vec{u} , we need to verify that the supremum is actually a maximum. To this end we use the Rellich-Kondrachov theorem to show that the set of functions we are trying to maximize over is compact. Specifically, we use the fact that the $W^{1,p}$ closed ball is compact for $1 \leq q < 6$ in 3-dimensions or less.

The generalizations of these embedding results to vector-valued functions $\vec{u} : \mathbb{R}^n \rightarrow \mathbb{R}^m$ is straightforward. For example, we may take $\|\vec{u}\|_p$ to mean

$$\|\vec{u}\|_p \equiv \left(\int_{\Omega} (\vec{u} \cdot \vec{u})^{p/2} \right)^{1/p}. \quad (3.12)$$

For the most part we can ignore the subtlety of using vector valued functions and proceed to applying estimates as if \vec{u} was just a scalar. For example, by Cauchy-Schwarz we have

$$|\phi \vec{u} \cdot \nabla \theta| \leq |\phi| \sqrt{\vec{u} \cdot \vec{u}} \sqrt{\nabla \theta \cdot \nabla \theta}. \quad (3.13)$$

hence,

$$\|\phi \vec{u} \cdot \nabla \theta\|_1 \leq \|\phi \sqrt{\vec{u} \cdot \vec{u}} \sqrt{\nabla \theta \cdot \nabla \theta}\|_1 \quad (3.14)$$

$$\leq \|\phi\|_6 \|\vec{u}\|_3 \|\nabla \theta\|_2 \quad (3.15)$$

by applying Hölder's inequality to the scalar functions ϕ , $\sqrt{\vec{u} \cdot \vec{u}}$ and $\sqrt{\nabla \theta \cdot \nabla \theta}$. All of the Sobolev embedding results as well as Rellich's theorem still hold as well.

Showing that the functional is differentiable and a maximizer exists would all be a futile effort if solutions to the advection-diffusion equation (3.2) didn't exist. To show that there exist unique solutions we use the famous Lax-Milgram theorem.

Lax-Milgram Theorem. *Let V be a Hilbert Space, $B : V \times V \rightarrow \mathbb{R}$ a bilinear form, and $L : V \rightarrow \mathbb{R}$ a linear form. Suppose that B and L are continuous, i.e., there exist constants $c > 0$ and $d > 0$ such that*

$$|B[u, v]| \leq c \|u\|_V \|v\|_V \quad (3.16)$$

$$|L[u]| \leq d \|u\|_V \quad (3.17)$$

for each $u, v \in V$, where $\|\cdot\|_V$ is the norm for V . Furthermore assume that $B[u, v]$ is coercive,

$$e\|v\|_V\|v\|_V \leq |B[v, v]| \quad (3.18)$$

for a constant $e > 0$ and each $v \in V$; then there is a unique $v \in V$ such that

$$B[u, v] = L[u] \quad (3.19)$$

for each $u \in V$.

3.3 Existence of a Maximizer and Differentiability

To show that the maximization problem is well-posed we will take the following steps:

1. First we will show that we can indeed find a T satisfying the steady advection-diffusion equation for $\vec{u} \in V$. To do so we will work with the weak form of the advection-diffusion equation and appeal to Lax-Milgram theorem (§3.2) to guarantee that solutions exist. In fact, due to the way we formulate the weak form of the advection diffusion equation, we will see that solutions exist as long as $\vec{u} \in L^3$.
2. We will show that the functional $\mathcal{F}[\vec{u}] = \langle w\theta \rangle$, where $\theta = T - (1 - z)$, is continuous with respect to the strong L^3 topology on \vec{u} . For incompressible flow fields with the boundary conditions considered in this thesis we have $\langle w\theta \rangle = \langle wT \rangle$.
3. By the Rellich-Kondrachov theorem (§3.2) we know that in three dimensions the closed H^1 ball is compact in L^p for $1 \leq p < 6$. This is enough to establish that a maximizer exists since we are maximizing a continuous (in L^3) function \mathcal{F} on a compact (in L^3) set $\{\vec{u} : \langle \nabla \vec{u} : \nabla \vec{u} \rangle \leq Pe\}$. Explicitly, our functional is continuous in the L^3 topology and the H^1 ball is compact in the L^3 topology and a continuous function on a compact set attains its maximum. Specifying boundary/integral conditions on \vec{u} become essential in this step.

Furthermore we show that the functional is differentiable with respect to the strong L^3 topology on \vec{u} , hence we can characterize the maximizer by looking at the first-order optimality conditions.

The choice of $\vec{u} \in L^3$ may seem unusual and it is indeed arbitrary. It is the largest class of flow fields that still preserves continuity and differentiability of the functional 3.1. It is

motivated by the desire to have control over a term arising in the weak form of the advection diffusion equation of the form $\|\varphi \vec{u} \cdot \nabla \theta\|_1$ where $\theta, \varphi \in H^1$. By applying Hölder's inequality we see that

$$\|\varphi \vec{u} \cdot \nabla \theta\|_1 \leq \|\varphi\|_{p_1} \|\vec{u}\|_{p_2} \|\nabla \theta\|_{p_3} \quad (3.20)$$

where

$$\frac{1}{p_1} + \frac{1}{p_2} + \frac{1}{p_3} = 1 \quad (3.21)$$

We would like to find the smallest p_2 such that the estimate is guaranteed to be finite in order to have the largest class of vector fields possible. This means that we must find the largest p_1 and p_3 such that the estimates are guaranteed to be finite. In the case of p_3 we can do no better than $p_3 = 2$ given that $\theta \in H^1$. For φ by the Sobolev embeddings in three dimensions $\|\theta\|_6 \leq c \|\nabla \theta\|_2$ for a constant c . Hence the largest value of p_1 that we may use is $p_1 = 6$. Solving for p_2 then yields $p_2 = 3$.

3.3.1 Existence of the Temperature Field

In order to establish the existence and uniqueness of the temperature function $T : \mathbb{R}^3 \rightarrow \mathbb{R}$

$$\vec{u} \cdot \nabla T = \Delta T \quad (3.22)$$

subject to $T(z = 0) = 1$ and $T(z = 1) = 0$ and appropriate¹ boundary conditions in the horizontal (x, y) directions, we will work instead with the function $\theta \equiv T - (1 - z)$ which satisfies homogeneous boundary conditions in the vertical direction and satisfies the equation

$$\vec{u} \cdot \nabla \theta = \Delta \theta + w, \quad (3.23)$$

where we have decomposed the vector \vec{u} into three components $\vec{u} = (u, v, w)$ and w is the velocity in the vertical direction whereas (u, v) are the components in the horizontal direction.

We now motivate the weak form of the equation. Multiplying through by a smooth

¹For example, we can work with periodic boundary conditions or no-flux boundary conditions on the side walls.

function ϕ with compact support and integrating yields the following equation

$$\int_{\Omega} (\phi \vec{u} \cdot \nabla \theta + \nabla \phi \cdot \nabla \theta) = \int_{\Omega} \phi w. \quad (3.24)$$

Integrating by parts on the $\frac{1}{2} \phi \vec{u} \cdot \nabla \theta$ term and using incompressibility yields

$$\int_{\Omega} \left(\frac{1}{2} [\phi \vec{u} \cdot \nabla \theta - \theta \vec{u} \cdot \nabla \phi] + \nabla \phi \cdot \nabla \theta \right) = \int_{\Omega} \phi w. \quad (3.25)$$

We will define this to be the weak form of our equation. This is convenient because the advective term is explicitly anti-symmetric which simplifies many of the proofs later on and guarantees coercivity as required by the Lax-Milgram theorem. Furthermore by taking (3.25) as the definition of the advection diffusion equation, ignoring the original derivation using incompressibility, we may consider a larger class of flows than incompressible ones. The functions θ and ϕ satisfy homogeneous boundary conditions on the $z = 0$ and $z = 1$ plane and, for example, periodic boundary conditions in the horizontal directions. What is essential is that $\|\nabla \theta\|_2$ defines a norm.

The bilinear form associated with the weak form is

$$B[\theta, \phi] = \int_{\Omega} \left(\frac{1}{2} [\phi \vec{u} \cdot \nabla \theta - \theta \vec{u} \cdot \nabla \phi] + \nabla \phi \cdot \nabla \theta \right). \quad (3.26)$$

We will now show that the conditions for the Lax-Milgram theorem are satisfied for the advection-diffusion equation. For a fixed $\vec{u} \in L^3$ this bilinear form is continuous by the following estimates,

$$|B[\theta, \phi]| = \left| \int_{\Omega} \left(\frac{1}{2} [\phi \vec{u} \cdot \nabla \theta - \theta \vec{u} \cdot \nabla \phi] + \nabla \phi \cdot \nabla \theta \right) \right| \quad (3.27)$$

$$\leq \frac{1}{2} (\|\phi \vec{u} \cdot \nabla \theta\|_1 + \|\theta \vec{u} \cdot \nabla \phi\|_1) + \|\nabla \phi \cdot \nabla \theta\|_1 \quad (3.28)$$

$$\leq \frac{1}{2} (\|\phi\|_6 \|\vec{u}\|_3 \|\nabla \theta\|_2 + \|\theta\|_6 \|\vec{u}\|_3 \|\nabla \phi\|_2) + \|\nabla \phi\|_2 \|\nabla \theta\|_2 \quad (3.29)$$

$$\leq c \|\nabla \phi\|_2 \|\vec{u}\|_3 \|\nabla \theta\|_2 + \|\nabla \phi\|_2 \|\nabla \theta\|_2 \quad (3.30)$$

$$\leq (c \|\vec{u}\|_3 + 1) \|\nabla \phi\|_2 \|\nabla \theta\|_2 \quad (3.31)$$

and coercive since

$$B[\theta, \theta] = \int_{\Omega} \left(\frac{1}{2} [\theta \vec{u} \cdot \nabla \theta - \theta \vec{u} \cdot \nabla \theta] + \nabla \theta \cdot \nabla \theta \right) = \int_{\Omega} \nabla \theta \cdot \nabla \theta = \|\nabla \theta\|_2^2. \quad (3.32)$$

The last thing that we need to verify is that the right side defines a continuous linear func-

tional. This is true since

$$\int_{\Omega} \phi w \leq \|\phi\|_2 \|w\|_2 \quad (3.33)$$

$$\leq C \|\nabla \phi\|_2 \|\vec{u}\|_3 \quad (3.34)$$

for a constant C by Sobolev embedding on ϕ and L^p inclusions on \vec{u} . Thus by the Lax-Milgram Theorem (§3.2) the solutions to the steady advection-diffusion equation exist as long as the vector field is in L^3 . Note that we did not use incompressibility of the vector field \vec{u} from 3.25 onwards.

3.3.2 Continuity and Existence of a Maximizer

We think of θ as an implicit function of \vec{u} and thus would like to know if it is continuous with respect to changes in \vec{u} . To this end let $\vec{u}, \vec{v} \in L^3$ be flow fields and denote the difference by $\delta\vec{u} = \vec{v} - \vec{u}$ and consider the equations

$$\int_{\Omega} \left(\frac{1}{2} [\phi \vec{u} \cdot \nabla \theta - \theta \vec{u} \cdot \nabla \phi] + \nabla \phi \cdot \nabla \theta \right) = \int_{\Omega} \phi f \quad (3.35)$$

$$\int_{\Omega} \left(\frac{1}{2} [\phi \vec{v} \cdot \nabla \varphi - \varphi \vec{v} \cdot \nabla \phi] + \nabla \phi \cdot \nabla \varphi \right) = \int_{\Omega} \phi g \quad (3.36)$$

There exists solutions θ and φ for each ϕ as long f, g are in the dual space of θ, ϕ by the Lax-Milgram theorem and the discussion in the previous paragraph. Taking the difference of the two equations yields the following equation for $\delta\theta \equiv \varphi - \theta$,

$$\begin{aligned} & \int_{\Omega} \left(\frac{1}{2} [\phi (\vec{u} + \delta\vec{u}) \cdot \nabla \delta\theta - \delta\theta (\vec{u} + \delta\vec{u}) \cdot \nabla \phi] + \nabla \phi \cdot \nabla \delta\theta \right) \\ &= \\ & \int_{\Omega} \left(\frac{1}{2} [\theta \delta\vec{u} \cdot \nabla \phi - \phi \delta\vec{u} \cdot \nabla \theta] + \phi \delta f \right), \end{aligned} \quad (3.37)$$

where $\delta f = f - g$. Set $\phi = \delta\theta$ to yield the following balance relation

$$\|\nabla \delta\theta\|^2 = \int_{\Omega} \left(\frac{1}{2} [\theta \delta\vec{u} \cdot \nabla \delta\theta - \delta\theta \delta\vec{u} \cdot \nabla \theta] + \delta\theta \delta f \right). \quad (3.38)$$

We may estimate the right hand side to get

$$\|\nabla\delta\theta\|_2^2 = \left| \int_{\Omega} \left(\frac{1}{2} [\theta\delta\vec{u} \cdot \nabla\delta\theta - \delta\theta\delta\vec{u} \cdot \nabla\theta] + \delta\theta\delta f \right) \right| \quad (3.39)$$

$$\leq \int_{\Omega} \left| \frac{1}{2} [\theta\delta\vec{u} \cdot \nabla\delta\theta - \delta\theta\delta\vec{u} \cdot \nabla\theta] + \delta\theta\delta f \right| \quad (3.40)$$

$$\leq \frac{1}{2} \|\theta\|_6 \|\delta\vec{u}\|_3 \|\nabla\delta\theta\|_2 + \frac{1}{2} \|\delta\theta\|_6 \|\delta\vec{u}\|_3 \|\nabla\theta\|_2 + \|\delta f\|_{6/5} \|\delta\theta\|_6 \quad (3.41)$$

$$\leq \frac{1}{2} \|\theta\|_6 \|\delta\vec{u}\|_3 \|\nabla\delta\theta\|_2 + \frac{c}{2} \|\nabla\delta\theta\|_2 \|\delta\vec{u}\|_3 \|\nabla\theta\|_2 + c \|\delta f\|_{6/5} \|\nabla\delta\theta\|_2 \quad (3.42)$$

$$= \left(\frac{1}{2} \|\theta\|_6 \|\delta\vec{u}\|_3 + \frac{c}{2} \|\delta\vec{u}\|_3 \|\nabla\theta\|_2 + c \|\delta f\|_{6/5} \right) \|\nabla\delta\theta\|_2, \quad (3.43)$$

where c is the Sobolev embedding constant such that $\|\theta\|_6 \leq c \|\nabla\theta\|_2$. For our problem (3.25) we have that $\|\delta f\|_{6/5} = \|\delta w\|_{6/5} \leq c' \|\delta\vec{u}\|_3$ for a constant c' . Again $\vec{u} = (u, v, w)$. Hence we have

$$\|\nabla\delta\theta\|_2^2 \leq \left(\frac{1}{2} \|\theta\|_6 \|\delta\vec{u}\|_3 + \frac{c}{2} \|\delta\vec{u}\|_3 \|\nabla\theta\|_2 + cc' \|\delta\vec{u}\|_3 \right) \|\nabla\delta\theta\|_2 \quad (3.44)$$

$$\Leftrightarrow \quad (3.45)$$

$$\|\nabla\delta\theta\|_2 \leq \left(\frac{1}{2} \|\theta\|_6 + \frac{c}{2} \|\nabla\theta\|_2 + c'c \right) \|\delta\vec{u}\|_3 \quad (3.46)$$

$$= d' \|\delta\vec{u}\|_3 \quad (3.47)$$

where $d' \equiv \frac{1}{2} \|\theta\|_6 + \frac{c}{2} \|\nabla\theta\|_2 + c'c$ is a constant that depends on θ (hence \vec{u}) and the Sobolev embeddings.

This is enough to show that the functional $\langle w\theta \rangle$ continuous with respect to the strong L^3 topology on \vec{u} since

$$\left| \int_{\Omega} (w + \delta w) (\theta + \delta\theta) - w\theta \right| = \left| \int_{\Omega} (w\delta\theta + \delta w\theta + \delta w\delta\theta) \right| \quad (3.48)$$

$$\leq \|w\delta\theta\|_1 + \|\delta w\theta\|_1 + \|\delta w\delta\theta\|_1 \quad (3.49)$$

$$\leq \|\vec{u}\|_3 \|\delta\theta\|_{3/2} + \|\delta\vec{u}\|_3 \|\theta\|_{3/2} + \|\delta\vec{u}\|_3 \|\delta\theta\|_{3/2} \quad (3.50)$$

$$\leq c (\|\vec{u}\|_3 + \|\delta\vec{u}\|_3) \|\nabla\delta\theta\|_2 + \|\delta\vec{u}\|_3 \|\theta\|_{3/2} \quad (3.51)$$

$$\leq [c (\|\vec{u}\|_3 + \|\delta\vec{u}\|_3) (\|\theta\|_6 + d') + \|\theta\|_{3/2}] \|\delta\vec{u}\|_3. \quad (3.52)$$

The last line followed from (3.46) and the previous lines from Sobolev embeddings and Hölder's inequalities. Thus our functional is controlled by the L^3 norm of the differences. Said differently we can invoke L^3 perturbations on our functional and still have values

remain “close” to one another.

Thus far no mention of boundary conditions on \vec{u} were necessary; however, to determine a global maximizer exists to (3.1) it is essential to be more specific. In fact, any boundary or integral conditions on \vec{u} such that $\|\nabla\vec{u}\|_2$ defines a norm would work. Otherwise we could instead work with $\|\vec{u}\|_2 + \gamma\|\nabla\vec{u}\|_2$ where $\gamma \in (0, \infty)$ is a fixed number, but then the connection to Rayleigh-Bénard convection would be lost. Example boundary conditions include:

1. Periodicity in the horizontal directions and no-slip boundary conditions in the vertical direction for all components of velocity.
2. Stress-Free boundary conditions and mean-zero on the horizontal velocities for the vertical boundary conditions, and homogeneous boundary conditions in the vertical direction for the vertical velocity. Periodic boundary conditions for the horizontal directions for all the components of velocity.
3. No-slip boundary conditions on the entire domain for all components of velocity.

To confirm that maximizers do indeed exist to the optimization problem (3.1) we may use the Rellich-Kondrachov theorem (§3.2). A consequence of this theorem is the compactness of the H^1 ball in the L^3 topology in three dimensions or less. Hence we are maximizing a continuous function on a compact set, thus a maximizer exists. More explicitly we can proceed as follows: Let C denote the Poincaré constant. The functional is bounded above by CPe by the calculation

$$\|\nabla\theta\|_2^2 = \int_{\Omega} w\theta \leq \|w\|_2\|\theta\|_2 \leq C\|\nabla\vec{u}\|_2\|\nabla\theta\|_2, \quad (3.53)$$

hence a supremum exists. Let \vec{u}_n be a sequence of vectors that converge to the supremum. Since the H^1 ball is compact in the weak H^1 topology by the Banach-Alaoglu Theorem there exists a subsequence such that \vec{u}_{n_k} converges weakly to a function \vec{u} . This \vec{u} is our candidate maximizer and we will indeed show that it is a maximizer. By the Rellich-Kondrachov theorem (§3.2) this sequence converges strongly in L^3 which by (3.52) implies that the value of the functional converges to $\langle w\theta \rangle$, meaning $\langle w_{n_k}\theta \rangle \rightarrow \langle w\theta \rangle$. But we also know that the sequence converges to the supremum, hence \vec{u} is our maximizer. If we instead restrict ourselves to incompressible flow fields the argument is exactly the same. In conclusion a maximizer to (3.1) does indeed exist.

3.3.3 Differentiability

We will now show that the functional

$$\mathcal{F}[\vec{u}] = \int_{\Omega} w\theta \quad (3.54)$$

where θ is defined as the solution to

$$\int_{\Omega} \left(\frac{1}{2} [\phi\vec{u} \cdot \nabla\theta - \theta\vec{u} \cdot \nabla\phi] + \nabla\theta \cdot \nabla\phi \right) = \int_{\Omega} \phi w \quad (3.55)$$

is Fréchet differentiable with respect to the L^3 topology on \vec{u} . By definition we must find a linear operator L (linear in $\delta\vec{u}$) such that

$$\left| \int_{\Omega} ((w + \delta w)(\theta + \delta\theta) - w\theta - L[\delta\vec{u}]) \right| \leq c\|\delta\vec{u}\|_3^2 \quad (3.56)$$

for some constant c , where $\theta + \delta\theta$ solves (3.25) for an advective term of $\vec{u} + \delta\vec{u}$, i.e.

$$\int_{\Omega} \left(\frac{1}{2} [\phi(\vec{u} + \delta\vec{u}) \cdot \nabla(\theta + \delta\theta) - \varphi(\vec{u} + \delta\vec{u}) \cdot \nabla\phi] + \nabla\phi \cdot \nabla\varphi \right) = \int_{\Omega} (\phi\delta\vec{u} \cdot \nabla\theta + \phi\delta w). \quad (3.57)$$

The choice

$$L[\delta\vec{u}] = \theta\delta w + \delta\varphi w \quad (3.58)$$

where $\delta\varphi$ is solution to

$$\int_{\Omega} \left(\frac{1}{2} [\phi\vec{u} \cdot \nabla\delta\varphi - \delta\varphi\vec{u} \cdot \nabla\phi] + \nabla\phi \cdot \nabla\delta\varphi \right) = \int_{\Omega} \left(\frac{1}{2} [\theta\delta\vec{u} \cdot \nabla\phi - \phi\delta\vec{u} \cdot \nabla\theta] \right) \quad (3.59)$$

is the linear operator that we are looking for. We have shown that solutions to this equation exist in §3.3.1 as long as the right hand side defines a continuous linear functional on $\phi \in H^1$. This is seen by using $\theta \in H^1$ and $\delta\vec{u} \in L^3$ and the estimate

$$\left| \int_{\Omega} \left(\frac{1}{2} [\theta\delta\vec{u} \cdot \nabla\phi - \phi\delta\vec{u} \cdot \nabla\theta] \right) \right| \leq \frac{1}{2} \|\theta\delta\vec{u} \cdot \nabla\phi\|_1 + \frac{1}{2} \|\phi\delta\vec{u} \cdot \nabla\theta\|_1 \quad (3.60)$$

$$\leq \frac{1}{2} \|\theta\|_6 \|\delta\vec{u}\|_3 \|\nabla\phi\|_2 + \frac{1}{2} \|\phi\|_6 \|\delta\vec{u}\|_3 \|\nabla\theta\|_2 \quad (3.61)$$

$$\leq c\|\delta\vec{u}\|_3 \|\nabla\theta\|_2 \|\nabla\phi\|_2. \quad (3.62)$$

This is the same equation as the one for $\delta\theta$ except without the second order $\delta\theta\delta\vec{u} \cdot \nabla\theta$ terms. Since we are solving a linear equation, the function $\delta\varphi$ is indeed linear in $\delta\vec{u}$ and hence the L operator is a linear function of $\delta\vec{u}$. To show differentiability we verify that

$$\left| \int_{\Omega} \delta\theta\delta w + w(\delta\theta - \delta\varphi) \right| \leq C\|\delta\vec{u}\|_3^2 \quad (3.63)$$

holds for some constant C that depends on what point in function space we are considering. The difference between the $\delta\theta$ and $\delta\varphi$ equations yield

$$\begin{aligned} & \int_{\Omega} \left(\frac{1}{2} [\phi\vec{u} \cdot \nabla(\delta\theta - \delta\varphi) - (\delta\theta - \delta\varphi)\vec{u} \cdot \nabla\phi] + \nabla\phi \cdot \nabla(\delta\theta - \delta\varphi) \right) \\ &= \\ & \int_{\Omega} \frac{1}{2} (\phi\delta\vec{u} \cdot \nabla\delta\theta - \delta\theta\delta\vec{u} \cdot \nabla\phi). \end{aligned} \quad (3.64)$$

choosing $\phi = \delta\theta - \delta\varphi$ allows us to estimate $\|\nabla(\delta\theta - \delta\varphi)\|_2$ since

$$\|\nabla(\delta\theta - \delta\varphi)\|_2^2 = \left| \int_{\Omega} \frac{1}{2} ((\delta\theta - \delta\varphi)\delta\vec{u} \cdot \nabla\delta\theta - \delta\theta\delta\vec{u} \cdot \nabla(\delta\theta - \delta\varphi)) \right| \quad (3.65)$$

$$\leq \frac{1}{2} \|(\delta\theta - \delta\varphi)\delta\vec{u} \cdot \nabla\delta\theta\|_1 + \frac{1}{2} \|\delta\theta\delta\vec{u} \cdot \nabla(\delta\theta - \delta\varphi)\|_1 \quad (3.66)$$

$$\leq \frac{1}{2} \|(\delta\theta - \delta\varphi)\|_6 \|\delta\vec{u}\|_3 \|\nabla\delta\theta\|_2 + \frac{1}{2} \|\delta\theta\|_6 \|\delta\vec{u}\|_3 \|\nabla(\delta\theta - \delta\varphi)\|_2 \quad (3.67)$$

$$\leq c \|\nabla(\delta\theta - \delta\varphi)\|_2 \|\delta\vec{u}\|_3 \|\nabla\delta\theta\|_2 \quad (3.68)$$

$$\leq cd' \|\nabla(\delta\theta - \delta\varphi)\|_2 \|\delta\vec{u}\|_3^2 \quad (3.69)$$

where we used integration Sobolev embedding, Hölder's inequality, and (3.46). The c and c' are constants. This is enough to show that the functional is differentiable

$$\left| \int_{\Omega} (\delta\theta\delta w + w(\delta\theta - \delta\varphi)) \right| \leq \|\delta\theta\delta\vec{u} \cdot \hat{e}_3\|_1 + \|w(\delta\theta - \delta\varphi)\|_1 \quad (3.70)$$

$$\leq \|\delta\theta\|_{3/2} \|\delta w\|_3 + \|\vec{u} \cdot \hat{e}_3\|_3 \|(\delta\theta - \delta\varphi)\|_{3/2} \quad (3.71)$$

$$\leq c' \|\nabla\delta\theta\|_2 \|\delta\vec{u}\|_3 + c' \|\vec{u}\|_3 \|\nabla(\delta\theta - \delta\varphi)\|_2 \quad (3.72)$$

$$\leq c'd' \|\delta\vec{u}\|_3^2 + c'd' \|\delta\vec{u}\|_3^2 \quad (3.73)$$

Since the functional $\langle w\theta \rangle$ is Fréchet differentiable with respect to any $\vec{u} \in L^3$ the maximizer to 3.1 also satisfies this condition. Thus our maximizer must satisfy first-order optimality conditions. Fréchet differentiability guarantees differentiability in any direction

and in particular we may constrain ourselves to the set $\{\vec{u} | \langle \nabla \vec{u} : \nabla \vec{u} \rangle = \text{Pe}^2\}$.

3.4 Upper Bound

From now on we would like to deduce properties of the maximizer and will proceed formally. We only proved existence of a maximizer and differentiability of the functional with respect to the time-independent case but we will no longer limit ourselves to time-independent flows to obtain an upper-bound. It is important to note that we will make no assumptions on the boundary conditions for the horizontal velocity. In fact we will only use the fact that $w = 0$ at $z = 0$ and $z = 1$. Furthermore, the estimates here apply to the rigorous time-independent problem for incompressible velocity fields.

To obtain the upper bound will make a background decomposition of the form

$$T = \theta + \tau(z) \tag{3.74}$$

where τ is the ‘‘background’’. The form of τ will be

$$\tau(z) = \begin{cases} 1 - \frac{1}{2\delta}z & \text{for } 0 \leq z < \delta \\ \frac{1}{2} & \text{for } \delta \leq z \leq 1 - \delta \\ \frac{1}{2} - \frac{1}{2\delta}(z - (1 - \delta)) & \text{for } 1 - \delta < z \leq 1 \end{cases} \tag{3.75}$$

so that

$$\tau'(z) = \begin{cases} -\frac{1}{2\delta} & \text{for } 0 < z < \delta \\ 0 & \text{for } \delta < z < 1 - \delta \\ -\frac{1}{2\delta} & \text{for } 1 - \delta < z < 1 \end{cases} \tag{3.76}$$

with $\delta > \frac{1}{2}$ being chosen later. Note that $\langle (\tau')^2 \rangle = (2\delta)^{-1}$.

We see that θ satisfies homogeneous boundary conditions. The equation of motion for θ is

$$\partial_t \theta + \vec{u} \cdot \nabla \theta = \Delta \theta + \tau'' - w\tau'. \tag{3.77}$$

This implies the following balance relation

$$0 = -\langle |\nabla \theta|^2 \rangle - \langle \tau' \partial_z \theta \rangle - \langle \theta w \tau' \rangle \tag{3.78}$$

and that the Nusselt number is

$$\text{Nu} = \langle |\nabla T|^2 \rangle \quad (3.79)$$

$$= \langle |\nabla\theta + \tau'\hat{z}|^2 \rangle \quad (3.80)$$

$$= \langle |\nabla\theta|^2 \rangle + 2\langle \tau'\partial_z\theta \rangle + \langle (\tau')^2 \rangle \quad (3.81)$$

Since $0 \leq T \leq 1$ our choice of background implies the boundedness of θ . Hence $\lim_{T \rightarrow \infty} \frac{\theta(T)}{T} = 0$. If we want to bound the Nusselt number we make the following observation

$$\text{Nu} = \langle |\nabla T|^2 \rangle \quad (3.82)$$

$$= \left\langle |\nabla T|^2 + \frac{\partial}{\partial t}\theta^2 + \alpha\text{Pe}^{2/3} \left(1 - \frac{|\nabla\vec{u}|^2}{\text{Pe}^2} \right) \right\rangle \quad (3.83)$$

$$= \langle (\tau')^2 \rangle + \alpha\text{Pe}^{2/3} - \langle |\nabla\theta|^2 + 2w\theta\tau' + \alpha\text{Pe}^{-4/3}|\nabla\vec{u}|^2 \rangle \quad (3.84)$$

where $\alpha \geq 0$ and the prefactor $\text{Pe}^{2/3}$ has been factored out in anticipation of the result. Recall that $|\nabla\vec{u}|^2 = \nabla\vec{u} : \nabla\vec{u}$. We would now like to choose δ such that for any $\theta, \vec{u} \in H^1$

$$\mathcal{Q}[\theta, \vec{u}] = \langle |\nabla\theta|^2 + 2w\theta\tau' + \alpha\text{Pe}^{-4/3}|\nabla\vec{u}|^2 \rangle \geq 0, \quad (3.85)$$

i.e. \mathcal{Q} is positive semi-definite. To do so we must balance the $2\langle w\theta\tau' \rangle$ term with the positive definite terms $|\nabla\theta|^2$ and $|\nabla\vec{u}|^2$. This was originally accomplished by Constantin and Doering [4], but for completeness the calculation is repeated in Appendix D. Specifically, it was shown that

$$2\langle w\theta\tau' \rangle \geq -\frac{\delta}{2} \left\langle c(\partial_z w)^2 + \frac{1}{c}(\partial_z \theta)^2 \right\rangle \geq -\frac{\delta}{2} \left\langle \frac{c}{4}|\nabla\vec{u}|^2 + \frac{1}{c}|\nabla\theta|^2 \right\rangle \quad (3.86)$$

for a constant $c > 0$ that will be chosen later. This implies

$$\mathcal{Q}[\theta, \vec{u}] = \langle |\nabla\theta|^2 + 2w\theta\tau' + \alpha\text{Pe}^{-4/3}|\nabla\vec{u}|^2 \rangle \quad (3.87)$$

$$\geq \left\langle \left(1 - \frac{\delta}{2c} \right) |\nabla\theta|^2 + \left(\alpha\text{Pe}^{-4/3} - \frac{c\delta}{8} \right) |\nabla\vec{u}|^2 \right\rangle. \quad (3.88)$$

Choosing $c = \delta/2$ so that

$$\mathcal{Q}[\theta, \vec{u}] \geq \left\langle \left(\alpha\text{Pe}^{-4/3} - \frac{\delta^2}{16} \right) |\nabla\vec{u}|^2 \right\rangle \quad (3.89)$$

and $\delta = 4\sqrt{\alpha}\text{Pe}^{-2/3}$ yields

$$\mathcal{Q}[\theta, \vec{u}] \geq 0. \quad (3.90)$$

Hence our upper bound for the Nusselt number is

$$\text{Nu} \leq \frac{1}{2\delta} + \alpha\text{Pe}^{2/3} \quad (3.91)$$

$$\leq \left(\frac{1}{8\sqrt{\alpha}} + \alpha \right) \text{Pe}^{2/3}. \quad (3.92)$$

We now pick $\alpha = 256^{-1/3}$ to minimize the prefactor and obtain,

$$\text{Nu} \leq \left(\frac{3}{4 \times 2^{2/3}} \right) \text{Pe}^{2/3} \leq 0.473\text{Pe}^{2/3}. \quad (3.93)$$

3.5 The Euler-Lagrange Equations

Let us proceed formally and look at the first-order optimality condition for incompressible vector fields \vec{u}

$$0 = \int_{\Omega} \theta \delta w + \delta \varphi w. \quad (3.94)$$

a little more closely. We think of θ as a functional output given a \vec{u} defined by the equation

$$\int_{\Omega} \phi \vec{u} \cdot \nabla \theta + \nabla \phi \cdot \nabla \theta = \int_{\Omega} \phi f \quad (3.95)$$

for each $\phi \in H^1$ and for a chosen forcing function f (in the context of this chapter $f = w$). Let us denote the (linear) mapping of $f \rightarrow \theta$ by $G_{\vec{u}}$, that is, $G_{\vec{u}}[f] = \theta$. The adjoint of this operator $G_{\vec{u}}^{\dagger}$ corresponds to a φ such that

$$\int_{\Omega} -\phi \vec{u} \cdot \nabla \varphi + \nabla \phi \cdot \nabla \varphi = \int_{\Omega} \phi f \quad (3.96)$$

for each $\phi \in H^1$, hence, $G_{\vec{u}}^{\dagger}[f] = \varphi$. The adjoint equation comes equipped with boundary conditions with the same boundary conditions as the one for θ if, for example, the horizontal directions satisfy periodic or homogeneous or no-flux boundary conditions and if the vertical direction satisfies homogenous boundary conditions. With this notation in place

we see that the first-order optimality condition becomes,

$$\int_{\Omega} \theta \delta w + \delta \varphi w = \int_{\Omega} G_{\vec{u}}[w] \delta w + w G_{\vec{u}}[-\delta \vec{u} \cdot \nabla \theta + \delta w] \quad (3.97)$$

$$= \int_{\Omega} G_{\vec{u}}[w] \delta w + G_{\vec{u}}^{\dagger}[w] (-\delta \vec{u} \cdot \nabla \theta + \delta w) \quad (3.98)$$

$$= \int_{\Omega} \delta \vec{u} \cdot \left(G_{\vec{u}}[w] \hat{e}_3 + G_{\vec{u}}^{\dagger}[w] \hat{e}_3 - G_{\vec{u}}^{\dagger}[w] \nabla G_{\vec{u}}[w] \right) \quad (3.99)$$

$$= \int_{\Omega} \delta \vec{u} \cdot (\theta \hat{e}_3 + \varphi \hat{e}_3 - \varphi \nabla \theta) \quad (3.100)$$

Imposing constraints on \vec{u} changes the null-space of the linear functional $\int_{\Omega} \delta \vec{u}$. Particularly, by imposing incompressibility and the $\langle \nabla \vec{u} : \nabla \vec{u} \rangle = \text{Pe}^2$ constraint we have

$$0 = \int_{\Omega} \delta \vec{u} \cdot \nabla p \quad (3.101)$$

$$0 = \int_{\Omega} \nabla \delta \vec{u} \cdot \nabla \vec{u} \quad (3.102)$$

for a $p \in H^1$. The first condition comes from noting that (with appropriate boundary conditions) the velocity field \vec{u} is orthogonal to gradients. The second condition may be calculated from,

$$\langle \nabla(\vec{u} + \delta \vec{u}), \nabla(\vec{u} + \delta \vec{u}) \rangle = \text{Pe}^2 \quad (3.103)$$

$$\langle \nabla \vec{u}, \nabla \vec{u} \rangle = \text{Pe}^2 \quad (3.104)$$

$$\Rightarrow \quad (3.105)$$

$$\langle \nabla \delta \vec{u}, \nabla \delta \vec{u} \rangle = -\langle \nabla \vec{u}, \nabla \delta \vec{u} \rangle - \langle \nabla \delta \vec{u}, \nabla \vec{u} \rangle, \quad (3.106)$$

noting that $\langle \nabla \delta \vec{u}, \nabla \delta \vec{u} \rangle$ is second order, and that $\langle f, g \rangle = \langle g, f \rangle$.

Although we have written the first-order optimality conditions, they are a bit inconvenient to use when trying to establish properties of the maximizer. Instead we will introduce Lagrange multipliers μ , φ , and p , to enforce the Péclet constraint, advection diffusion equation, and the incompressibility constraint. Furthermore we will now consider the time-dependent problem as well. Note that we have not proven that solutions exist to the time-dependent problem, nor have we shown what space \vec{u} must belong in order for the problem to make sense. Nevertheless we will proceed formally hoping that the calculations may someday be made rigorous.

The solution to the time-dependent maximization problem (3.1) is characterized by the

critical points of the augmented Lagrangian

$$\mathcal{F} = \left\langle w\theta - \varphi (\partial_t \theta + \vec{u} \cdot \nabla \theta - \Delta \theta - w) + p(\nabla \cdot \vec{u}) + \frac{\mu}{2}(\text{Pe}^2 - \nabla \vec{u} : \nabla \vec{u}) \right\rangle. \quad (3.107)$$

The first-order optimality conditions are given by the variations with respect to $(\vec{u}, \theta, \varphi, p, \mu)$. Variations with respect to the Lagrange multipliers yield the constraint equations

$$0 = \frac{\delta \mathcal{F}}{\delta \varphi} = \partial_t \theta + \vec{u} \cdot \nabla \theta - \Delta \theta - w \quad (3.108)$$

$$0 = \frac{\delta \mathcal{F}}{\delta p} = \nabla \cdot \vec{u} \quad (3.109)$$

$$0 = \frac{\delta \mathcal{F}}{\delta \mu} = \frac{1}{2} \langle \text{Pe}^2 - \nabla \vec{u} : \nabla \vec{u} \rangle \quad (3.110)$$

variations with respect to the state θ and the control \vec{u} yield the adjoint equation and the optimality condition respectively,

$$0 = \frac{\delta \mathcal{F}}{\delta \theta} = -\partial_t \varphi - \vec{u} \cdot \nabla \varphi - \Delta \varphi - w \quad (3.111)$$

$$0 = \frac{\delta \mathcal{F}}{\delta \vec{u}} = \mu \Delta \vec{u} + (\theta + \varphi) \hat{e}_3 - \varphi \nabla \theta - \nabla p. \quad (3.112)$$

Using the Euler-Lagrange equations we will show that the maximum must indeed occur when $\langle \nabla \vec{u} : \nabla \vec{u} \rangle = \text{Pe}^2$ under the assumption that

$$\langle \varphi \partial_t \theta \rangle = \langle \theta \partial_t \varphi \rangle = 0. \quad (3.113)$$

This is not a restriction in the steady case, but in the time-dependent case this becomes dubious; however, by assuming that there exists an optimal time period $0 < T^* < \infty$ that maximizes heat transport and that the functional evaluated on an optimal trajectory is differentiable with respect to T , variations with respect to T imply

$$0 = \frac{\delta \mathcal{F}}{\delta T} = -\frac{\mathcal{F}}{T} + \frac{1}{\Gamma_1 \Gamma_1} \int_0^{\Gamma_1} \int_0^{\Gamma_2} \int_0^1 \mathcal{H}^t dz dy dx \quad (3.114)$$

$$\mathcal{H}^t = \mathcal{L} - \partial_t \theta \varphi. \quad (3.115)$$

Time averaging (3.114) yields (3.113). See Appendix A. This may be useful when calculating periodic trajectories, but since we expect steady state solutions to be most optimal the assumption that there exists a T^* for which the above holds should be called into question. In fact we expect that the computation of such a gradient would imply that $T^* \rightarrow \infty$ for solutions to time-dependent problems where $\varphi(\vec{x}, T) = \theta(\vec{x}, 0) = 0$ or time-periodic

problems.

From the augmented Lagrangian we make one further observation. Optimizing over horizontal boundary conditions implies that the conjugate momenta associated with the variable must be zero on the boundary, see §A.1.1 and §A.2.2. In the context of this functional this means that the horizontal velocities must satisfy stress-free boundary conditions. In so far as a maximum exists and is differentiable with respect to varying boundary data for horizontal components of \vec{u} this would imply that stress-free boundary conditions yield the absolute optimal transport of heat.

The Euler-Lagrange equations for the system are

$$\partial_t \theta + \vec{u} \cdot \nabla \theta = \Delta \theta + w \quad (3.116)$$

$$-\partial_t \varphi - \vec{u} \cdot \nabla \varphi = \Delta \varphi + w \quad (3.117)$$

$$-\mu \Delta \vec{u} = \hat{e}_3 \theta - \varphi \nabla \theta + \hat{e}_3 \varphi - \nabla p \quad (3.118)$$

$$0 = \nabla \cdot \vec{u} \quad (3.119)$$

$$0 = \frac{1}{2}(\text{Pe}^2 - |\nabla \vec{u}|^2). \quad (3.120)$$

In addition consider the equations for the sum and difference of θ and φ

$$\vec{u} \cdot \nabla (\theta - \varphi) = \Delta (\theta + \varphi) + 2w \quad (3.121)$$

$$-\vec{u} \cdot \nabla (\theta + \varphi) = \Delta (\theta - \varphi). \quad (3.122)$$

From these we have the following integral relations

$$-\langle \theta \Delta \theta \rangle = \langle \nabla \theta \cdot \nabla \theta \rangle = \langle \theta w \rangle \quad (3.123)$$

$$-\langle \theta \Delta \varphi \rangle = \langle \nabla \varphi \cdot \nabla \varphi \rangle = \langle \varphi w \rangle \quad (3.124)$$

$$-\langle (\theta - \varphi) \Delta (\theta + \varphi) \rangle = 2 \langle w (\theta - \varphi) \rangle \quad (3.125)$$

$$-\langle (\theta + \varphi) \Delta (\theta - \varphi) \rangle = 0 \quad (3.126)$$

we rely on the assumption that $\langle \varphi \partial_t \theta \rangle = \langle \theta \partial_t \varphi \rangle = 0$ when deriving (3.125) and (3.126). The latter two were derived by multiplying the $\theta \pm \varphi$ equations by $\theta \mp \varphi$ respectively and integrating by parts.

Using (3.126) with (3.125) allows us to conclude

$$\langle w \theta \rangle = \langle w \varphi \rangle \quad (3.127)$$

from whence we see

$$\langle w\theta \rangle = \langle w\varphi \rangle = \langle \nabla\theta \cdot \nabla\theta \rangle = \langle \nabla\varphi \cdot \nabla\varphi \rangle. \quad (3.128)$$

Dotting the optimality condition (3.118) by \vec{u} and averaging gives

$$-\mu\langle \vec{u} \cdot \Delta\vec{u} \rangle = \langle w\theta + w\varphi \rangle - \langle \varphi\vec{u} \cdot \nabla\theta \rangle - \langle \vec{u} \cdot \nabla p \rangle \quad (3.129)$$

\Rightarrow

$$-\mu\langle \vec{u} \cdot \Delta\vec{u} \rangle = 2\langle \nabla\theta \cdot \nabla\theta \rangle - \langle \varphi\vec{u} \cdot \nabla\theta \rangle. \quad (3.130)$$

Multiplying (3.116) by φ and (3.117) by θ and averaging yields

$$\langle \varphi\vec{u} \cdot \nabla\theta \rangle = \langle \varphi\Delta\theta \rangle + \langle w\varphi \rangle = -\langle \nabla\varphi \cdot \nabla\theta \rangle + \langle \nabla\theta \cdot \nabla\theta \rangle \quad (3.131)$$

$$-\langle \theta\vec{u} \cdot \nabla\varphi \rangle = \langle \theta\Delta\varphi \rangle + \langle w\theta \rangle = -\langle \nabla\varphi \cdot \nabla\theta \rangle + \langle \nabla\theta \cdot \nabla\theta \rangle. \quad (3.132)$$

Here we used the assumption that $\langle \varphi\partial_t\theta \rangle = \langle \theta\partial_t\varphi \rangle = 0$. Using these integral balance relations we may reduce (3.130) to

$$-\mu\langle \vec{u} \cdot \Delta\vec{u} \rangle = 2\langle \nabla\theta \cdot \nabla\theta \rangle - \langle -\nabla\varphi \cdot \nabla\theta + \nabla\theta \cdot \nabla\theta \rangle \quad (3.133)$$

\Rightarrow

$$-\mu\langle \vec{u} \cdot \Delta\vec{u} \rangle = \langle \nabla\theta \cdot \nabla\theta + \nabla\varphi \cdot \nabla\theta \rangle = \langle \nabla\varphi \cdot \nabla\varphi + \nabla\varphi \cdot \nabla\theta \rangle. \quad (3.134)$$

We are now finally in the position to show that the maximum of Nu must occur on the boundary. Observe that if the maximum occurred for $\langle |\nabla\vec{u}|^2 \rangle < \text{Pe}^2$ we would not need to enforce the Pe constraint in the Euler-Lagrange equations, hence $\mu = 0$. If $\mu = 0$ then

$$0 = \langle \nabla\theta \cdot \nabla\theta + \nabla\varphi \cdot \nabla\theta \rangle \quad (3.135)$$

$$0 = \langle \nabla\varphi \cdot \nabla\varphi + \nabla\varphi \cdot \nabla\theta \rangle \quad (3.136)$$

\Rightarrow

$$0 = \langle \nabla(\theta + \varphi) \cdot \nabla(\theta + \varphi) \rangle \quad (3.137)$$

The last equation lets us conclude that $\theta = -\varphi$, and using

$$-\vec{u} \cdot \nabla(\theta + \varphi) = \Delta(\theta - \varphi)$$

gets us that $\theta = \varphi$, and hence $\theta = 0 = \varphi$. But if this is true then $w = 0$ from either the advection-diffusion equation or the adjoint equation. Hence $\mu = 0$ implies $w = 0$ as long

as $\langle \varphi \partial_t \theta \rangle = \langle \theta \partial_t \varphi \rangle = 0$. These are the minimizers of the functional. Since there exist non-zero solutions to the advection-diffusion equation, it must be the case that there are no maximizers on the interior of the H^1 ball. It is worth noting that these conclusions do not depend on the exact boundary conditions on \vec{u} , in so far as the conditions on \vec{u} define a well-formulated variational problem.

3.6 Possible Avenues for Improving the Upper Bound

From computations in Chapter 4 it seems to be the case that the upper bound from §3.4 is suboptimal. There are various properties of the advection-diffusion equation and incompressibility that were not used in the derivation of the upper bound. In particular we did not use the fact that θ satisfies the advection-diffusion equation, the maximum principle for θ ($\|\theta\|_\infty \leq 1$), the optimality condition for the velocity field, nor did we use any boundary conditions for the horizontal velocity.

The Euler-Lagrange equations imply that the optimal velocity field satisfies Stoke's equation,

$$\mu \partial_{jj} u_i = f_i + \partial_i p \quad (3.138)$$

$$\partial_i u_i = 0 \quad (3.139)$$

hence we have the following equation for pressure,

$$\partial_{kk} p = -\partial_k f_k \quad (3.140)$$

which may be eliminated to yield,

$$\mu \partial_{kk} \partial_{jj} u_i = \partial_{kk} f_i + \partial_i \partial_{kk} p \quad (3.141)$$

$$= \partial_{kk} f_i - \partial_{ik} f_k \quad (3.142)$$

$$= \partial_k (f_{i,k} - f_{k,i}) \quad (3.143)$$

For the Euler-Lagrange equations this means that

$$-\mu \Delta^2 w = \nabla \cdot (\nabla(\theta + \varphi - \varphi \partial_z \theta) - \partial_z(\theta + \varphi) \hat{e}_3 + \partial_z \varphi \nabla \theta + \varphi \nabla \partial_z \theta) \quad (3.144)$$

$$= (\partial_{xx} + \partial_{yy})(\theta + \varphi) + \nabla \cdot (\partial_z \varphi \nabla \theta - \partial_z \theta \nabla \varphi) \quad (3.145)$$

$$= (\partial_{xx} + \partial_{yy})(\theta + \varphi) + \partial_z \varphi \Delta \theta - \partial_z \theta \Delta \varphi + \nabla \partial_z \varphi \cdot \nabla \theta - \nabla \partial_z \theta \cdot \nabla \varphi. \quad (3.146)$$

Multiplying through by any function g that vanishes on the boundary and integrate by parts we get

$$\mu \langle g \Delta^2 w \rangle = \langle g (\partial_{xx} + \partial_{yy}) (\theta + \varphi) \rangle + \langle \nabla g \cdot (\partial_z \theta \nabla \varphi - \partial_z \varphi \nabla \theta) \rangle. \quad (3.147)$$

The difficulty preventing us from properly exploiting the Euler-Lagrange equations comes from the

$$\nabla g \cdot (\partial_z \theta \nabla \varphi - \partial_z \varphi \nabla \theta) \quad (3.148)$$

term. The z component of $\partial_z \theta \nabla \varphi - \partial_z \varphi \nabla \theta$ vanishes. Perhaps it is possible to use (3.147) to improve the analytic upper bound, but even if this is possible one would need to know a relation between μ and Pe .

3.6.1 Insights on How to Improve the Upper Bound

In order to improve the upper bound it is necessary to look at the essential ingredients that go into such an analysis. It is known that minimizing the quadratic functional (3.85) over all incompressible velocity fields \vec{u} and $\theta \in H^1$ is equivalent to looking for eigenfunctions of the operator ($\gamma \geq 0$)

$$\mathcal{Q}[\theta, \vec{u}] = \begin{bmatrix} \theta & \vec{u} \end{bmatrix} \begin{bmatrix} -\Delta & \tau' \hat{e}_3 \\ \tau' \hat{e}_3 & -\gamma \Delta \end{bmatrix} \begin{bmatrix} \theta \\ \vec{u} \end{bmatrix}, \quad (3.149)$$

and finding the τ that gives the lowest value of $\langle (\tau')^2 \rangle$ subject to the constraint that the lowest eigenvalue is non-negative. In Constantin and Doering [4], a relaxation of this was found for the operator

$$\mathcal{Q}_R[\theta, w] = \begin{bmatrix} \theta & w \end{bmatrix} \begin{bmatrix} -\frac{d^2}{dz^2} & \tau' \\ \tau' & -\frac{d^2}{dz^2} \end{bmatrix} \begin{bmatrix} \theta \\ w \end{bmatrix}. \quad (3.150)$$

Interestingly both spectral constraints produce the same scaling exponent, suggesting that incompressibility is not important for the ultimate scaling in the background method [31].

Here we will look at a particular relaxation of the full optimal control problem in order

to develop some intuition. The full optimal control problem is

$$\text{Maximize } \langle w\theta \rangle \quad (3.151)$$

subject to

$$\vec{u} \cdot \nabla \theta = \Delta \theta + w \quad (3.152)$$

$$\langle \nabla \vec{u} : \nabla \vec{u} \rangle \leq \text{Pe}^2 \quad (3.153)$$

$$\nabla \cdot \vec{u} = 0. \quad (3.154)$$

Observe that for incompressible flow fields

$$\vec{u} \cdot \nabla \theta = \beta \vec{u} \cdot \nabla \theta + (1 - \beta) \nabla \cdot (\vec{u}\theta) \quad (3.155)$$

$$\langle w\theta \rangle = \alpha \langle w\theta \rangle + (1 - \alpha) \langle |\nabla \theta|^2 \rangle \quad (3.156)$$

for parameters $\alpha, \beta \in \mathbb{R}$. Hence (3.151) is equivalent to

$$\text{Maximize } \alpha \langle w\theta \rangle + (1 - \alpha) \langle |\nabla \theta|^2 \rangle \quad (3.157)$$

subject to

$$\beta \vec{u} \cdot \nabla \theta + (1 - \beta) \nabla \cdot (\vec{u}\theta) = \Delta \theta + w \quad (3.158)$$

$$\langle \nabla \vec{u} : \nabla \vec{u} \rangle \leq \text{Pe}^2 \quad (3.159)$$

$$\nabla \cdot \vec{u} = 0. \quad (3.160)$$

Let us denote the global maximum to (3.151) by Nu_1 . Now denote the global maximum of the less restricted problem

$$\text{Maximize } \alpha \langle w\theta \rangle + (1 - \alpha) \langle |\nabla \theta|^2 \rangle \quad (3.161)$$

subject to

$$\beta \vec{u} \cdot \nabla \theta + (1 - \beta) \nabla \cdot (\vec{u}\theta) = \Delta \theta + w \quad (3.162)$$

$$\langle \nabla \vec{u} : \nabla \vec{u} \rangle \leq \text{Pe}^2 \quad (3.163)$$

by Nu_2 . This is less constrained because we have removed the incompressibility constraint. It is the case that $\text{Nu}_1 \leq \text{Nu}_2$ for any choice of parameters α and β since (3.161) includes solutions of (3.157) as a special case. Getting rid of the incompressibility constraint suggests that we would not want to use any of the enstrophy budget on horizontal directions or velocities. Physically this would correspond to a flow field that would purely transport heat from the bottom plate to the top plate, not wasting any time transporting horizontally.

Thus we consider the following optimization problem

$$\text{Maximize } \alpha \langle w\theta \rangle + (1 - \alpha) \langle (\partial_z \theta)^2 \rangle \quad (3.164)$$

subject to

$$\beta w \partial_z \theta + (1 - \beta) \partial_z (w\theta) = \partial_{zz}^2 \theta + w \quad (3.165)$$

$$\langle \|\partial_z w\|_2^2 \rangle \leq \text{Pe}. \quad (3.166)$$

as a model for (3.161) with boundary conditions $\theta(0) = \theta(1) = w(0) = w(1) = 0$. We will not solve this optimal control problem, but rather look at some particular flow fields that achieve the same scaling as the bound from §3.4 ($\text{Nu} \lesssim \text{Pe}^{2/3}$). In light of examining these flows we then switch to a special class of incompressible flows that share a similar structure and show how incompressibility ruins this scaling. Thus we come to the conclusion that we have to both fully enforce incompressibility and the advection-diffusion equation to understand the true scaling, independent of enforcing the Navier-Stokes equations.

We expect that the flow field should essentially try to remain as large as possible everywhere to transport as much heat as possible, hence we will look at the particular flow field

$$w(z) = \begin{cases} \frac{\text{Pe}}{\sqrt{2\delta}} z & \text{for } 0 \leq z \leq \delta \\ \text{Pe} \frac{\sqrt{\delta}}{\sqrt{2}} & \text{for } \delta \leq z \leq 1 - \delta \\ \frac{\text{Pe}}{\sqrt{2\delta}} (1 - z) & \text{for } 1 - \delta \leq z \leq 1 \end{cases} \quad (3.167)$$

for $0 < \delta \leq 1/2$. This flow field satisfies the enstrophy budget constraint and the boundary conditions, but depends on finding an optimal parameter δ . On one hand the smaller the δ the more the flow field is essentially like constant, on the other hand the lower the infinity norm of w .

We will look at the particular case $\beta = 1$ and $\alpha = 0$. For this case we can reduce the advection-diffusion equation

$$w \frac{d}{dz} \theta = \frac{d^2}{dz^2} \theta + w \quad (3.168)$$

to quadrature,

$$\theta(z) = z - \frac{1}{\int_0^1 g(\zeta) d\zeta} \int_0^z g(\zeta) d\zeta \quad (3.169)$$

$$g(\zeta) = \exp\left(\int_0^\zeta w(\xi) d\xi\right). \quad (3.170)$$

The benefit of using this value of β is revealed by examining the structure of the solution. It satisfies the maximum principle since

$$-1 \leq -\frac{1}{\int_0^1 g(\zeta) d\zeta} \int_0^z g(\zeta) d\zeta \leq \theta(z) \leq z \leq 1. \quad (3.171)$$

The inequalities follow from the positivity of $g(\zeta)$ and z . Numerical solutions to (3.168) with w as in (3.167) suggest that the optimal scaling of a Nusselt number defined by $\alpha = 0$ seems to be $\text{Pe}^{2/3}$, that is to say, asymptotically $\text{Nu} \sim \text{Pe}^{2/3}$ as was derived by the background method.

Finding analytic representations to for θ that satisfy the advection-diffusion equation for non-constant incompressible flow fields is difficult, but there are a few cases that can be solved exactly. For example, as noted in §3.5, if the vertical velocity is zero, i.e. $w = 0$, the only solution is $\theta = 0$, regardless of the functional form of the horizontal velocities. Hasanazadeh et al. in [32] found non-trivial asymptotic solutions to the advection-diffusion equation. The derivation is as follows. We start with the ansatz

$$u = A \cos(kx) F'(z) \quad (3.172)$$

$$w = Ak \sin(kx) F(z) \quad (3.173)$$

$$\theta + \varphi = \sin(kx) G_1(z) \quad (3.174)$$

$$\theta - \varphi = G_2(z) \quad (3.175)$$

Here $k = \frac{\pi}{\Gamma}$. Where $\theta + \varphi$ and $\theta - \varphi$ satisfy

$$u\partial_x\theta + w\partial_z\theta = \partial_{xx}\theta + \partial_{zz}\theta + w \quad (3.176)$$

$$-u\partial_x\varphi - w\partial_z\varphi = \partial_{xx}\varphi + \partial_{zz}\varphi + w \quad (3.177)$$

\Rightarrow

$$u\partial_x(\theta - \varphi) + w\partial_z(\theta - \varphi) = \partial_{xx}(\theta + \varphi) + \partial_{zz}(\theta + \varphi) + 2w \quad (3.178)$$

$$u\partial_x(\theta + \varphi) + w\partial_z(\theta + \varphi) = \partial_{xx}(\theta - \varphi) + \partial_{zz}(\theta - \varphi) \quad (3.179)$$

These equations with our ansatz become ordinary differential equations for $G_1(z)$, $G_2(z)$, and F

$$AkFG'_2 = -k^2G_1 + G''_1 + 2AkF \quad (3.180)$$

$$FG'_1 + F'G_1 = \frac{2}{Ak}G''_2 \quad (3.181)$$

$$FG'_1 = G_1F', \quad (3.182)$$

along with boundary conditions $F(0) = F(1) = G_1(1) = G_1(0) = G_2(0) = G_2(1) = 0$. The solutions to these set of equations are well represented by exponentials as noted in [32], thus the asymptotic solution takes the form,

$$u(x, z) = \frac{1}{\sqrt{2\mu}} \left(1 - \frac{\pi}{2\Gamma} \sqrt{2\mu}\right) \cos\left(\frac{\pi}{\Gamma}x\right) H'(z) \quad (3.183)$$

$$w(x, z) = \frac{1}{\sqrt{2\mu}} \frac{\pi}{\Gamma} \left(1 - \frac{\pi}{2\Gamma} \sqrt{2\mu}\right) \sin\left(\frac{\pi}{\Gamma}x\right) H(z) \quad (3.184)$$

$$\theta(x, z) = \frac{1}{2} \left(1 - \frac{\pi}{2\Gamma} \sqrt{2\mu}\right) \left(\sin\left(\frac{\pi}{\Gamma}x\right) + 2z - 1\right) H(z) \quad (3.185)$$

$$\varphi(x, z) = \frac{1}{2} \left(1 - \frac{\pi}{2\Gamma} \sqrt{2\mu}\right) \left(\sin\left(\frac{\pi}{\Gamma}x\right) - 2z + 1\right) H(z) \quad (3.186)$$

$$H(z) = \tanh\left(\frac{z}{\delta}\right) \tanh\left(\frac{1-z}{\delta}\right) \quad (3.187)$$

$$\delta^{-1} \equiv \left(1 - \frac{\pi}{2\Gamma} \sqrt{2\mu}\right) \frac{\pi}{2\Gamma\sqrt{2\mu}}. \quad (3.188)$$

It is required that $\pi\sqrt{2\mu} < 2\Gamma$ for the solutions to remain valid. The parameter μ is related to Pe implicitly and may be calculated by noting that, asymptotically,

$$\int_0^1 [H(z)]^2 dz \sim 1 - 2\delta \quad (3.189)$$

$$\int_0^1 [H'(z)]^2 dz \sim \frac{4}{3}\delta^{-1} \quad (3.190)$$

$$\int_0^1 [H''(z)]^2 dz \sim \frac{16}{15}\delta^{-3}. \quad (3.191)$$

The original motivation for considering this class of solutions comes from examining a related optimal control problem where the constraint on the velocity field is not $\langle \nabla \vec{u} : \nabla \vec{u} \rangle = \text{Pe}^2$ but rather $\langle \vec{u} \cdot \vec{u} \rangle$. Note that $H(z)$ resembles the piecewise function (3.167).

Solving for the best aspect ratio² in order to maximize the Nusselt number yields a

²For our purposes one may use $\Gamma = \pi\sqrt{8\mu}$. This makes it so that Nu scales like μ^{-1} and Pe^2 scales like μ^{-4} .

transport value of $Nu-1 \sim Pe^{1/2}$, well below the $Pe^{2/3}$ scaling of the bound in §3.4. The smallness of the boundary layers for the vertical component w incurs a large penalty on magnitude of the $\langle(\partial_z u)^2\rangle$ term, which introduces an extremely large value of Pe into the system. This aspect of penalty is what prevents this flow field from achieving the optimal possible scaling. Indeed, if we could neglect the $\langle(\partial_z u)^2\rangle$ term, we would achieve an upper bound scaling of $Pe^{2/3}$. Here it is the incompressibility constraint that is preventing us from achieving a supposedly “optimal” scaling. Taking everything together we see that we must consider both the incompressibility constraint and the enforcement of the advection-diffusion equation in order to improve the bounds.

CHAPTER 4

Numerical Discretization and Solutions

We now turn attention to numerically solving the Euler-Lagrange equations for the optimal velocity field. In Hassanzadeh et al. [33] the Euler-Lagrange equations for 2D stress-free boundary conditions were solved numerically by using Newton’s method. However, there were limitations in spatial resolution due to the inversion of large matrix sizes. If there are relatively few degrees of freedom this is not a problem but even modest accuracy for the Euler-Lagrange equations involves inverting matrices of sizes $10^2 \times 10^2$. In the asymptotic regime where nonlinearity dominates (for Péclet of around 10^3) the matrices are $10^4 \times 10^4$ or larger in two dimensions.

Utilizing Newton’s method also leads to less confidence that one has found the global optimum. Typically a computation is performed in the linear regime and then numerically continued in the nonlinear regime. It is possible to “miss” more optimal solutions due to saddle node bifurcations. Furthermore, if one wants to generalize to three dimensions or time dependent flows, it is necessary to use a different method.

To remedy the some of these problems we employ gradient ascent strategy to solve for local maxima. Discretizations using gradient ascent in this setting presents some additional subtleties. In §4.1 we formulate the time-stepping procedure for gradient ascent in the following contexts: steady state, periodic, and time-dependent flows. This leads us to consider various methods for handling time-evolution as well.

The time evolution (in either gradient ascent or the time-dependent optimal control problem) reduces to solving two boundary value problems, a modified Poisson’s equation and a modified Stokes equation, that we describe how to solve in §4.2. Spectral methods are natural for these problems since our domain is periodic in the horizontal directions and bounded in the vertical. We represent numerical solutions by Fourier series in the horizontal directions and Chebyshev series in the vertical but we do not use the usual methods [34, 35] for the Chebyshev direction. We instead adopt spectral integration as the method of choice for solving the resulting boundary value problems. The modified Stokes equation and

modified Poisson’s equation are discussed in this context. We then apply these techniques to solve the first-order optimality conditions and present solutions to the Euler-Lagrange equations as well as various scalings with respect to the Péclet constraint in §4.3.

4.1 Gradient Ascent

Finding the global maximum of a function is a challenging task for a generic function, even in the one dimensional context. One can compute a finite set of test points and choose the one that does the best, but this leads to little confidence that one has found a good candidate for a maximum. However, the maximum of a differentiable function $f : \mathbb{R}^n \rightarrow \mathbb{R}$ is characterized the first-order optimality condition

$$0 = \nabla f(x) \tag{4.1}$$

where $\nabla f : \mathbb{R}^n \rightarrow \mathbb{R}^n$. Typically there are fewer points that satisfy (4.1) but there are still problems with this approach. One is that the set of solutions to equation 4.1 could still be large, leading to the same problem as before. Another is that equation 4.1 could give spurious answers; saddle points and minima also satisfy the equation. Lastly, (4.1) may be difficult to solve.

A standard method to solve the (4.1) is gradient ascent. This involves introducing a time derivative on the left hand side and considering the dynamical system

$$\dot{x} = \nabla f(x), \tag{4.2}$$

where every local maximum of $\nabla f(x)$ is an attracting fixed point of the system. Thus for generic initial conditions¹ the gradient ascent procedure will provide a method for marching towards a local maximum. There are few variations of this theme.

Adding higher order derivatives on the left hand side leads to the time-marching method

$$\ddot{x} + \beta \dot{x} = \nabla f, \tag{4.3}$$

where β is some real number. With a proper choice of β one may attain significantly enhanced convergence [36]. Here one is lead to having a “momentum” term in the gradient ascent procedure.

Applying an invertable “preconditioner” $P : \mathbb{R}^n \rightarrow \mathbb{R}^n$ such that $P(0) = 0$ leads to a

¹If one starts at a local minima or saddle point $\nabla f = 0$. In the presence of rounding error, time-marching would move us away from these unstable fixed points but it may take a long time depending on the stability.

different system of equations to solve

$$0 = P(\nabla f(x)). \quad (4.4)$$

The zeros of this system are the same as 4.1 since $\nabla f(x^*) = 0$ implies $P(\nabla f(x^*)) = 0$ and visa-versa. This new equation is time-marched via

$$\dot{x} = P(\nabla f(x)). \quad (4.5)$$

For example Newton's method may be viewed as choosing the inverse negative Jacobian of ∇f , $P = -J^{-1}(x)$, and using an Euler time-stepping scheme with timestep equal to 1,

$$\dot{x} = -J^{-1}(x)(\nabla f(x)) \Rightarrow x^{n+1} = x^n - J^{-1}(x^n)(\nabla f(x^n)). \quad (4.6)$$

There is a danger that the preconditioner will change the stability of the fixed point, meaning that we may no longer be converging to a local maxima, but rather a saddle point or minima.

Yet another option, perhaps best suited for finding global optima, is to implement stochastic gradient ascent

$$\dot{x} = \nabla f(x) + \chi\eta \quad (4.7)$$

where η is a noise term and $\chi : \mathbb{R}^n \rightarrow \mathbb{R}^n$ is a correlation matrix. In the infinite dimensional context we penalize the excitation of small scales through a proper choice of correlation matrix.

There is little change when generalizing all of these procedures to the infinite dimensional context; however, care must be taken when discretizing the infinite dimensional system to a finite one. Additionally there is a subtlety of when one chooses to discretize. If one discretizes the functional f and then computes the gradient associated with the finite dimensional system, this normally does not correspond to calculating the functional derivative of f and then discretizing. Succinctly stated, the operations of discretizing and differentiating do not normally commute. In this work we will numerically solve the maximization problem by discretizing the functional derivative.

Including constraints presents additional subtleties. As an example, let us look at

$$\text{Maximize } xy \tag{4.8}$$

subject to

$$y = 1 - x. \tag{4.9}$$

Think of y as the “state” and x as the “control”. This is equivalent to maximizing $x(1 - x)$ in which case $x = 1/2$ is the maximizer. We would like to see what happens when we introduce a Lagrange multiplier λ and perform gradient ascent.

The augmented function is

$$g(x, y, \lambda) = xy + \lambda(1 - x - y) \tag{4.10}$$

and the first-order optimality condition is

$$0 = \frac{\partial g}{\partial x} = y - \lambda \tag{4.11}$$

$$0 = \frac{\partial g}{\partial y} = x - \lambda \tag{4.12}$$

$$0 = \frac{\partial g}{\partial \lambda} = 1 - x - y. \tag{4.13}$$

This critical point is a saddle point of the function g as can be seen by calculating the Hessian, H ,

$$H = \begin{bmatrix} 0 & 1 & -1 \\ 1 & 0 & -1 \\ -1 & -1 & 0 \end{bmatrix} \tag{4.14}$$

which has eigenvalues and eigenvectors $-1, [-1, 0, 1]^T$, $-1, [-1, 2, 1]^T$ and $2, [1, 1, -1]^T$.

Thus gradient ascent in the form

$$\frac{d}{dt} \begin{bmatrix} x \\ y \\ \lambda \end{bmatrix} = \begin{bmatrix} 0 & 1 & -1 \\ 1 & 0 & -1 \\ -1 & -1 & 0 \end{bmatrix} \begin{bmatrix} x \\ y \\ \lambda \end{bmatrix} + \begin{bmatrix} 0 \\ 0 \\ 1 \end{bmatrix} \tag{4.15}$$

will not converge to a local maximum. If we explicitly enforce the y and λ equations–

implying that $x = \lambda$ and $y = 1 - x$ —and time march forward, we would instead be evolving

$$\dot{x} = 1 - 2x, \quad (4.16)$$

which converges to $x = 1/2$, as expected.

With proper preconditioning we can still use gradient ascent on the full system. Interchanging where we place the evolution of the adjoint and the state variables leads to

$$\frac{d}{dt} \begin{bmatrix} x \\ \lambda \\ y \end{bmatrix} = \begin{bmatrix} 0 & 1 & -1 \\ 1 & 0 & -1 \\ -1 & -1 & 0 \end{bmatrix} \begin{bmatrix} x \\ y \\ \lambda \end{bmatrix} + \begin{bmatrix} 0 \\ 0 \\ 1 \end{bmatrix} \quad (4.17)$$

$$\Leftrightarrow \quad (4.18)$$

$$\frac{d}{dt} \begin{bmatrix} x \\ y \\ \lambda \end{bmatrix} = \begin{bmatrix} 0 & 1 & -1 \\ -1 & -1 & 0 \\ 1 & 0 & -1 \end{bmatrix} \begin{bmatrix} x \\ y \\ \lambda \end{bmatrix} + \begin{bmatrix} 0 \\ 1 \\ 0 \end{bmatrix}. \quad (4.19)$$

This new matrix has eigenvalues $\{\frac{1}{2}(-1 + i\sqrt{7}), \frac{1}{2}(-1 - i\sqrt{7}), -1\}$ and thus will evolve towards $[x, y, \lambda] = [1/2, 1/2, 1/2]$. This amounts to using a preconditioner of the form

$$P = \begin{bmatrix} 1 & 0 & 0 \\ 0 & 0 & 1 \\ 0 & 1 & 0 \end{bmatrix}. \quad (4.20)$$

Heuristically, the success of this preconditioner may be reasoned as follows: For an x that is independent of time the equation $\dot{y} = 1 - x - y$ will evolve towards $y = 1 - x$ and $\dot{\lambda} = x - \lambda$ will evolve towards x . The time evolution of y and λ is an iterative way to solve the linear equations $0 = 1 - x - y$ and $0 = x - \lambda$. At each time step the evolution of the y and λ equations give an approximation to the gradient associated with the ascent procedure that fully enforces the constraints.

This method of solving the first-order optimality condition is very similar to the method that we will use to solve the Euler-Lagrange equations. Additional subtleties related to the implementation of a numerical scheme are discussed in the following subsections.

4.1.1 Gradient Ascent in the Optimal Control System

In order to numerically solve

$$\text{Maximize } \langle wT \rangle \quad (4.21)$$

subject to

$$\partial_t T + \vec{u} \cdot \nabla T = \Delta T \quad (4.22)$$

$$\langle \nabla \vec{u} : \nabla \vec{u} \rangle = \text{Pe}^2 \quad (4.23)$$

$$\nabla \cdot \vec{u} = 0 \quad (4.24)$$

with suitable boundary conditions we form the augmented functional (substituting $\theta = T - (1 - z)$),

$$\mathcal{F} = \left\langle w\theta - \varphi (\partial_t \theta + \vec{u} \cdot \nabla \theta - \Delta \theta - w) + p(\nabla \cdot \vec{u}) + \frac{\mu}{2}(\text{Pe}^2 - \nabla \vec{u} : \nabla \vec{u}) \right\rangle, \quad (4.25)$$

and derive the Euler-Lagrange equations:

$$0 = \frac{\delta \mathcal{F}}{\delta \varphi} = \partial_t \theta + \vec{u} \cdot \nabla \theta - \Delta \theta - w \quad (4.26)$$

$$0 = \frac{\delta \mathcal{F}}{\delta p} = \nabla \cdot \vec{u} \quad (4.27)$$

$$0 = \frac{\delta \mathcal{F}}{\delta \mu} = \frac{1}{2} \langle \text{Pe}^2 - \nabla \vec{u} : \nabla \vec{u} \rangle \quad (4.28)$$

$$0 = \frac{\delta \mathcal{F}}{\delta \theta} = -\partial_t \varphi - \vec{u} \cdot \nabla \varphi - \Delta \varphi - w \quad (4.29)$$

$$0 = \frac{\delta \mathcal{F}}{\delta \vec{u}} = \mu \Delta \vec{u} + (\theta + \varphi) \hat{e}_3 - \varphi \nabla \theta - \nabla p. \quad (4.30)$$

The domain is periodic in the $x \in [0, \Gamma_1]$ and $y \in [0, \Gamma_2]$ variables, bounded in the $z \in [0, 1]$, and either independent of t (steady state), periodic, or long time² $t \in [0, \mathcal{T}]$ where \mathcal{T} is “large”. In the time-dependent problem we take the initial solution to be in the conductive state $\theta = 0$ in which case the natural³ final condition for the adjoint is $\varphi = 0$.

²As a practical point we cannot compute the answer on the infinite domain. Since we expect the answer to be mostly steady one criteria that may be used to evaluate that one has waited long enough is to compute $\partial_t \vec{u}$ with respect to a norm and quantify \mathcal{T} as large if $\|\partial_t \vec{u}\|$ is small.

³One may choose this in two equivalent ways, the first is by demanding that the integration by parts formula works when deriving the Euler-Lagrange equations. The second is by setting variational derivative with respect to all final conditions of φ equal to zero.

Denote the Lagrangian density⁴ by

$$\mathcal{L} = w\theta - \nabla\varphi \cdot \nabla\theta - \varphi\partial_t\theta - \varphi\vec{u} \cdot \nabla\theta + \varphi w - \nabla p \cdot \vec{u} + \frac{\mu}{2}(\text{Pe}^2 - \nabla\vec{u} : \nabla\vec{u}), \quad (4.31)$$

and the Hamiltonian densities by

$$(\phi_1, \phi_2, \phi_3, \phi_4, \phi_5, \phi_6) = (u, v, w, \theta, \varphi, p) \quad (4.32)$$

$$\mathcal{H}^t = \partial_t\phi_j \frac{\partial\mathcal{L}}{\partial\partial_t\phi_j} - \mathcal{L} \quad (4.33)$$

$$\mathcal{H}^x = \partial_x\phi_j \frac{\partial\mathcal{L}}{\partial\partial_x\phi_j} - \mathcal{L} \quad (4.34)$$

$$\mathcal{H}^y = \partial_y\phi_j \frac{\partial\mathcal{L}}{\partial\partial_y\phi_j} - \mathcal{L}, \quad (4.35)$$

where repeated j indices are summed over for $j = 1, \dots, 6$. For the steady state case we augment the Euler-Lagrange equations with conditions that pick out the optimal domain size,

$$0 = \frac{\delta\mathcal{F}}{\delta\Gamma_1} = -\frac{1}{\Gamma_1}\langle\mathcal{L}\rangle - \frac{1}{\Gamma_1\Gamma_2} \int_0^{\Gamma_2} \int_0^1 \mathcal{H}^x dz dy \quad (4.36)$$

$$0 = \frac{\delta\mathcal{F}}{\delta\Gamma_2} = -\frac{1}{\Gamma_2}\langle\mathcal{L}\rangle - \frac{1}{\Gamma_1\Gamma_2} \int_0^{\Gamma_1} \int_0^1 \mathcal{H}^y dz dx \quad (4.37)$$

and in the periodic case we augment with a condition that picks out an optimal time period \mathcal{T} (if one exists),

$$0 = \frac{\delta\mathcal{F}}{\delta\mathcal{T}} = -\frac{1}{\mathcal{T}}\langle\mathcal{L}\rangle - \frac{1}{\mathcal{T}\Gamma_1\Gamma_2} \int_0^{\Gamma_1} \int_0^{\Gamma_2} \int_0^1 \mathcal{H}^t dz dy dx. \quad (4.38)$$

See Appendix A for details of the derivation.

The optimism with regards to the existence of an optimal domain size comes from previous experience with the system in the case of stress-free boundary conditions by Hasanzadeh et al. [33]. In that study it appeared that there is a unique optimal aspect ratio that maximizes the Nusselt number. The pessimism with regards to an optimal time period T for periodic solutions comes from experience with the Lorenz and Double Lorenz systems where the steady state solutions were the global optimizers.

The gradient ascent procedure needs to be modified depending on what we assume for the time domain. We will discuss three different cases for performing gradient ascent and heuristic reasoning as to why we expect convergence. As a matter of terminology

⁴Note that $\langle\mathcal{L}\rangle = \mathcal{F}$ via integration by parts.

we will use “ascent-time” for time-steps associated with the gradient ascent procedure to differentiate it from “regular” time.

We make the following observations that will help us with the gradient ascent procedure:

1. If $\frac{\delta \mathcal{F}}{\delta \varphi} = 0$ then we are enforcing the advection-diffusion equation. Here θ is a unique function of \vec{u} for a fixed initial condition or in the long time limit in the periodic/steady state cases for any initial condition. However, \vec{u} is not a unique function of θ . For example both $\vec{u} = 0$ and $\vec{u} = u(z)\hat{x} + 0\hat{z}$ have $\theta = 0$ as a solution in the steady case.
2. The previous statement holds for $\frac{\delta \mathcal{F}}{\delta \theta} = 0$ as well, the adjoint equation.
3. If \vec{u} has a symmetry we may not need to solve both $\frac{\delta \mathcal{F}}{\delta \theta} = 0$ and $\frac{\delta \mathcal{F}}{\delta \varphi} = 0$, but rather solve one and use symmetry to compute the other.
4. It is unnecessary to enforce $0 = \frac{\delta \mathcal{F}}{\delta \mu} = (\text{Pe}^2 - \nabla \vec{u} : \nabla \vec{u})$ since a choice of μ implicitly determines Pe. In other words we may fix μ and determine the value of Pe after convergence.
5. If $\frac{\delta \mathcal{F}}{\delta \varphi} = 0$ and $\frac{\delta \mathcal{F}}{\delta p} = 0$, then \vec{u} is a unique function of θ , φ , and μ . However, this equation alone does not uniquely determine θ and φ given \vec{u} and μ . This optimality condition is Stokes equation and this equation must hold at each point in time.

In the next three subsections we present gradient ascent procedures for the three different situations—time dependent, time periodic, and steady—as well as methods for evolving equations forward in time.

4.1.2 Time Dependent

For the time-dependent problem we fix μ , take the initial temperature to be in the conductive state, and the final adjoint to be zero. The high level overview for the type of gradient ascent

procedure that we use will be as follows:

$$0 = \frac{\delta \mathcal{F}}{\delta \varphi} = \partial_t \theta + \vec{u} \cdot \nabla \theta - \Delta \theta - w \quad (4.39)$$

$$0 = \frac{\delta \mathcal{F}}{\delta p} = \nabla \cdot \vec{u} \quad (4.40)$$

$$0 = \frac{\delta \mathcal{F}}{\delta \theta} = -\partial_t \varphi - \vec{u} \cdot \nabla \varphi - \Delta \varphi - w \quad (4.41)$$

$$\partial_\tau \vec{u} = P \left(\frac{\delta \mathcal{F}}{\delta \vec{u}} \right) = P (\mu \Delta \vec{u} + (\theta + \varphi) \hat{e}_3 - \varphi \nabla \theta - \nabla p), \quad (4.42)$$

where P is an appropriate preconditioner described shortly. Algorithmically we proceed as follows,

1. Fix μ and choose an incompressible flow field at each point in space and time.
2. Solve the time-dependent advection-diffusion/adjoint equation by marching forwards/backwards.
3. Update the optimality condition and at each point in time and space via (4.42).
4. Repeat steps 2 and 3 until convergence is achieved.

For step 1 we may generate a good guess for \vec{u} by numerical continuation from previous values of μ (implicitly Pe). For example, we may compute solutions in the low Péclet (high μ) regime and numerically continue to higher Péclet (low μ). Since we expect the steady solutions to be the most optimal, we can start with a time-independent field as a preliminary guess to the time-dependent \vec{u} and then allow the gradient ascent procedure to modify the \vec{u} to a fully time-dependent solution. It is expected that the solution remains steady for the majority of the time, with minor modifications at the initial and final time. The initial time serves as a wind up period to “kick” the temperature field out of the conductive state and into the optimal steady state whereas the final time has an analogous wind up period (backwards in time) for the adjoint field. There is a danger that using the steady as the initial guess only generates a local maximum.

Let us go into step 2 into more detail. To solve the advection-diffusion/adjoint equation we must evolve the state equation

$$\partial_t \theta = -\vec{u} \cdot \nabla \theta + \Delta \theta + w \quad (4.43)$$

forward in time and the adjoint equation

$$\partial_t \varphi = \vec{u} \cdot \nabla \varphi + \Delta \varphi + w \quad (4.44)$$

backward in time. There are various methods that one may employ to evolve such equations forward. In order to use Runge-Kutta methods we would need to interpolate the control variable \vec{u} at intermediary points in ascent-time. This introduces interpolation errors and additional computational costs. Instead we opt for simpler multi-step schemes that automatically take into account the already-computed times for the control \vec{u} . These multi-step methods are described in §4.1.5. These methods result in boundary-value problems to be solved at every time-step. We discuss how to solve these in §4.2.1.

To evolve (4.42) we time-march according to the methods in §4.1.5 and focus on two different preconditioners: the identity operator and the inverse Stokes operator. The inverse Stokes operator is defined as the solution to Stokes equation

$$\Delta \vec{u} = \vec{f} - \nabla p \tag{4.45}$$

$$\nabla \cdot \vec{u} = 0 \tag{4.46}$$

with respect to appropriate boundary conditions. We write $S^{-1}\vec{f} = \vec{u}$ and show how to solve the resulting boundary value problems in §4.2.2.

From a computational aspect there is a large memory requirement since $\vec{u}(x, t)$ needs to be stored at each point in time and in order to update \vec{u} via the optimality condition we need to know $\theta(x, t)$ and $\varphi(x, t)$ for each t . Checkpointing is a popular strategy in other optimal control problems, but that heavily relies on the fact that one is solving for an initial condition as opposed to a flow field at each point in time. It can be used in a limited sense in this context since one does not have to store θ and φ at each point in time, but rather can reconstruct them at certain checkpoints. But this still does not circumvent the necessity of knowing \vec{u} at each point in time and space. In two dimensions this is not too much of a limitation, but even in the low Pe setting approximately 1000 evenly spaced time-steps were necessary for proper convergence of the time-dependent problem.

We opted for limiting computational results to the steady case due to the additional computational complexity of the fully time-dependent problem as well as insights from the Lorenz and Double Lorenz system where steady solutions were shown to be optimal. For the cases that we have attempted, time-dependence seemed to merely kick the conductive state into the steady state case, with “wind up” and “settling down” periods at the initial and final times. These computations were by no means exhaustive and further study regarding the necessity of time-dependence is required.

4.1.3 Time Periodic

The top level algorithm for solving the time-periodic problem resembles the time-dependent algorithm of the previous section. We use the same gradient ascent procedure,

$$0 = \frac{\delta \mathcal{F}}{\delta \varphi} = \partial_t \theta + \vec{u} \cdot \nabla \theta - \Delta \theta - w \quad (4.47)$$

$$0 = \frac{\delta \mathcal{F}}{\delta p} = \nabla \cdot \vec{u} \quad (4.48)$$

$$0 = \frac{\delta \mathcal{F}}{\delta \theta} = -\partial_t \varphi - \vec{u} \cdot \nabla \varphi - \Delta \varphi - w \quad (4.49)$$

$$\partial_\tau \vec{u} = P \left(\frac{\delta \mathcal{F}}{\delta \vec{u}} \right) = P (\mu \Delta \vec{u} + (\theta + \varphi) \hat{e}_3 - \varphi \nabla \theta - \nabla p), \quad (4.50)$$

with a similar loop structure:

1. Fix μ and choose an incompressible time-periodic flow field \vec{u} at each point in space and time.
2. Solve for time-periodic solutions to the advection-diffusion/adjoint equation, by marching forwards/backwards until convergence to a time-periodic solution occurs.
3. Update the optimality condition and at each point in time and space via (4.42).
4. Repeat steps 2 and 3 until convergence has been achieved.

We solve the problem in the linear regime for an initial flow field and numerically continue to higher values of Péclet (equivalently smaller values of μ). Or we could just as readily construct a suboptimal flow field and let the gradient ascent procedure converge to the optimal solution.

Consider step 2 in more detail. Given a time-periodic vector field \vec{u} with period \mathcal{T} , we will show that θ must also converge to a time periodic function in the long time limit. First observe that $\theta(x, t)$ and $\theta(x, t + \mathcal{T})$ satisfy the same equation of motion since

$$\partial_t \theta(\vec{x}, t) + \vec{u}(\vec{x}, t) \cdot \nabla \theta(\vec{x}, t) = \Delta \theta(\vec{x}, t) + w(\vec{x}, t) \quad (4.51)$$

\Rightarrow

$$\partial_t \theta(\vec{x}, t + \mathcal{T}) + \vec{u}(\vec{x}, t + \mathcal{T}) \cdot \nabla \theta(\vec{x}, t + \mathcal{T}) = \Delta \theta(\vec{x}, t + \mathcal{T}) + w(\vec{x}, t + \mathcal{T}) \quad (4.52)$$

\Rightarrow

$$\partial_t \theta(\vec{x}, t + \mathcal{T}) + \vec{u}(\vec{x}, t) \cdot \nabla \theta(\vec{x}, t + \mathcal{T}) = \Delta \theta(\vec{x}, t + \mathcal{T}) + w(\vec{x}, t) \quad (4.53)$$

where the last line follows by the periodicity of \vec{u} . Taking the difference of the two equations, multiplying through by $\theta(x, t) - \theta(x, t + \mathcal{T})$, integrating with respect to the spatial coordinates, integrating by parts, and making use of incompressibility yields

$$\partial_t \int_{\Omega} [\theta(x, t) - \theta(x, t + \mathcal{T})]^2 = - \int_{\Omega} |\nabla [\theta(x, t) - \theta(x, t + \mathcal{T})]|^2 \quad (4.54)$$

$$\leq -C \int_{\Omega} [\theta(x, t) - \theta(x, t + \mathcal{T})]^2 \quad (4.55)$$

\Rightarrow

$$\int_{\Omega} [\theta(x, t) - \theta(x, t + \mathcal{T})]^2 \leq \int_{\Omega} [\theta(x, 0) - \theta(x, 0 + \mathcal{T})]^2 \exp(-Ct), \quad (4.56)$$

where C is the Poincaré constant. From this we see that $\theta(x, t) - \theta(x, t + \mathcal{T}) \rightarrow 0$ as $t \rightarrow \infty$, suggesting that θ will converge to a periodic solution with period \mathcal{T} . The same result holds for φ evolved backwards in time. Note that if θ and φ are periodic with period \mathcal{T} the optimality condition for \vec{u} is also guaranteed to be \mathcal{T} periodic. Hence if we guess periodic solutions the gradient-ascent procedure will continue to generate periodic solutions.

4.1.4 Steady

For the steady solution we do not use the algorithms described in the previous section but instead specialize to take advantage of the structure of the time-independent solutions. The top level algorithm is more complicated but results in much faster convergence than using the previous schemes. This method was developed due to the slow convergence of the steady advection-diffusion equation and the primary insight to its development came from the observation with regards to constrained optimization in §4.1.

Fix $\text{Pe} > 0$. The gradient ascent procedure in two dimensions is:

$$-\partial_{\tau_{\theta}} \theta = \frac{\delta \mathcal{F}}{\delta \varphi} = \vec{u} \cdot \nabla \theta - \Delta \theta - w \quad (4.57)$$

$$0 = \frac{\delta \mathcal{F}}{\delta p} = \nabla \cdot \vec{u} \quad (4.58)$$

$$\varphi = \mathcal{S}(\theta) \quad (4.59)$$

$$\partial_{\tau} \vec{u} = S^{-1} \left(\frac{\delta \mathcal{F}}{\delta \vec{u}} \right) = S^{-1} (\mu \Delta \vec{u} + (\theta + \varphi) \hat{e}_3 - \varphi \nabla \theta - \nabla p) \quad (4.60)$$

$$\partial_{\tau_1} \Gamma_1 = (\Gamma_1)^2 \left\langle \frac{\delta \mathcal{F}}{\delta \Gamma_1} \right\rangle = \Gamma_1 \langle \mathcal{H}^x - \mathcal{L} \rangle \quad (4.61)$$

$$\partial_{\tau_{\mu}} \mu = \frac{\mu}{\text{Pe}^2} \frac{\delta \mathcal{F}}{\delta \mu} = \mu \left(1 - \frac{\langle \nabla \vec{u} : \nabla \vec{u} \rangle}{\text{Pe}^2} \right) \quad (4.62)$$

where \mathcal{S} is a function that computes φ from θ using symmetry, and S^{-1} is the inverse Stokes operator. In (4.61) multiplication by $(\Gamma_1)^2$ is an invertible preconditioner whose effect is to invoke percentage, as opposed to absolute, changes to Γ_1 once we discretize time. The same holds for the μ evolution equation. The reason why we compute the average value of $\delta\mathcal{F}/\delta\Gamma_1$ as opposed to its value at the endpoint may seem like a relaxation, but this is not the case. Hamiltonians that satisfy the Euler-Lagrange equations are independent of where they are evaluated.

Algorithmically we proceed as follows,

1. Fix Pe and choose an incompressible steady flow field.
2. March one time step of the time-dependent advection-diffusion equation.
3. Use symmetry to compute adjoint equation.
4. Update the optimality condition and at each point in time and space via (4.60).
5. Compute the Hamiltonian and the Nusselt number in order to update the aspect ratio via (4.61).
6. Update the Lagrange multiplier μ via (4.62).
7. Repeat steps 2-5 until convergence has been achieved.

One difference between this algorithm and the previous ones is that the evolution equation for φ and θ are being time-stepped together with the optimality equation. Furthermore we are computing the aspect ratio evolution as well as the μ evolution. This means that the domain is changing every time-step as well as the value of μ .

In step 3 the symmetry condition was imposed based off of the structure of optimal flow fields from the more standard evolution (as in the previous section). It turns out that for those flow fields

$$\varphi(x, z) = \theta(x, -(z + 1/2) + 1/2), \quad (4.63)$$

meaning that φ is θ reflected on the $z = 1/2$ plane. The reason these two may be related comes from the symmetry of the optimal flow field itself.

As in the previous algorithms the method for guessing an optimal flow field \vec{u} for step 1 comes from numerical continuation from low to high values of the Péclet constraint. For low values of Pe the linearized problem may be related to linearized Rayleigh-Bénard

convection under the transcription

$$\frac{2}{\mu} \mapsto \text{Ra}. \quad (4.64)$$

Thus we may verify that Γ_1 and μ are converging to the correct aspect ratio and critical Rayleigh number for the onset of convection.

4.1.5 Time Evolution Discretization

Suppose that

$$\dot{x} = \mathcal{L}x + \mathcal{N}(x) + f \quad (4.65)$$

where x is the state vector, \mathcal{L} is a linear operator (i.e. Laplacian here), \mathcal{N} is a nonlinear operator (terms involving the advection operator $\vec{u} \cdot \nabla$), and f is a forcing function (such as pressure). Both the advection-diffusion/adjoint equation and the gradient-ascent procedures generate evolutions of this form. We follow Viswanath in [37] and consider time-stepping schemes of the form

$$\frac{1}{\Delta t} \left(\gamma x^{n+1} + \sum_{j=0}^{s-1} a_j x^{n-j} \right) = \sum_{j=0}^{s-1} b_j \mathcal{N}(x^{n-j}) + \mathcal{L}x^{n+1} + f^{n+1}. \quad (4.66)$$

where s is the order of the time-stepping scheme, a_i and b_i are parameters, and Δt is the time-step size. The parameters values for orders $s = 1, 2$ and 3 are

$$s = 1, \quad \gamma = 1, \quad a_0 = -1, \quad b_0 = 1 \quad (4.67)$$

$$s = 2, \quad \gamma = 3/2, \quad a_0 = -2, \quad a_1 = 1/2, \quad b_0 = 2, \quad b_1 = -1 \quad (4.68)$$

$$s = 3, \quad \gamma = 11/6, \quad a_0 = -3, \quad a_1 = 3/2, \quad a_2 = -1/3, \quad b_0 = 3, \quad b_1 = -3, \quad b_2 = 1. \quad (4.69)$$

For example with $s = 1$ and the advection-diffusion equation

$$\partial_t \theta = -\vec{u} \cdot \nabla \theta + \Delta \theta + w \quad (4.70)$$

we use

$$\left(\Delta - \frac{1}{\Delta t} \mathbb{I} \right) \theta^{n+1} = \vec{u}^n \cdot \nabla \theta^n - w^n - \frac{1}{\Delta t} \theta^n. \quad (4.71)$$

Thus for each time-step we must solve a modified Poisson's equation of the form

$$(\Delta - c\mathbb{I})\theta = f \quad (4.72)$$

where $c \geq 0$ and we have made the transcription

$$\theta^{n+1} \mapsto \theta \quad (4.73)$$

$$\frac{1}{\Delta t} \mapsto c \quad (4.74)$$

$$\vec{u}^n \cdot \nabla \theta^n - w^n - \frac{1}{\Delta t} \theta^n \mapsto f. \quad (4.75)$$

For updating the optimality condition with $s = 1$ one option is to use

$$\left(\mu \Delta - \frac{1}{\Delta \tau} \mathbb{I} \right) \vec{u}^{n+1} = -(\varphi^n + \theta^n) \hat{e}_3 + \varphi^n \nabla \theta^n - \frac{1}{\Delta \tau} \vec{u}^n + \nabla p^{n+1} \quad (4.76)$$

$$\nabla \cdot \vec{u}^{n+1} = 0. \quad (4.77)$$

Each time-step involves solving modified Stokes equation

$$(\Delta - c\mathbb{I}) \vec{u} = \vec{f} + \nabla p \quad (4.78)$$

$$\nabla \cdot \vec{u} = 0 \quad (4.79)$$

where $c \geq 0$ and we have made the transcription

$$\vec{u}^{n+1} \mapsto \vec{u} \quad (4.80)$$

$$p^{n+1} \mapsto p \quad (4.81)$$

$$\frac{1}{\Delta \tau} \mapsto c \quad (4.82)$$

$$(\varphi^n + \theta^n) \hat{e}_3 + \varphi^n \nabla \theta^n - \frac{1}{\Delta \tau} \vec{u}^n \mapsto \vec{f}. \quad (4.83)$$

In the following section we describe how to solve these boundary value problems.

4.2 Spectral Methods

Taking the Fourier transform of (4.72) and (4.78) in the horizontal directions leads to the following set of ODE's to solve

$$(D^2 - \beta_{nl}^2) \theta_{nl} = f_{nl} \quad (4.84)$$

and

$$(D^2 - \beta_{nl}^2) \vec{u}_{nl} = \vec{f}_{nl} + Dp_{nl}\hat{z} + ik_n p_{nl}\hat{x} + ik_\ell p_{nl}\hat{y} \quad (4.85)$$

$$ik_n u_{nl} + ik_\ell v_{nl} + Dw_{nl} = 0 \quad (4.86)$$

for $n, \ell \in \mathbb{Z}$, where D the derivative in the vertical direction, and

$$k_{nl}^2 = (k_n)^2 + (k_\ell)^2 \quad (4.87)$$

$$\beta_{nl}^2 = k_{nl}^2 + c \quad (4.88)$$

$$k_n = \frac{n\pi}{\Gamma_1} \quad (4.89)$$

$$k_\ell = \frac{\ell\pi}{\Gamma_2} \quad (4.90)$$

$$i = \sqrt{-1}. \quad (4.91)$$

The square root denotes the principle branch. Although we could discretize the spatial coordinates using Chebyshev matrices, we instead use spectral integration. This method of solving boundary value problems of the form

$$(D - k)y = f \quad (4.92)$$

subject to boundary conditions has numerous advantages over the differentiation matrix approach as in [35]. With spectral integration the operators that must be inverted have bounded condition numbers and are banded matrices as opposed to dense matrices with unbounded condition numbers.

Instead of solving for functions on $z \in [0, 1]$ it is more convenient to take $z \in [-1, 1]$ and then convert results back to the original domain. Solutions in the $z \in [0, 1]$ domain—denoted by subscripted 1's as in θ_1, \vec{u}_1 —are related to solutions in the $z \in [-1, 1]$ domain—denoted by subscripted 2's as in θ_2, \vec{u}_2 —via the following relations

$$\theta_1 = \frac{1}{2}\theta_2, \vec{u}_1 = 2\vec{u}_2, \text{Pe}_1 = 4\text{Pe}_2, (\text{Nu} - 1)_1 = (\text{Nu} - 1)_2, \mu_1 = \mu_2/16. \quad (4.93)$$

When performing calculations we use the $[-1, 1]$ domain but report results in terms of the original $z \in [0, 1]$ domain.

Computing averages (such as the Nusselt number) can be achieved with spectral accuracy. As mentioned in [34] the trapezoidal rule is spectrally accurate for periodic functions and for bounded domains there are quadrature weight formulas both in terms of the Chebyshev nodal and modal values.

4.2.1 Spectral Integration

As stated in the previous section all the numerical problems of this Chapter reduce to solving differential equations of the form

$$(D - k)y = f, \tag{4.94}$$

where $k \in \mathbb{R}$ and $z \in [-1, 1]$. The differential equation has the solution

$$y(z) = Ce^{kz} + e^{-kz} \int_{-1}^z e^{kx} f(x) dx, \tag{4.95}$$

where C enforces boundary or integral constraints. This reduces the problem to quadrature and indeed the method that we adopt implicitly constructs the solution in this manner as noted in [38].

To solve (4.94) we use a modern form of spectral integration developed by Viswanath [38]. The general principle is remarkably simple. First compute the homogeneous solution

$$(D - k)y^h = 0 \tag{4.96}$$

and then the particular solution

$$(D - k)y^p = f \tag{4.97}$$

so that the general solution is then a linear combination of the particular and homogeneous solution

$$y = Cy^h + y^p \tag{4.98}$$

where C is a constant that enforces boundary conditions or integral constraints. This basic decomposition of the general solution of an ordinary differential equation serves as the primary building block in the construction of solutions to (4.72) and (4.78).

We will now discuss how to construct y^h and y^p in the domain $z \in [-1, 1]$. First write y as Chebyshev expansion of the form

$$y(z) = \frac{y_0}{2}P_0 + \sum_{n=1}^{\infty} y_n P_n(z) \quad (4.99)$$

where $P_n(x)$ $n = 0, 1, 2, \dots$ are the Chebyshev polynomials defined by

$$P_n(z) = \cos(n \cos^{-1}(z)). \quad (4.100)$$

The factor of $1/2$ in front of the y_0 term is standard and convenient for formulas later on.

Let $\mathcal{T}_n(y)$ denote the n 'th Chebyshev coefficient of y , e.g.

$$\mathcal{T}_n(y) = y_n \quad (4.101)$$

$$\mathcal{T}_n\left(\int y\right) = \begin{cases} 0 & \text{for } n = 0 \\ \frac{y_{n-1} - y_{n+1}}{2n} & \text{for } n > 0 \end{cases} \quad (4.102)$$

where $\int y$ here denotes a particular anti-derivative of y . The coefficients may be computed by the linear operator

$$y_n = \frac{2}{\pi} \int_{-1}^1 y(x) \frac{P_n(x)}{\sqrt{1-x^2}} dx. \quad (4.103)$$

Instead of working with (4.94) directly we will work with the equation in integral form

$$y - k \int y = \int f + C \quad (4.104)$$

where C is a constant of integration. An important observation is that if $f = Dg$ for some function g , then we do not need to differentiate g to write it in the form (4.104) but rather we can directly use

$$y - k \int y = g + C. \quad (4.105)$$

In other words we can avoid numerically differentiating g .

Use the relation (4.102) to construct (4.104) as a system of equations for the Chebyshev

coefficients, i.e.

$$\mathcal{T}_n(y) - k\mathcal{T}_n\left(\int y\right) = \mathcal{T}_n\left(\int f\right) + \mathcal{T}_n(C) \quad (4.106)$$

\Rightarrow

$$y_0 = 2C \text{ for } n = 0 \quad (4.107)$$

$$y_n - k\frac{y_{n-1} - y_{n+1}}{2n} = \frac{f_{n-1} - f_{n+1}}{2n} \text{ for } n > 0 \quad (4.108)$$

The f_n are the Chebyshev coefficients of the forcing function f . Note that any choice of C will yield a particular solution to the problem, but will not enforce the proper boundary conditions. This is an infinite dimensional tridiagonal system of equations for the Chebyshev coefficients of y .

In order to be amenable to computation any such system of equations must be truncated. Thus we will assume that the solution y and forcing function f is well represented by a finite truncation

$$y(z) = \frac{y_0}{2} + \sum_{n=1}^{N-2} y_n P_n(z) + \frac{y_{N-1}}{2} P_{N-1}(z) \quad (4.109)$$

$$f(z) = \frac{f_0}{2} + \sum_{n=1}^{N-2} f_n P_n(z) + \frac{f_{N-1}}{2} P_{N-1}(z). \quad (4.110)$$

For example, with $N = 6$ we would have the following system of equations to solve,

$$\begin{bmatrix} 1 & 0 & 0 & 0 & 0 & 0 \\ -\frac{k}{2} & 1 & \frac{k}{2} & 0 & 0 & 0 \\ 0 & -\frac{k}{2.2} & 1 & \frac{k}{2.2} & 0 & 0 \\ 0 & 0 & -\frac{k}{2.3} & 1 & \frac{k}{2.3} & 0 \\ 0 & 0 & 0 & -\frac{k}{2.4} & 1 & 0 \\ 0 & 0 & 0 & 0 & -\frac{k}{2.5} & 1 \end{bmatrix} \begin{bmatrix} y_0 \\ y_1 \\ y_2 \\ y_3 \\ y_4 \\ y_5 \end{bmatrix} = \begin{bmatrix} 2C \\ \frac{f_0 - f_2}{2} \\ \frac{f_1 - f_3}{2.2} \\ \frac{f_2 - f_4}{2.3} \\ \frac{f_3 - f_5}{2.4} \\ \frac{f_4}{2.5} \end{bmatrix}. \quad (4.111)$$

The use of this finite representation has additional benefits. The Chebyshev spectral coefficients of y are related to the nodal values of y evaluated at $\cos(\pi j / (N - 1))$ for $j = 0, 1, \dots, N - 1$ via the fast-cosine transform. This allows us to quickly convert spectral coefficients into real space, and herein lies one of the many advantages of using a Chebyshev series.

We are now in a position to show how to construct numerical homogeneous and partic-

ular solutions y^h and y^p . To construct y^h we solve the following problem

$$(D - k)v = \frac{k}{2} \quad (4.112)$$

subject to $\mathcal{T}_0(v) = 0$. The general solution to (4.112) is

$$v = Cy^h + v^p \quad (4.113)$$

$$v^p = -1/2 \quad (4.114)$$

$$y^h(z) = e^{kz} \quad (4.115)$$

where $v^p = -1/2$ is the particular solution. The condition $\mathcal{T}_0(v) = 0$ guarantees that $C \neq 0$ since

$$C\mathcal{T}_0(y^h) = \mathcal{T}_0(v - v^p) = \mathcal{T}_0(v) - \mathcal{T}_0(v^p) = 0 - (-1) = 1 \quad (4.116)$$

and $\mathcal{T}_0(v^h) \neq 0$. Thus the homogeneous solution is $y^h = v + 1/2$. Denoting the Chebyshev series of v by v_n for $n = 0, \dots, N - 1$, we find v by solving the system of equations

$$v_0 = v_{N-1} = 0 \quad (4.117)$$

$$v_n - k \frac{v_{n-1} - v_{n+1}}{2n} = \frac{f_{n-1} - f_{n+1}}{2n} \text{ for } 0 < n < N - 1. \quad (4.118)$$

We set the $N - 1$ 'st Chebyshev coefficient of v and f as zero for convenience. For example, for $N = 6$ we solve the system of equations,

$$\begin{bmatrix} 1 & 0 & 0 & 0 & 0 & 0 \\ -\frac{k}{2} & 1 & \frac{k}{2} & 0 & 0 & 0 \\ 0 & -\frac{k}{2 \cdot 2} & 1 & \frac{k}{2 \cdot 2} & 0 & 0 \\ 0 & 0 & -\frac{k}{2 \cdot 3} & 1 & \frac{k}{2 \cdot 3} & 0 \\ 0 & 0 & 0 & -\frac{k}{2 \cdot 4} & 1 & 0 \\ 0 & 0 & 0 & 0 & 0 & 1 \end{bmatrix} \begin{bmatrix} v_0 \\ v_1 \\ v_2 \\ v_3 \\ v_4 \\ v_5 \end{bmatrix} = \begin{bmatrix} 0 \\ -\frac{k}{2} \\ 0 \\ 0 \\ 0 \\ 0 \end{bmatrix} \quad (4.119)$$

for the Chebyshev coefficients of v and then add 1 to v_0 to construct y^h .

For the construction of the particular solution y^p we solve (4.97) subject to $\mathcal{T}_0(y^p) = 0$.

Thus we solve the system of equations

$$v_0 = v_{N-1} = 0 \quad (4.120)$$

$$v_n - k \frac{v_{n-1} - v_{n+1}}{2n} = \frac{f_{n-1} - f_{n+1}}{2n} \text{ for } 0 < n < N - 1. \quad (4.121)$$

For $N = 6$ implies solving the tridiagonal system

$$\begin{bmatrix} 1 & 0 & 0 & 0 & 0 & 0 \\ -\frac{k}{2} & 1 & \frac{k}{2} & 0 & 0 & 0 \\ 0 & -\frac{k}{2 \cdot 2} & 1 & \frac{k}{2 \cdot 2} & 0 & 0 \\ 0 & 0 & -\frac{k}{2 \cdot 3} & 1 & \frac{k}{2 \cdot 3} & 0 \\ 0 & 0 & 0 & -\frac{k}{2 \cdot 4} & 1 & 0 \\ 0 & 0 & 0 & 0 & 0 & 1 \end{bmatrix} \begin{bmatrix} y_0^p \\ y_1^p \\ y_2^p \\ y_3^p \\ y_4^p \\ y_5^p \end{bmatrix} = \begin{bmatrix} 0 \\ \frac{f_0 - f_2}{2} \\ \frac{f_1 - f_3}{2 \cdot 2} \\ \frac{f_2 - f_4}{2 \cdot 3} \\ \frac{f_3 - f_5}{2 \cdot 4} \\ 0 \end{bmatrix}. \quad (4.122)$$

Now that we have constructed the homogeneous and particular solutions we can enforce boundary conditions. Given $y(a) = b$ for $a \in [-1, 1]$ the value of the constant C is determined:

$$y(a) = C y^h(a) + y^p(a) \Rightarrow C = \frac{b - y^p(a)}{y^h(a)}. \quad (4.123)$$

Typically we enforce the boundary conditions at the endpoint $z = \pm 1$ for which we have readily available formulas to compute the values of y^h and y^p in terms of their Chebyshev

coefficients. For $f = f_0/2 + \sum_{n=1}^{N-2} f_n P_n + P_{N-1} f_{N-1}/2$ we compute

$$f(-1) = f_0/2 + \sum_{j=1}^{N-2} (-1)^j f_j + (-1)^{N-1} f_{N-1}/2 \quad (4.124)$$

$$f(1) = f_0/2 + \sum_{j=1}^{N-2} f_j + f_{N-1}/2 \quad (4.125)$$

$$f'(-1) = \sum_{j=1}^{N-2} (-1)^{j+1} j^2 f_j + (-1)^N (N-1)^2 f_{N-1}/2 \quad (4.126)$$

$$f'(1) = \sum_{j=1}^{N-2} j^2 f_j + (N-1)^2 f_{N-1}/2 \quad (4.127)$$

$$f''(1) = \frac{1}{3} \sum_{j=2}^{N-2} (j^4 - j^2) f_j + [(N-1)^4 - (N-1)^2] f_{N-1}/2 \quad (4.128)$$

$$f''(-1) = \frac{1}{3} \sum_{j=2}^{N-2} (-1)^j (j^4 - j^2) f_j + (-1)^{N-1} [(N-1)^4 - (N-1)^2] f_{N-1}/2. \quad (4.129)$$

We will now show how to construct solutions to the second order equation

$$(D^2 - k^2)y = f. \quad (4.130)$$

For this problem we have two homogeneous solutions and one particular solution so that the general solution to this differential equation is of the form

$$y = C_1 y^{h_1} + C_2 y^{h_2} + y^p. \quad (4.131)$$

We solve this as a system of two different equations

$$(D - k)v = f \quad (4.132)$$

$$(D + k)y = v. \quad (4.133)$$

First we find the particular and homogeneous solution to

$$(D - k)v = f \quad (4.134)$$

as described previously so that we have

$$v = C v^{h_1} + v^p. \quad (4.135)$$

Then we find y^{h_2} and y^p by solving

$$(D + k)y^{h_2} = y^{h_1} \quad (4.136)$$

$$(D + k)y^p = v^p \quad (4.137)$$

subject to $\mathcal{T}_0(y^{h_2}) = 0$ and $\mathcal{T}_0(y^p) = 0$ via spectral integration for the particular solution. Note that y^{h_2} constructed in this manner is linearly independent from y^{h_1} . To enforce boundary conditions we must now invert a matrix for the coefficients C_1 and C_2 . For example for boundary condition enforced at the endpoints $z = \pm 1$ we have

$$\begin{bmatrix} y^{h_1}(-1) & y^{h_2}(-1) \\ y^{h_1}(1) & y^{h_2}(1) \end{bmatrix} \begin{bmatrix} C_1 \\ C_2 \end{bmatrix} = \begin{bmatrix} y(-1) - y^p(-1) \\ y(1) - y^p(1) \end{bmatrix} \quad (4.138)$$

for the coefficients a and b .

Once we have our solution y we find derivatives without recourse to differentiation matrices or Fourier transform methods. Indeed, in the first-order case, i.e. for y that satisfy

$$(D - k)y = f, \quad (4.139)$$

we find the derivative by simply rearranging the equation

$$Dy = f + ky. \quad (4.140)$$

Hence differentiating is obtained by merely summing the the forcing function and the solution multiplied by k . For the second order case, i.e. for y that satisfy

$$C_1 y^{h_1} + C_2 y^{h_2} + y^p = y \quad (4.141)$$

$$(D^2 - k^2)y = f \quad (4.142)$$

$$(D - k)y^{h_1} = 0 \quad (4.143)$$

$$(D + k)y^{h_2} = y^{h_1} \quad (4.144)$$

$$(D - k)y^{dp} = f \quad (4.145)$$

$$(D + k)y^p = y^{dp}, \quad (4.146)$$

we compute

$$Dy = D(C_1y^{h_1} + C_2y^{h_2} + y^p) \quad (4.147)$$

$$= kC_1y^{h_1} + C_2(y^{h_1} - ky^{h_2}) - ky^p + y^{dp} \quad (4.148)$$

$$D^2y = k^2y + f. \quad (4.149)$$

It seems that computing derivatives in this manner lead to an order of magnitude improvement of the relative error over other methods (either differentiation matrices or Fourier methods). Using these formulas we compute the derivatives of y at the endpoints in an alternative manner. Instead of using (4.126) and (4.127) to the solution y , we apply (4.124) and (4.124) to (4.147). From numerical experimentation it does not seem to matter which way the derivatives were evaluated at the endpoint.

We now have all the pieces to solve the modified Poisson's equation (4.72). As was the case with the Chebyshev series we must truncate the number of horizontal Fourier wave-modes in hopes that we achieve a good representation of our solution. This problem is linear thus we solve

$$(D^2 - \beta_{n\ell}^2)\theta_{n\ell} = f_{n\ell} \quad (4.150)$$

subject to $\theta_{n\ell}(z = \pm 1) = 0$, mode by mode. Here

$$k_{n\ell}^2 = (k_n)^2 + (k_\ell)^2 \quad (4.151)$$

$$\beta_{n\ell}^2 = k_{n\ell}^2 + c \quad (4.152)$$

$$c \geq 0 \quad (4.153)$$

$$k_n = \frac{n\pi}{\Gamma_1} \text{ for } n = -N/2 + 1, \dots, 0, \dots, N/2 \quad (4.154)$$

$$k_\ell = \frac{\ell\pi}{\Gamma_2} \text{ for } \ell = -L/2 + 1, \dots, 0, \dots, L/2. \quad (4.155)$$

and N, L are even. Thus we solve $N \times L$ second order boundary value problems. By using symmetry or realness of the variables we reduce computation. The $n = \ell = 0$ mode for $c = 0$ must be handled separately depending on boundary conditions. For example, if $\partial_z \theta_{00}(z = \pm 1) = 0$ there is the solvability requirement that $0 = \int_{z=-1}^1 f_{00}(z)dz$ otherwise no solution exists. Changing the value of θ_{00} by any constant still produces a solution, thus instead we replace one of the boundary conditions with a normalization condition such as $\int_{-1}^1 \theta_{00}dz = 0$.

Solving the modified Stokes equation (4.78) is more complicated and is the subject of

the next section.

4.2.2 Kleiser-Schumann Algorithm

The Kleiser-Schumann algorithm is a method for solving the modified Stokes problem (4.78), see [39, 37]. Since the modified Stokes problem is linear we solve wave-number by wave-number equations of the form

$$(D^2 - \beta_{n\ell}^2)\vec{u}_{n\ell} = \vec{f}_{n\ell} - \hat{\nabla}p_{n\ell} \quad (4.156)$$

$$\hat{\nabla} \cdot \vec{u}_{n\ell} = 0 \quad (4.157)$$

where

$$k_{n\ell}^2 = (k_n)^2 + (k_\ell)^2 \quad (4.158)$$

$$\beta_{n\ell}^2 = k_{n\ell}^2 + c \quad (4.159)$$

$$\hat{\nabla} = \imath k_n \hat{x} + \imath k_\ell \hat{y} + D \hat{z} \quad (4.160)$$

$$k_n = \frac{n\pi}{\Gamma_1} \text{ for } n = -N/2 + 1, \dots, 0, \dots, N/2 \quad (4.161)$$

$$k_\ell = \frac{\ell\pi}{\Gamma_2} \text{ for } \ell = -L/2 + 1, \dots, 0, \dots, L/2 \quad (4.162)$$

$$\vec{f}_{n\ell} = f_{n\ell}^1 \hat{x} + f_{n\ell}^2 \hat{y} + f_{n\ell}^3 \hat{z} \quad (4.163)$$

$$\vec{u}_{n\ell} = u_{n\ell} \hat{x} + v_{n\ell} \hat{y} + w_{n\ell} \hat{z}. \quad (4.164)$$

Here $\imath = \sqrt{-1}$ where the square-root is interpreted as the principle branch. From now on we will drop the subscript $n\ell$ with the understanding that the modified Stokes problem must be solved for all values of n and ℓ individually. For now we consider the $k \neq 0$ case and discuss how to handle this mode separately at the end.

The single wave-number problem is to solve

$$(D^2 - \beta^2)\vec{u} = \vec{f} - \hat{\nabla}p \quad (4.165)$$

$$\hat{\nabla} \cdot \vec{u} = 0. \quad (4.166)$$

Taking the divergence of the first equation yields the following equation for p

$$(D^2 - k^2)p = \hat{\nabla} \cdot \vec{f}. \quad (4.167)$$

As we have seen before we may write the general solution to this problem as the sum of

two homogeneous terms and a particular solution

$$p = C_1 p^{h_1} + C_2 p^{h_2} + p^p. \quad (4.168)$$

Hence we may write the equation for \vec{u} as

$$(D^2 - \beta^2)\vec{u} = \vec{f} - \hat{\nabla} p^p - C_1 \hat{\nabla} p^{h_1} - C_2 \hat{\nabla} p^{h_2}. \quad (4.169)$$

We will now split the problem of finding solutions to \vec{u} into three parts. Let \vec{u}^i for $i = 1, 2, 3$ be solutions to

$$(D^2 - \beta^2)\vec{u}^1 = \hat{\nabla} p^{h_1} \quad (4.170)$$

$$(D^2 - \beta^2)\vec{u}^2 = \hat{\nabla} p^{h_2} \quad (4.171)$$

$$(D^2 - \beta^2)\vec{u}^3 = \vec{f} - \hat{\nabla} p^p. \quad (4.172)$$

where each \vec{u}^i for $i = 1, 2, 3$ satisfies the boundary conditions for \vec{u} . With this we write \vec{u} as

$$\vec{u} = \vec{u}^3 - C_1 \vec{u}^1 - C_2 \vec{u}^2. \quad (4.173)$$

To find C_1 and C_2 we use auxiliary conditions derived by enforcing incompressibility on the boundary.

For no-slip boundary conditions we have $\partial_z w(z = \pm 1) = 0$ and for stress-free boundary conditions $\partial_{zz} w(z = \pm 1) = 0$. That is to say (4.173) applies to each component hence to the vertical velocity w

$$w = w^3 - C_1 w^1 - C_2 w^2. \quad (4.174)$$

For example with no-slip boundary conditions we apply the vertical derivative D to both sides and solve the following system of equations for C_1 and C_2

$$\begin{bmatrix} Dw^1(z=1) & Dw^2(z=1) \\ Dw^1(z=-1) & Dw^2(z=-1) \end{bmatrix} \begin{bmatrix} C_1 \\ C_2 \end{bmatrix} = \begin{bmatrix} Dw^3(z=1) \\ Dw^3(z=-1) \end{bmatrix} \quad (4.175)$$

For fixed time-step sizes the matrix for are precomputed and factorized only once. Furthermore \vec{u}^1 and \vec{u}^2 is precomputed. Hence at each time step we only need to solve for \vec{u}^3 and the coefficients C_1 and C_2 .

For this problem the $k = 0$ case must be handled separately as well. This is due to

the fact that the homogeneous solution for the pressure is of the form $p^{h_1} = 1/2$ and $p^{h_2} = z/2$. Letting $\vec{u}^1 = (u^1, v^1, w^1)$ the $k = 0$ case implies that $\vec{u}^1 = 0$ for no-slip boundary conditions and stress-free boundary conditions. For $\beta = 0$ one has $(u^1, v^1, w^1) = (D_1, D_2, 0)$ in the stress-free case where D_1 and D_2 are arbitrary constants. By specifying that (u^1, v^1) are mean zero we may set these arbitrary constants to zero. The constant C_1 becomes a free parameter that doesn't affect the physical flow field \vec{u} . This corresponds to the fact that the pressure may be changed by an arbitrary constant. We may choose this value such that the average of p is zero, but this is by no means necessary. Now we must find C_2 . From incompressibility and from the boundary conditions we see that $Dw = 0 \Rightarrow w = 0$ which implies⁵ $C_2 w^2 = w^3$. Taking the derivative we find that $Dw^3(z \pm 1)/Dw^2(z \pm 1) = C_2$. This may appear overconstrained, but since we are guaranteed that that the functions w^2 and w^3 are proportional to one another we could take either conditions to evaluate the constant C_2 .

4.3 Numerical Results

We now assemble the methods of previous sections to examine optimal flow fields for various different values of Péclet. As mentioned in §3.5 we expect stress-free boundary conditions to be the most optimal boundary conditions, hence no-slip velocity fields should have a lower Nu than the stress-free boundary conditions. This turns out to be the case for the numerically computed solutions here.

The stress-free calculation was carried out by Hassanzadeh et al. [33] albeit for different boundary conditions in the horizontal directions. In that study it was found that, for a fixed aspect ratio, it was more optimal to have a multiple convection rolls as the enstrophy budget increased. The solutions to the equations developed recirculation regions within a single cell. We repeat the calculation here as verification for the algorithm in §4.1.4 and to compute high resolution velocity fields with stress-free boundary conditions. The Nu-Pe scalings presented for the stress-free case here are directly related to what was found in [33]. The highest resolution (in the optimal domain size) used for the stress-free case was 256×257 Fourier-Chebyshev points reaching a Péclet value of 5×10^4 and for the no-slip case we used 512×1025 Fourier-Chebyshev grid in the optimal domain size which reached a Péclet of 2.5×10^5 .

As a point of comparison three different computations of upperbounds to 2D Rayleigh-Bénard with stress-free boundaries are shown in Figure 4.1. Here we see the rigorous

⁵Note that for $\beta = 0$ we have $w^2 = (z^2 - 1)/4$ and for $\beta \neq 0$ we have $w^2 = -\frac{1}{2\beta^2} + \frac{\sinh(\beta) \cosh(\beta z)}{\beta^2 \sinh(2\beta)}$.

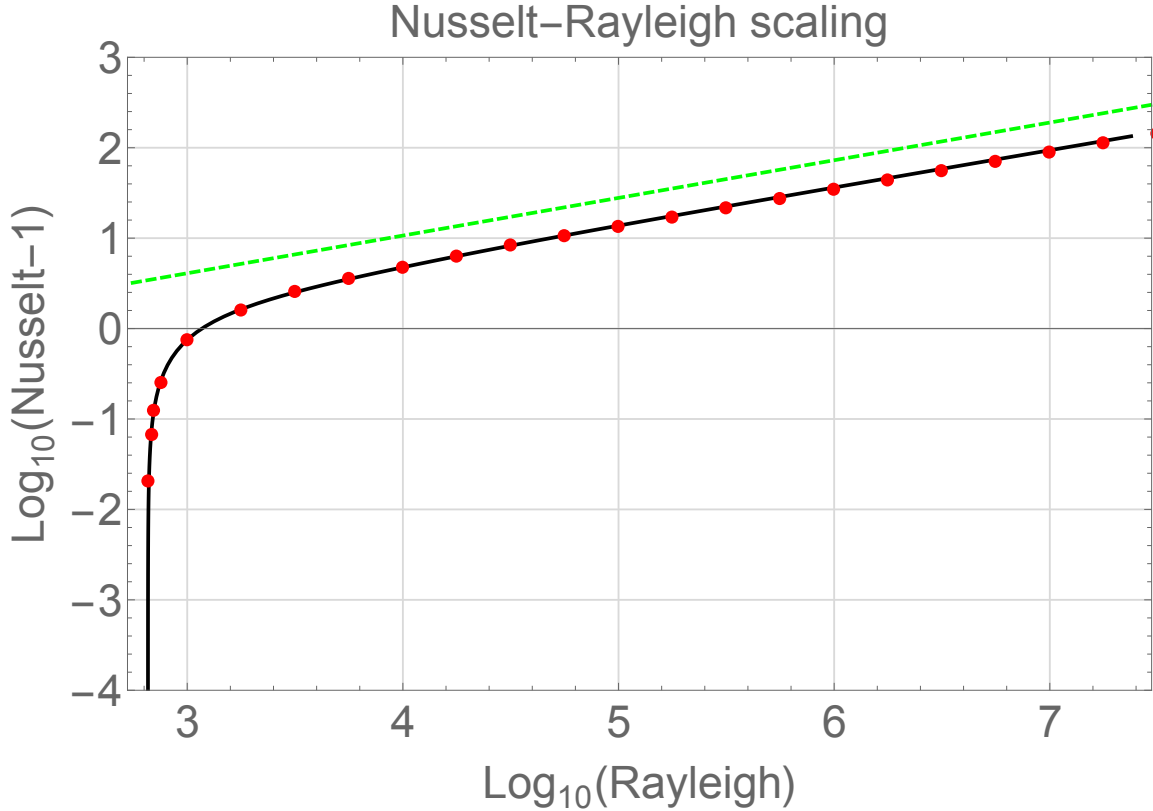


Figure 4.1: Upper bounds to the Nusselt number in 2D Rayleigh-Bénard convection with stress-free boundary conditions. The dashed green line is the rigorous upper bound by Whitehead and Doering [3]. The red dots are numerically computed solutions to the background method problem by Wen et al.[2]. The black line corresponds to numerically computed optimizers of the steady optimal control problem with stress-free boundary conditions.

upper bound obtained by Whitehead and Doering [3], the numerically computed solutions to the background method problem by Wen et al. [2], and the upper bound computed by the methods of this chapter (which corresponds to the envelope over all fixed aspect-ratio solutions in Hassanzadeh et al. [33]). Astonishingly the numerical solutions to the background method problem and the optimal control problem seem to coincide over the range of Rayleigh numbers shown in the figure.

In Figure 4.2 and Figure 4.3 we display the stream-lines and resulting temperature field for the best known 2D steady optimizers in the stress-free and no-slip case, respectively. In both cases the unicellular solutions are optimal in the low Pe regime as suggested by linear theory. The linear optimal aspect ratio is $2\sqrt{2} \approx 2.82843$ in the stress-free case and about 2.01622 in the no-slip case. As the Péclet budget increases it becomes more optimal to have multiple convection cells for a fixed aspect-ratio. The structure of the solution for the

stress-free case displays a more prominent “recirculation zone” near the $z = 0$ and $z = 1$ walls. The no-slip solution also displays this structure, but one must zoom in to see this feature. When the gradient ascent procedure was initially performed the large aspect ratio circulation solutions eventually lost stability and converged to the smaller circulations.

In Figure 4.4 and Figure 4.5 we zoom in to a particular cell to more closely examine the structure of the optimal flow fields. The aspect ratio changes as the enstrophy budget increases and all computations using the method of §4.1.4 were performed in the reduced domain as opposed to the full one. In these plots one can see that the optimal stress-free solutions have pronounced recirculation zones near the boundaries. On the other hand the no-slip solutions develop an additional “recirculation zone” in the bulk, with less recirculation near the walls. It seems that the purpose of these regions is to prevent premature downwelling/upwelling of hot/cold fluid elements. Said differently, the optimal flow field prevents hot fluid elements from transporting downwards and cold fluid elements from transporting upwards.

The asymptotic solutions in §3.6.1 achieve the same effect but with a different mechanism. There the thinness of the boundary layers are what prevents downwelling/upwelling of hot/cold fluid elements. However, as discussed in §3.6.1, the thinness of the boundary layers comes at a much greater enstrophy cost. With this in mind the recirculation zones may be viewed as a compromise. It allows one to have larger boundary layers (hence reduced enstrophy cost) while still preventing downwelling/upwelling of hot/cold fluid elements. Furthermore one is allowed to have more convection roles for a given aspect ratio.

Finally in Figure 4.6 and Figure 4.7 we display the optimal Nusselt number and aspect-ratio as a function of the Péclet budget. In these plots there are 20 points per decade. Given the straightness of the curves in the linear and fully nonlinear regime (on a Log-Log scale) we can differentiate to examine the local scaling exponents of the Nusselt number and optimal aspect ratio with respect to the Péclet budget. Interestingly the aspect ratio scaling exponent in both cases seem to be a damped oscillation converging to an eventual constant value whereas the Nusselt number’s scaling exponent is a monotone decay. These figures suggest that $Nu \sim Pe^{0.58}$ and $Nu \sim Pe^{0.54}$ for the stress-free and no-slip cases respectively. As stated previously the stress-free case transports more heat than the no-slip case.

We additionally mention the asymptotic scalings of the additional quantities E, \mathcal{I}, μ where

$$E^2 = \langle \vec{u} \cdot \vec{u} \rangle \tag{4.176}$$

$$\mathcal{I} = \max\{\|u\|_\infty, \|w\|_\infty\} \tag{4.177}$$

and μ is the Lagrange multiplier that enforces the Pe constraint. For the case of no-slip boundary conditions we have

$$E \sim \text{Pe}^{0.64}, \mathcal{I} \sim \text{Pe}^{0.75}, \mu \sim \text{Pe}^{-1.45}, \quad (4.178)$$

and for stress-free boundary conditions

$$E \sim \text{Pe}^{0.66}, \mathcal{I} \sim \text{Pe}^{0.83}, \mu \sim \text{Pe}^{-1.42}. \quad (4.179)$$

In all cases the scaling exponents are approximate and should be correct to within ± 0.03 .

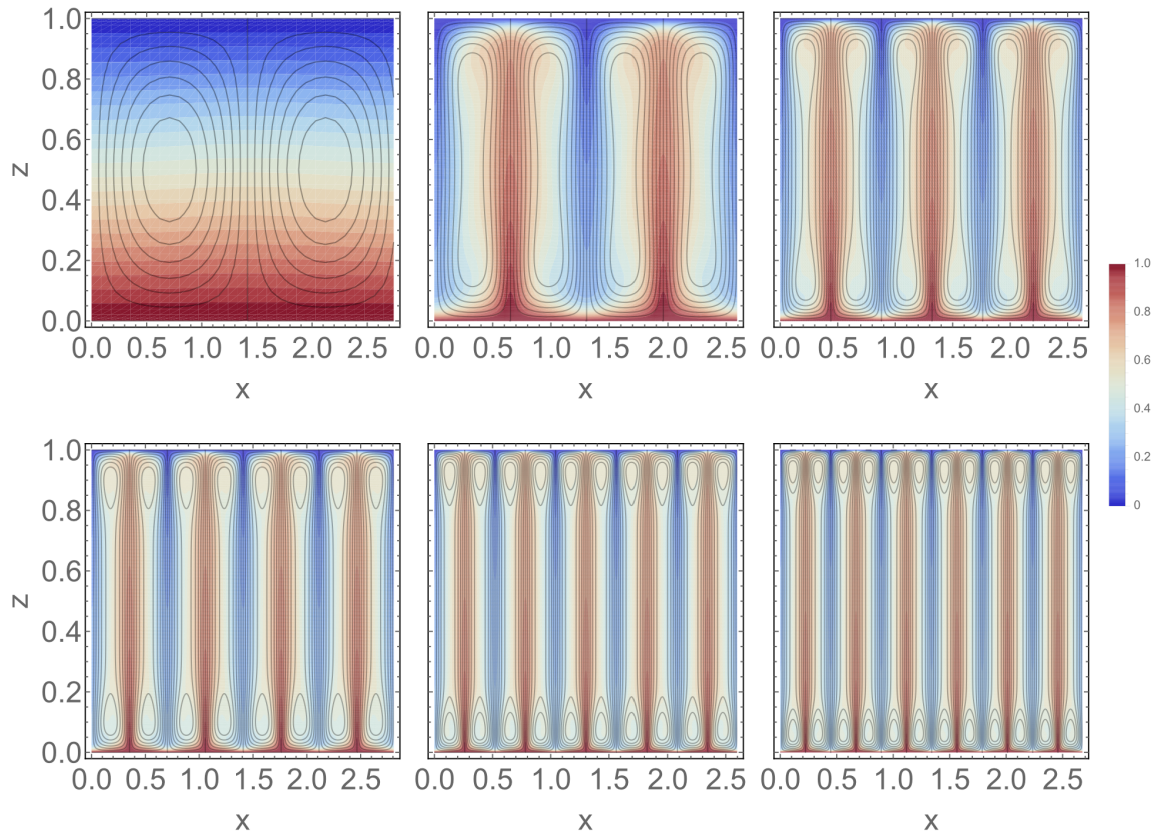


Figure 4.2: Optimal stress-free solutions for different entrophy budgets in the full domain. The black contour lines are the streamlines and the colors represent the temperature field. From left to right, top to bottom the Péclet numbers are 4.0×10^{-1} , 5.0×10^2 , 1.6×10^3 , 3.2×10^3 , 8.0×10^3 , 1.2×10^4 . The best known optimizers consist of a multiplicity of convection cells for a fixed domain size as the entrophy budget increases.

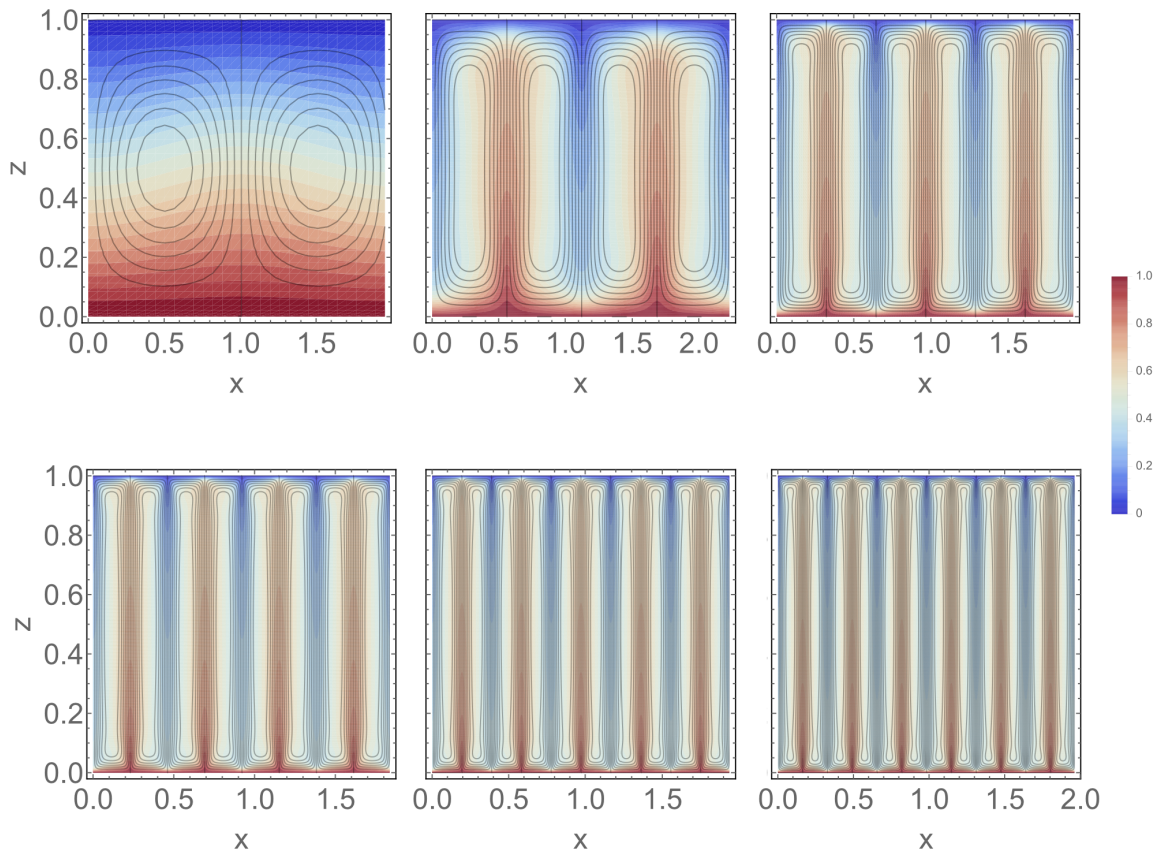


Figure 4.3: Optimal no-slip solutions for different enstrophy budgets in the full domain. The black contour lines are the streamlines and the colors represent the temperature field. From left to right, top to bottom the Péclet numbers are 4.0×10^{-1} , 4.0×10^2 , 1.8×10^3 , 5.0×10^3 , 8.0×10^3 , 1.3×10^4 . The best known optimizers consist of a multiplicity of convection cells for a fixed domain size as the enstrophy budget increases.

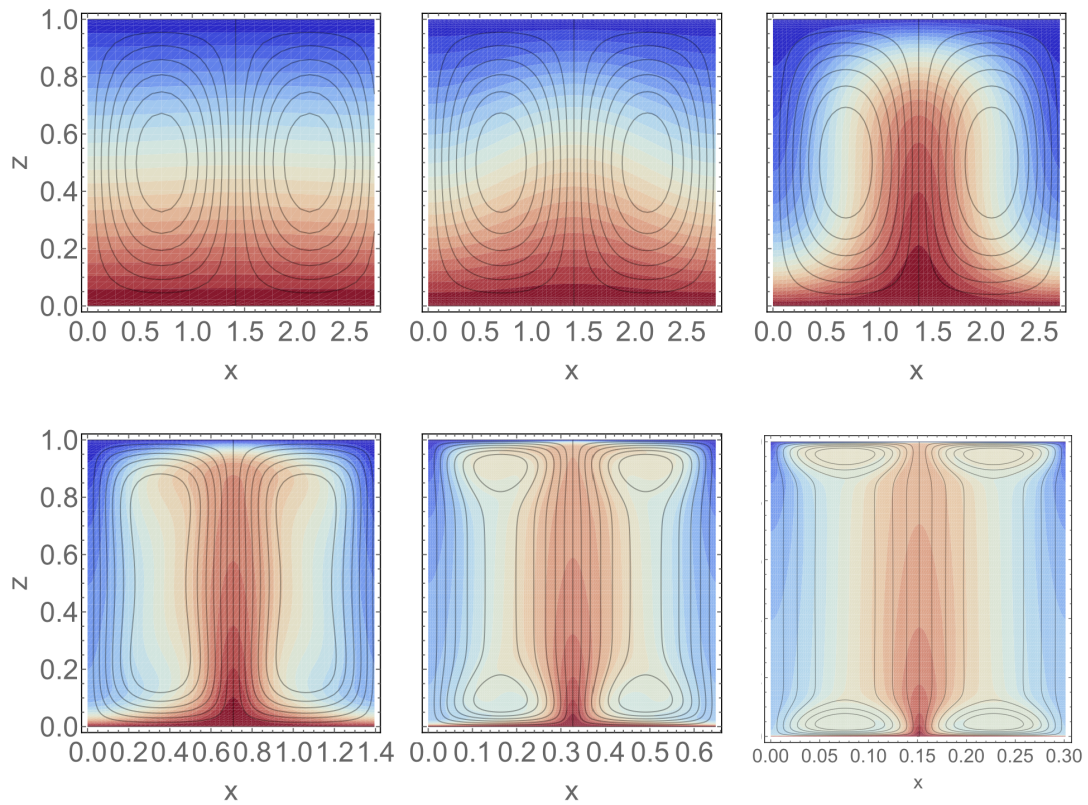


Figure 4.4: Optimal stress-free solutions for different enstrophy budgets in a single cell. The black contour lines are the streamlines and the colors represent the temperature field. From left to right, top to bottom the Péclet numbers are 4.0×10^{-1} , 4.0×10^0 , 4.0×10^1 , 4.0×10^2 , 4.0×10^3 , 4.0×10^4 . The domain size in the horizontal x direction shrinks as the Péclet number increases.

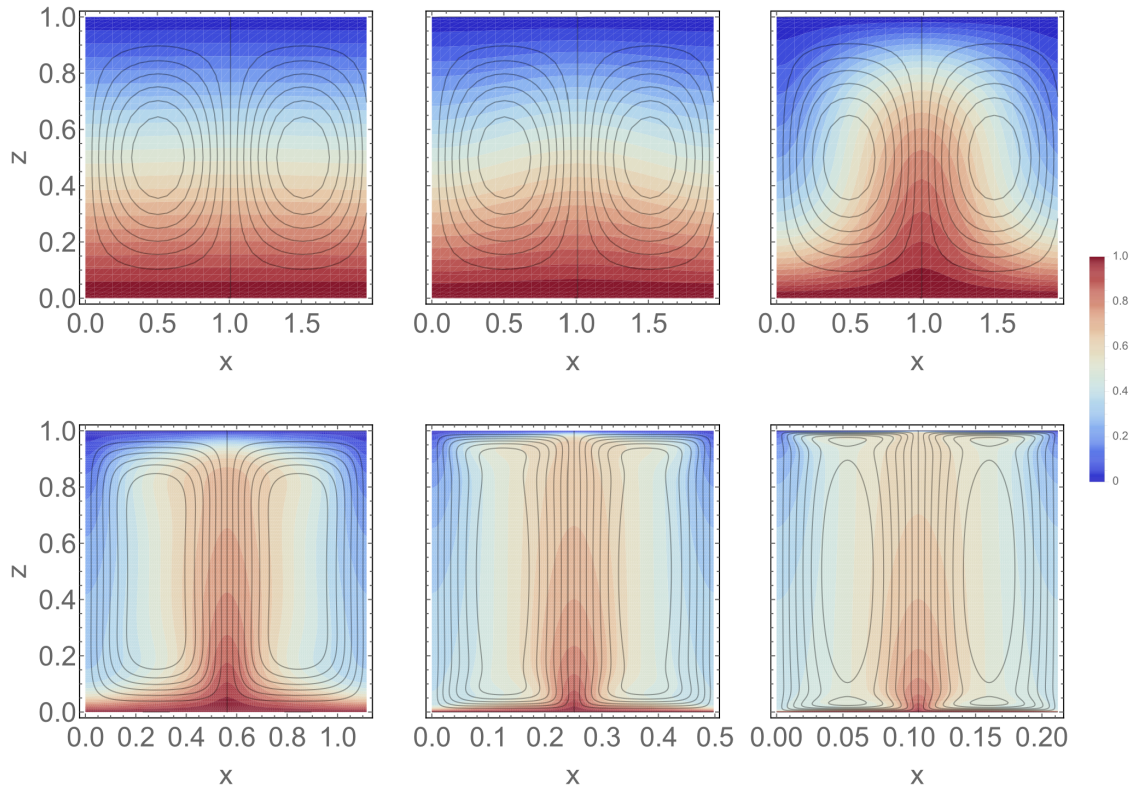


Figure 4.5: Optimal no-slip solutions for different enstrophy budgets in a single cell. The black contour lines are the streamlines and the colors represent the temperature field. From left to right, top to bottom the Péclet numbers are 4.0×10^{-1} , 4.0×10^0 , 4.0×10^1 , 4.0×10^2 , 4.0×10^3 , 4.0×10^4 . The domain size in the horizontal x direction shrinks as the Péclet number increases.

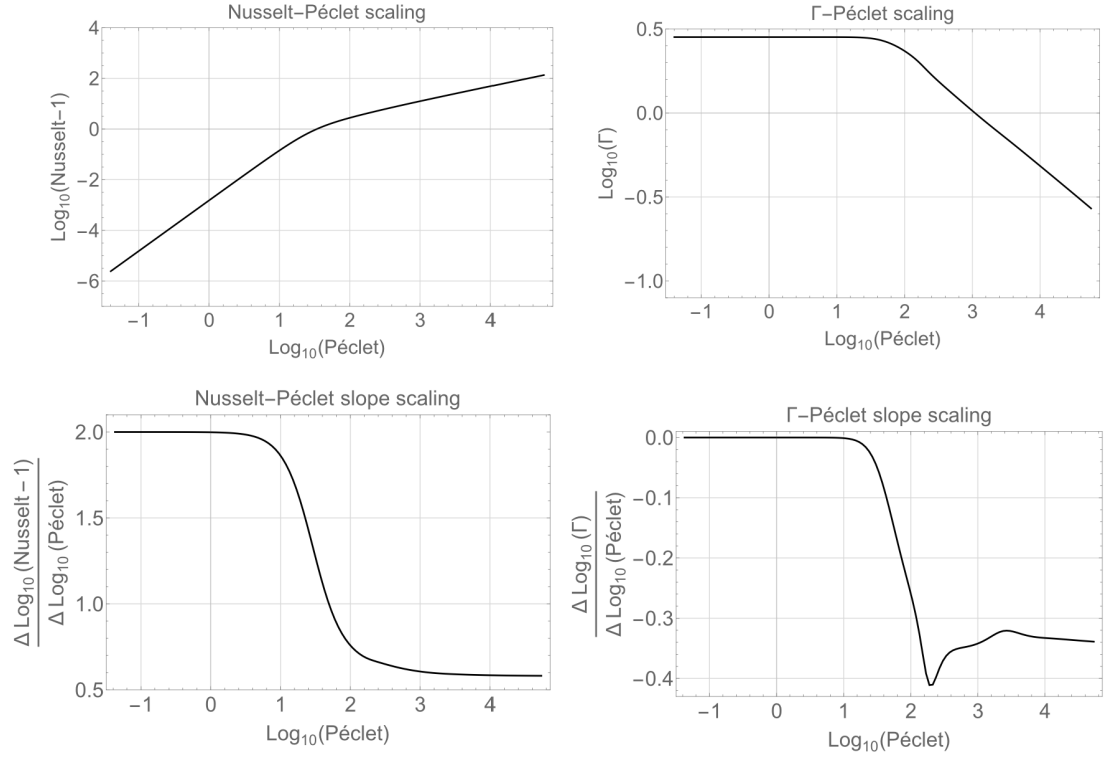


Figure 4.6: Computed optimal Nusselt number (Nu) and aspect ratio (Γ) as a function of the enstrophy budget (Pe), for stress-free boundary conditions. Top Left: Log-Log plot of Pe vs $\text{Nu}-1$. Bottom Left: The instantaneous slope of the top left plot, Pe vs $d \log(\text{Nu} - 1)/(d \log \text{Pe})$. Top Right: Log-Log plot of Pe vs Γ . Bottom Right: The instantaneous slope of the top right plot, Pe vs $d \log(\Gamma)/(d \log \text{Pe})$. The last instantaneous slope for the bottom left plot is 0.582 and the last instantaneous slope for the bottom right plot is -0.339 . The largest computed value of Pe is 5.65×10^4 corresponding to a μ value of 2.4×10^{-8} .

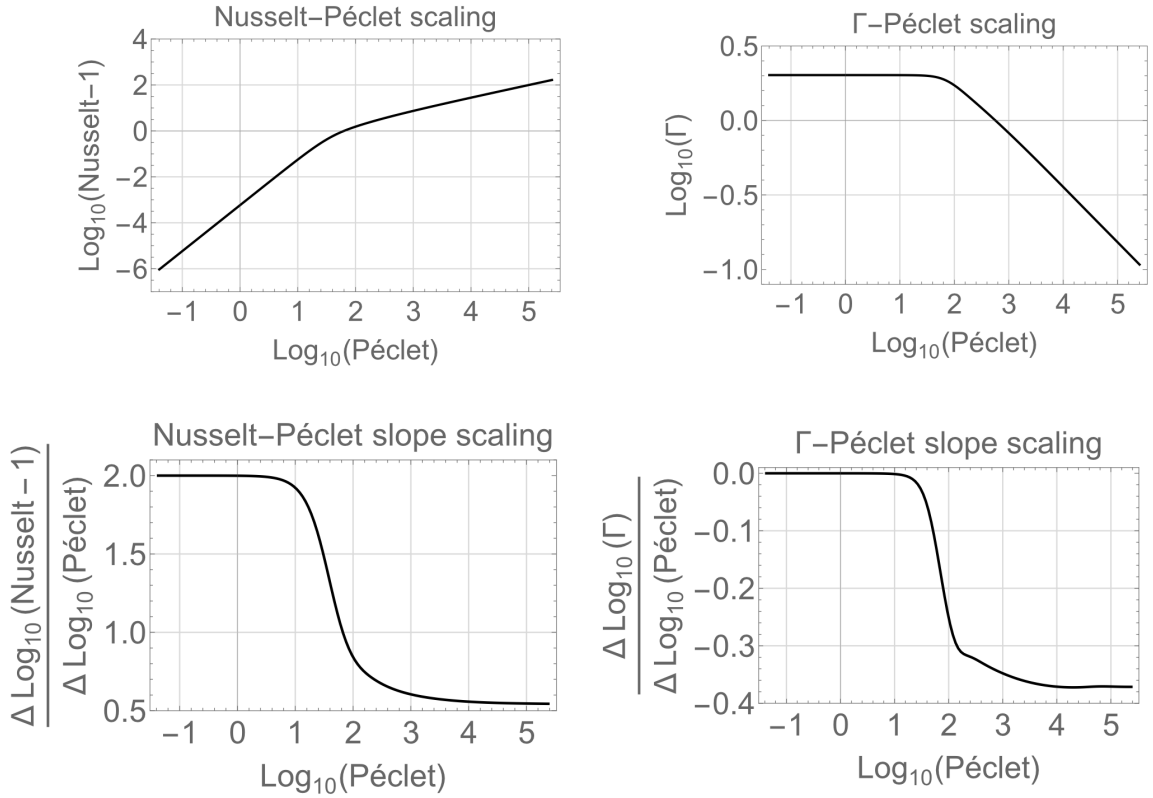


Figure 4.7: Computed optimal Nusselt number (Nu) and aspect ratio (Γ) as a function of the enstrophy budget (Pe), for no-slip boundary conditions. Top Left: Log-Log plot of Pe vs $\text{Nu}-1$. Bottom Left: The instantaneous slope of the top left plot, Pe vs $d \log(\text{Nu} - 1)/(d \log \text{Pe})$. Top Right: Log-Log plot of Pe vs Γ . Bottom Right: The instantaneous slope of the top right plot, Pe vs $d \log(\Gamma)/(d \log \text{Pe})$. The last instantaneous slope for the bottom left plot is 0.544 and the last instantaneous slope for the bottom right plot is -0.371 . The largest computed value of Pe is 2.5×10^5 corresponding to a μ value of 1.4×10^{-9} .

CHAPTER 5

Discussion

In this thesis we examined transport in solutions of the advection-diffusion equation,

$$\partial_t T + \vec{u} \cdot \nabla T = 0 \quad (5.1)$$

where \vec{u} is incompressible, i.e. $\nabla \cdot \vec{u} = 0$, the domain is $[0, \Gamma_1] \times [0, \Gamma_2] \times [0, 1]$, and the boundary conditions for T are $T(x, y, z = 0) = 1$, $T(x, y, z = 1) = 0$ and periodic in x, y . Transport refers to the transfer of passive tracers, characterized by concentration T , from the $z = 0$ boundary to the $z = 1$ boundary as measured by the space and time averaged vertical heat flux which we call the Nusselt number:

$$\text{Nu} = \limsup_{\tau \rightarrow \infty} \frac{1}{\tau \Gamma_1 \Gamma_2} \int_0^\tau \int_0^{\Gamma_1} \int_0^{\Gamma_2} \int_0^1 (wT - \partial_z T) dz dy dx dt = 1 + \langle wT \rangle \quad (5.2)$$

where w is the component of velocity in the vertical direction. In all cases the vertical velocity vanished on the $z = 0$ and $z = 1$ boundaries. Specifically we were interested in upper bounds to the heat transport in terms of a bulk integral intensity constraint on the velocity field \vec{u} , namely the magnitude of the enstrophy of the velocity field $\langle \nabla \vec{u} : \nabla \vec{u} \rangle = \langle |\nabla \times \vec{u}|^2 \rangle$ which we called the Péclet number.

We studied reduced models in Chapter 2 in order to understand transport properties in a simplified setting, build intuition, test theoretical and numerical tools, as well as to compare “natural” to optimal flows . The reduced models we analyzed were the Lorenz equations and the so-called Double Lorenz equations. In both cases, we found that steady solutions of the optimal control problem achieved maximal transport. This was numerically investigated (and in fact motivated) by computations of optimal non-steady periodic solutions of the optimal Lorenz and optimal Double Lorenz equations. We proved that there existed steady “natural” solutions that coincide with the optimal solutions in the Lorenz equations and that any sustained time dependence must strictly lower heat transport. On the other hand the Double Lorenz equations have no steady solutions that coincide with the optimal

flow fields, nor does it seem like any time dependent flow could reach the optimal transport values.

We rigorously formulated and analyzed the steady optimal transport problem in Chapter 3. There we showed that the problem is indeed well-posed, i.e. that a maximizer exists and bounds the Nusselt number $\langle wT \rangle$ in the following manner: $\langle wT \rangle \leq 0.5 \text{ Pe}^{2/3}$. Furthermore it was established that the functional associated with the optimization procedure is differentiable and hence that the optimizers are characterized by first-order optimality conditions.

Utilizing the Euler-Lagrange equations we then demonstrated that maximizers must indeed occur when $\langle \nabla \vec{u} : \nabla \vec{u} \rangle = \text{Pe}^2$. It was also shown that, as long as a maximum exists and the functional is differentiable with respect to boundary values, that stress-free boundary conditions achieve the highest heat transport among all boundary conditions for the horizontal components of velocity. We explored possible avenues for improving the analytic $\text{Pe}^{2/3}$ upper bound and examined the structure of flow fields that achieve an apparently suboptimal $\text{Pe}^{1/2}$ scaling.

In order to develop deeper insight and inspire further analysis we developed computational methods for solving the Euler-Lagrange equations in Chapter 4. The method of choice was gradient ascent because of its ability to generalize to the fully three dimensional time-dependent problem. We developed a framework to apply the gradient ascent procedure to time-dependent, time-periodic, and steady solutions to the Euler-Lagrange equations. Methods for discretizing time and space were described in detail. The method of spatial discretization developed by Viswanath [38] was advantageous since boundary value problems involved tridiagonal matrices with bounded condition numbers and traditional numerical differentiation could be avoided: numerical differentiation in the vertical direction reduced to multiplication by wave-vectors and summation.

We then presented numerically computed 2D steady state solutions to the Euler-Lagrange equations for both stress-free boundary conditions and no-slip boundary conditions. These numerical solutions suggest a global upper bound that scales like $\text{Nu} \sim \text{Pe}^{0.58}$ for 2D stress-free boundary conditions and $\text{Nu} \sim \text{Pe}^{0.54}$ for no-slip boundary conditions.

There are several advantages to investigating bounds for convective heat transport in the optimal control framework. The first is that it produces saturating flow fields. This has practical engineering applications since one can specifically examine the fluid dynamical mechanisms that achieve optimal heat transfer with the hope of designing devices capable of producing such flows. Another advantage is that numerical evidences suggests that it produces sharper upper bounds than previous methods.

There are, however, a number of substantial challenges that need to be addressed.

1. We do not know if the time-dependent problem is well-formulated, i.e., that a maximizer to the optimal transport problem exists. Furthermore even if the optimizer does exist, we do not know if it is characterized by the first-order optimality conditions.
2. The variational problem is a non-convex optimization problem so further analysis is necessary to close the gap between the numerical evidence ($\text{Nu} \lesssim \text{Pe}^{0.58}$) and rigorous results ($\text{Nu} - 1 \leq 0.5 \text{Pe}^{2/3}$).

With regards to the first point could circumvent this issue entirely by showing that steady flows are optimal. If this proves to be untenable then it may be possible to show that the optimizing solution must obey a Pontryagin's maximum principle as is the case for finite dimensional optimization. It is not immediately evident that the methods of Chapter 3 generalize to the time-dependent setting due to the lack of compactness in the time-direction. Perhaps working with a constraint of the form $\langle \gamma |\partial_t \vec{u}|^2 + \nabla \vec{u} : \nabla \vec{u} \rangle$ would provide the necessary compactness. This modification loses immediate connection to Rayleigh-Bénard convection, but if the $\gamma \rightarrow 0$ limit is well defined this would serve as a way to regularize the problem.

The second issue is serious because it prevents assertions that one has truly achieved the global upper bound in any numerically computed solution. For the optimization problem studied here it is possible to be more optimistic: it appears that merely local maxima in a fixed aspect ratio eventually lose dynamical stability in the gradient ascent procedure for ever increasing Péclet. This inspires some confidence that numerically computed solutions presented here are indeed optimal.

The original motivation for studying optimal transport to solutions of the advection-diffusion equation was to deduce upper bounds in turbulent Rayleigh-Bénard convection. In light of the relation $\text{Pe}^2 = \text{Ra}(\text{Nu} - 1)$ the numerically computed solutions in Chapter 4 suggest upper bounds $\text{Nu} \lesssim \text{Ra}^{0.41}$ for stress-free boundary conditions and $\text{Nu} \lesssim \text{Ra}^{0.37}$ for no-slip boundary conditions.

APPENDIX A

Variations of Boundary Conditions and Domain Size

Inspiration for the aspect ratio condition and to optimize over all boundary conditions came from an exercise in Feynman and Hibb's Quantum Mechanics book [40]. There the reader was tasked with showing that, for trajectories that satisfied the Euler-Lagrange equations, derivatives of the action with respect to time were related to the Hamiltonian of a system and derivatives of the action with respect to boundary values were related to conjugate momenta. In this appendix we revisit those exercises in the one-dimensional context, as well as the finite-dimensional context for separable domains of the form $\prod_{\mu=1}^N [a^\mu, b^\mu]$ where $a^\mu, b^\mu \in \mathbb{R}$ and $a^\mu \leq b^\mu$ for $\mu = 1, \dots, N$.

In the Lagrangian density setting we will again see that derivatives with respect to changes in the domain can be related to Hamiltonians and that variations with respect to boundary values can be related to conjugate momenta. We will give both a one-dimensional example and a non-trivial two-dimensional example in the context of the linearized optimal control problem.

A.1 Lagrangians

Suppose that we find the critical points of the functional

$$\mathcal{F}[x] = \int_0^T \mathcal{L}(x, \dot{x}) dt \quad (\text{A.1})$$

subject to $x(0) = a$ and $x(T) = b$. Under suitable conditions the optimal solution x^* satisfies the Euler-Lagrange equations

$$\frac{\partial \mathcal{L}}{\partial x} - \frac{d}{dt} \frac{\partial \mathcal{L}}{\partial \dot{x}} = 0. \quad (\text{A.2})$$

The value of the functional at an optimal solution will depend on the domain size T , the imposed value of the field at the $t = 0$ boundary ($x(0) = a$), and imposed the value of the field at the $t = T$ boundary ($x(T) = b$). That is, the the critical values of the functional are

$$\mathcal{F}[x^*] = f(a, b, T). \quad (\text{A.3})$$

For example if $\mathcal{L} = \frac{1}{2}(\dot{x})^2$ then the optimal solution is

$$x^*(t) = a + \frac{b-a}{T}t, \quad (\text{A.4})$$

in which case

$$\mathcal{F}[x^*] = \frac{(b-a)^2}{2T}. \quad (\text{A.5})$$

In general, looking at variations with respect to boundary data may be related to conjugate momenta. For example

$$\frac{\partial}{\partial b} \mathcal{F}[x^*] = \frac{\partial}{\partial b} f(a, b, T) = \frac{\partial L}{\partial \dot{x}}(T) = p(T), \quad (\text{A.6})$$

and variations with respect to domain size may be related to Hamiltonians, e.g.

$$\frac{\partial}{\partial T} \mathcal{F}[x^*] = \frac{\partial}{\partial T} f(a, b, T) = \mathcal{L}(T) - \dot{x} \frac{\partial L}{\partial \dot{x}}(T) = -H(T). \quad (\text{A.7})$$

In the particular case $\mathcal{L} = \frac{1}{2}(\dot{x})^2$, we have

$$-H(T) = -\frac{1}{2}(\dot{x}^*)^2 = -\frac{1}{2} \left(\frac{b-a}{T} \right)^2 = \frac{\partial}{\partial T} \mathcal{F}[x^*] \quad (\text{A.8})$$

and

$$p(T) = \dot{x}^* = \frac{b-a}{T} = \frac{\partial}{\partial b} \mathcal{F}[x^*] \quad (\text{A.9})$$

The same idea generalizes to Hamiltonian and Lagrangian densities as well. In the following subsections we derive these relations in the general one-dimensional case.

A.1.1 Variations with Respect to Boundary Data

We now characterize the dependence of our optimal solution on boundary values. Consider the functional

$$\mathcal{F}[x] = \int_0^T \mathcal{L}(x, \dot{x}) dt \quad (\text{A.10})$$

subject to $x(0) = a$ and $x(T) = b$ and examine variations with respect to the final condition $x(T) = b$. A similar result holds for $x(0) = a$.

Let x be the optimal solution with $x(T) = b$ and y be the optimal solution with $y(T) = b + \delta b$ and assume that the difference $\delta x(t) \equiv y(t) - x(t)$ is “small”. The strategy will be to write y as $x + \delta x$ and then Taylor expand the functional in terms of δx . Here the variations are no longer zero on the boundary.

Look at the difference $\mathcal{F}[y] - \mathcal{F}[x]$ to first-order:

$$F[y] - F[x] = \int_0^T \mathcal{L}(y, \dot{y}) dt - \int_0^T \mathcal{L}(x, \dot{x}) dt \quad (\text{A.11})$$

$$= \int_0^T \mathcal{L}(\delta x + x, \delta \dot{x} + \dot{x}) dt - \int_0^T \mathcal{L}(x, \dot{x}) dt \quad (\text{A.12})$$

$$\approx \int_0^T \left[\frac{\partial \mathcal{L}}{\partial x}(x, \dot{x}) \delta x + \frac{\partial \mathcal{L}}{\partial \dot{x}}(x, \dot{x}) \delta \dot{x} \right] dt \quad (\text{A.13})$$

$$= \int_0^T \delta x \left[\frac{\partial \mathcal{L}}{\partial x}(x, \dot{x}) - \frac{d}{dt} \frac{\partial \mathcal{L}}{\partial \dot{x}}(x, \dot{x}) \right] dt + \delta x(T) \frac{\partial \mathcal{L}}{\partial \dot{x}}(x(T), \dot{x}(T)) \quad (\text{A.14})$$

$$= \delta x(T) \frac{\partial \mathcal{L}}{\partial \dot{x}}(x, \dot{x}) \quad (\text{A.15})$$

$$= \delta b \frac{\partial \mathcal{L}}{\partial \dot{x}}(x(T), \dot{x}(T)) \quad (\text{A.16})$$

where we neglected higher order terms in the approximation. Going from (A.13) to (A.14) involved integration by parts. To first-order we see that $F[y] - F[x]$ is the conjugate momenta evaluated at the endpoint acted upon by a linear functional that characterizes the difference between the values of y and x on the boundary. In this case the linear functional is just multiplication by δb , but in the multi-dimensional setting this changes. Thus if we want to optimize with respect to endpoints we set the first variation, the conjugate momenta, equal to zero at the boundary. This is a special case of the transversality condition from calculus of variations.

A.1.2 Variations with Respect to Domain Interval

We want to characterize the dependence of our optimal solution on the domain size T . Specifically we will look at $\frac{\partial}{\partial T} \mathcal{F}[x^*]$. To do this we must consider differences of an optimal solution with domain size $T + \delta T$ and the optimal solution with domain size T to first-order in δT . We use the notation \mathcal{F}_T to signify the functional associated with the T domain and $\mathcal{F}_{T+\delta T}$ for the functional associated with the $T + \delta T$ domain. We will consider $\delta T > 0$ case but the same result holds for $\delta T < 0$. The two cases have to be considered separately because we shall expand the solution in the larger domain in terms of the solution in the smaller domain. The results here also hold for periodic domains.

Let y denote the optimal solution for the $[0, T + \delta T]$ interval and x be the optimal solution for the $[0, T]$ interval. Denote the difference $y - x = \delta x$ and assume that this is “small”. The strategy is to write y as $x + \delta x$ and Taylor expand the Lagrangian in terms of δx . Carrying out the calculation,

$$\mathcal{F}_{T+\delta T}[y] - \mathcal{F}_T[x] = \int_0^{T+\delta T} \mathcal{L}(y, \dot{y}) dt - \int_0^T \mathcal{L}(x, \dot{x}) dt \quad (\text{A.17})$$

$$= \int_T^{T+\delta T} \mathcal{L}(y, \dot{y}) dt + \int_0^T [\mathcal{L}(y, \dot{y}) - \mathcal{L}(x, \dot{x})] dt \quad (\text{A.18})$$

$$\approx \int_T^{T+\delta T} \mathcal{L}(y, \dot{y}) dt + \int_0^T \left[\frac{\partial \mathcal{L}}{\partial x}(x, \dot{x}) \delta x + \frac{\partial \mathcal{L}}{\partial \dot{x}}(x, \dot{x}) \delta \dot{x} \right] dt \quad (\text{A.19})$$

$$= \int_T^{T+\delta T} \mathcal{L}(y, \dot{y}) dt + \delta x \left. \frac{\partial \mathcal{L}}{\partial \dot{x}} \right|_0^T \quad (\text{A.20})$$

where (A.20) utilizes the Euler-Lagrange equations.

Now consider the following approximations

$$\int_T^{T+\delta T} \mathcal{L}(y, \dot{y}) dt \approx \delta T \mathcal{L}(x(T), \dot{x}(T)) \quad (\text{A.21})$$

and

$$\delta x(T) \approx \dot{x}(T), \quad (\text{A.22})$$

where (A.22) follows Taylor expanding y , i.e.

$$y(T) = y(T + \delta T - \delta T) \approx y(T + \delta T) - \delta T \dot{y}(T + \delta T) \quad (\text{A.23})$$

$$\approx y(T + \delta T) - \delta T \dot{y}(T) \approx y(T + \delta T) - \delta T \dot{x}(T) \quad (\text{A.24})$$

and using $y(T + \delta T) = x(T)$. In conclusion we get

$$\mathcal{F}_{T+\delta T}[y] - \mathcal{F}_T[x] \approx \delta T \left(\mathcal{L}(x(T), \dot{x}(T)) - \dot{x}(T) \frac{\partial \mathcal{L}}{\partial \dot{x}}(x(T), \dot{x}(T)) \right) \quad (\text{A.25})$$

where we used $\delta x(t = 0) = 0$. This is the negative of the Hamiltonian evaluated at the endpoint. If the Lagrangian has no explicit time dependence then the Hamiltonian is independent of time and may be evaluated anywhere on the domain $[0, T]$. The calculation is as follows

$$\frac{d}{dt} H(t) = \frac{d}{dt} \left(\dot{x} \frac{\partial \mathcal{L}}{\partial \dot{x}} \right) - \frac{d}{dt} \mathcal{L} \quad (\text{A.26})$$

$$= \ddot{x} \frac{\partial \mathcal{L}}{\partial \dot{x}} + \dot{x} \frac{d}{dt} \frac{\partial \mathcal{L}}{\partial \dot{x}} - \dot{x} \frac{\partial \mathcal{L}}{\partial x} - \ddot{x} \frac{\partial \mathcal{L}}{\partial \dot{x}} \quad (\text{A.27})$$

$$= \dot{x} \left(\frac{d}{dt} \frac{\partial \mathcal{L}}{\partial \dot{x}} - \frac{\partial \mathcal{L}}{\partial x} \right) \quad (\text{A.28})$$

$$= 0. \quad (\text{A.29})$$

The last line is zero since optimal trajectories satisfy the Euler-Lagrange equations. If we want to optimize the domain interval $[0, T]$ we set the Hamiltonian equal to zero. This is also special case of the transversality condition¹.

A.2 Lagrangian densities

Let us now deal with the more general case where our functional \mathcal{F} is described by a Lagrangian density that depends on several fields ϕ_j for $j = 1, \dots, M$, coordinates x^μ for $\mu = 1, \dots, N$, and are first-order in derivatives. That is,

$$\mathcal{F}[\phi_j] = \int \mathcal{L}(\phi_j, \partial_\mu \phi_j) \quad (\text{A.30})$$

where the integral is over the domain $\prod_{\mu=1}^N [a^\mu, b^\mu]$ and ∂_μ denotes the partial derivative with respect to the x^μ coordinate. Under suitable conditions, the extrema of these functionals satisfy the system of Euler-Lagrange equations

$$\frac{\partial \mathcal{L}}{\partial \phi_i} - \partial_\mu \frac{\partial \mathcal{L}}{\partial \partial_\mu \phi_i} = 0 \quad (\text{A.31})$$

¹At this point one may obtain the transversality condition using the chain rule. Indeed $d/dt(f(a, b(t), t) = \dot{b} \partial_b f + \partial_t f = L + (b - \dot{x}) \partial L / \partial \dot{x}$.

for $\mu = 1, \dots, N$, each field ϕ_i , and where repeated indices of μ are summed over. These equations are derived in the following manner. Introduce perturbations to the fields ϕ_i in the form $\delta\phi_i$ where $\delta\phi_i$ are vanish on the boundaries and consider differences in values of the functional, i.e.

$$\mathcal{F}[\phi_j + \delta\phi_j] - \mathcal{F}[\phi_j] = \int \mathcal{L}(\phi_j + \delta\phi_j, \partial_\mu\phi_j + \partial_\mu\delta\phi_j) - \int \mathcal{L}(\phi_j, \partial_\mu\phi_j) \quad (\text{A.32})$$

$$= \int \left(\delta\phi_i \frac{\partial\mathcal{L}}{\partial\phi_i} + (\partial_\mu\delta\phi_i) \frac{\partial\mathcal{L}}{\partial\partial_\mu\phi_i} \right) \quad (\text{A.33})$$

$$= \int \delta\phi_i \left(\frac{\partial\mathcal{L}}{\partial\phi_i} - \partial_\mu \frac{\partial\mathcal{L}}{\partial\partial_\mu\phi_i} \right), \quad (\text{A.34})$$

where (A.34) follows from integration by parts and making use of the fact that the perturbations are zero on the boundary. The integrand of (A.34) are the Euler-Lagrange equations which must hold for all perturbations $\delta\phi_i$ hence (A.31).

We now introduce notation. Let \int_ℓ denote an integral over the domain in all the coordinates except x^ℓ , hence an integral over the entire domain may be symbolically broken down into the following form

$$\int = \int_{a^\ell}^{b^\ell} \int_\ell \quad (\text{A.35})$$

We shall also use $\int_{\nu\ell}$ to denote an integral over the domain in all the coordinates except x^ν, x^ℓ , e.g.,

$$\int = \int_{a^\ell}^{b^\ell} \int_{a^\nu}^{b^\nu} \int_{\nu\ell}. \quad (\text{A.36})$$

We will take on the convention that repeated ℓ and i indices will never be summed over. We will also sometimes suspend Einstein convection and explicitly write out the sums for additional clarity.

As before we examine what happens when we perturb boundary values on a particular boundary as well as perturbations to endpoints b^ℓ for a fixed index ℓ . Let ϕ_j satisfy (A.31) with a prescribed boundary condition. Now perturb the boundary values on the $x^\ell = b^\ell$ boundary by $\delta\phi_i$ for fixed indices ℓ and i and denote the extrema to this perturbed problem by φ_j for all indices j . (Perturbing the boundary value of one of the fields on a single boundary potentially changes all the other fields as well.) Furthermore assume that $\varphi_j - \phi_j$

is small. Then

$$\mathcal{F}[\varphi_j] - \mathcal{F}[\phi_j] = \int_{\ell} \delta\phi_i(x^\ell = b^\ell) \frac{\partial \mathcal{L}}{\partial \partial_\ell \phi_i}(x^\ell = b^\ell) \quad (\text{A.37})$$

where \int_{ℓ} denotes an integral over all coordinates except x^ℓ here the repeated ℓ and i indices are not summed over. Note that $\frac{\partial \mathcal{L}}{\partial \partial_\ell \phi_i}$ is the conjugate momenta of ϕ_i associated with the x^ℓ direction and that $\delta\phi_i(x^\ell = b^\ell)$ is the perturbation invoked on the $x^\ell = b^\ell$ boundary

Now fix the boundary conditions but look at variations with respect to the domain size in a particular coordinate. Choose an index ℓ and let us perturb the domain by $b^\ell + \delta b^\ell$. Denote the extrema with respect to the original domain by ϕ_j and the extrema with respect to the perturbed domain by φ_j . Assume that $\phi_j - \varphi_j$ is small. Then

$$\mathcal{F}[\varphi_j] - \mathcal{F}[\theta_j] = \delta b^\ell \int_{\ell} \left(\mathcal{L} - \phi_j \frac{\partial \mathcal{L}}{\partial \partial_\ell \phi_j} \right) \quad (\text{A.38})$$

$$= -\delta b^\ell H^\ell(x^\ell = b^\ell) \quad (\text{A.39})$$

where $-H^\ell(x^\ell) = \int_{\ell} \left(\mathcal{L} - \phi_j \frac{\partial \mathcal{L}}{\partial \partial_\ell \phi_j} \right)$ and the repeated indices with respect to j are summed over but the repeated indices with respect to ℓ are not. As is the case in the one-dimensional setting the Hamiltonian will, in fact, be independent of x^ℓ provided

$$0 = \sum_j \sum_{\mu \neq \ell} \int_{\mu\ell} \partial_\ell \phi_j \frac{\partial \mathcal{L}}{\partial \partial_\mu \phi_j} \Big|_{x^\mu = a^\mu}^{x^\mu = b^\mu} \quad (\text{A.40})$$

where we wrote out the summations explicitly.

A.2.1 Variations with Respect to Boundary Values

Let ϕ_j satisfy the Euler-Lagrange equations (A.31) with a prescribed boundary condition. Now let us perturb the boundary values on the $x^\ell = b^\ell$ boundary by $\delta\phi_i$ for fixed indices ℓ and i and denote the extrema to this perturbed problem by φ_j for all indices j . Furthermore assume that $\delta\phi_j \equiv \varphi_j - \phi_j$ is small. (Note that the notation is consistent since the restriction of $\delta\phi_j$ for $j = i$ to the boundary coincides with the previous definition.)

The strategy will be to Taylor expand the Lagrangian density evaluated at φ_j in powers of $\delta\phi_j$. Unlike the perturbations that lead to (A.34) they are non-zero on the $x^\ell = b^\ell$

boundary but zero on every other boundary. The calculation is

$$\mathcal{F}[\varphi_j] - \mathcal{F}[\theta_j] = \mathcal{F}[\phi_j + \delta\phi_j] - \mathcal{F}[\phi_j] \quad (\text{A.41})$$

$$= \int [\mathcal{L}(\phi_j + \delta\phi_j, \partial_\mu\phi_j + \partial_\mu\delta\phi_j) - \mathcal{L}(\phi_j, \partial_\mu\phi_j)] \quad (\text{A.42})$$

$$\approx \int \left(\delta\phi_j \frac{\partial\mathcal{L}}{\partial\phi_j} + (\partial_\mu\delta\phi_j) \frac{\partial\mathcal{L}}{\partial\partial_\mu\phi_j} \right) \quad (\text{A.43})$$

$$= \int \delta\phi_j \left(\frac{\partial\mathcal{L}}{\partial\phi_j} - \partial_\mu \frac{\partial\mathcal{L}}{\partial\partial_\mu\phi_j} \right) + \int_\ell \delta\phi_i(x^\ell = b^\ell) \frac{\partial\mathcal{L}}{\partial\partial_\ell\phi_i}(x^\ell = b^\ell) \quad (\text{A.44})$$

$$= \int_\ell \delta\phi_i(x^\ell = b^\ell) \frac{\partial\mathcal{L}}{\partial\partial_\ell\phi_i}(x^\ell = b^\ell). \quad (\text{A.45})$$

Again repeated i and ℓ indices are not summed over but repeated j and μ are summed over.

Optimizing over all boundary conditions on the $x^\ell = b^\ell$ boundary for the ϕ_i field yields the condition

$$0 = \frac{\partial\mathcal{L}}{\partial\partial_\ell\phi_i}(x^\ell = b^\ell). \quad (\text{A.46})$$

Thus if there exists a “best” boundary condition and the functional \mathcal{F} is differentiable with respect to boundary values, then this optimality condition characterizes the “best” boundary condition.

In the context of the optimization problem of this thesis (A.46) implies that stress-free boundary conditions are extrema of the functional.

A.2.2 Variations with Respect to Boundaries

Now look at variations with respect to the domain size in a particular coordinate while keeping boundary conditions the same. Fix an index ℓ and let us perturb the domain $\prod_{\mu=1}^N [a^\mu, b^\mu]$ by $b^\ell + \delta b^\ell$ so that our new domain is $\prod_{\mu \neq \ell} [a^\mu, b^\mu] \times [a^\ell, b^\ell + \delta b^\ell]$. Denote the extrema with respect to the original domain by ϕ_j , the extrema with respect to the perturbed domain by φ_j , and the difference by $\delta\phi_j \equiv \phi_j - \varphi_j$. We need to specify the boundary data along the extended domain in order for the problem to be well defined, e.g., the boundary associated with $x^\nu = b^\nu$ where $\nu \neq \ell$ has an extra $\prod_{\mu \neq \nu \text{ and } \mu \neq \ell} [a^\mu, b^\mu] \times [b^\ell, b^\ell + \delta b^\ell]$ chunk where the boundary data needs to be defined. For the most part how the extension is done is irrelevant. For example if we assume Dirichlet boundary conditions keeping the boundary conditions fixed means $\delta\phi_j(x^\nu = b^\nu) = 0$ for $\nu \neq \ell$ and $\varphi_j(x^\ell = b^\ell) = \varphi_j(x^\ell = b^\ell + \delta b^\ell)$. If the x^ν coordinate is periodic we apply periodicity to the extended domain as well and results again carry through. We can also directly with the Neumann boundary conditions

in certain circumstances. If Neumann boundary conditions imply that the conjugate momenta associated with a specific boundary are zero on said boundary—as is the case for stress-free boundary conditions in the optimal transport problem of this thesis—the results of this section again carry through. In what follows we will assume Dirichlet boundary conditions.

Denote the functional associated with the original domain size by \mathcal{F}_{b^ℓ} , the functional associated with the perturbed domain size by $\mathcal{F}_{b^\ell+\delta b^\ell}$, and \int as an integral over the unperturbed domain. Assume that $\delta\phi_j \equiv \phi_j - \varphi_j$ is small. The strategy to derive (A.38) is to Taylor expand the Lagrangian density evaluated at φ_j in powers of $\delta\phi_j$.

We calculate as follows:

$$\mathcal{F}_{b^\ell+\delta b^\ell}[\varphi_j] - \mathcal{F}_{b^\ell}[\theta_j] = \int_{a^\ell}^{b^\ell+\delta b^\ell} \int_\ell \mathcal{L}(\varphi_j, \partial_\mu \varphi_j) - \int_{a^\ell}^{b^\ell} \int_\ell \mathcal{L}(\phi_j, \partial_\mu \phi_j) \quad (\text{A.47})$$

$$= \int_{b^\ell}^{b^\ell+\delta b^\ell} \int_\ell \mathcal{L}(\varphi_j, \partial_\mu \varphi_j) + \int_{a^\ell}^{b^\ell} \int_\ell [\mathcal{L}(\varphi_j, \partial_\mu \varphi_j) - \mathcal{L}(\phi_j, \partial_\mu \phi_j)] \quad (\text{A.48})$$

$$\approx \int_{b^\ell}^{b^\ell+\delta b^\ell} \int_\ell \mathcal{L}(\varphi_j, \partial_\mu \varphi_j) + \int \left(\delta\phi_j \frac{\partial \mathcal{L}}{\partial \phi_j} + (\partial_\mu \delta\phi_j) \frac{\partial \mathcal{L}}{\partial \partial_\mu \phi_j} \right). \quad (\text{A.49})$$

For the first term we approximate as follows

$$\int_{b^\ell}^{b^\ell+\delta b^\ell} \int_\ell \mathcal{L}(\varphi_j, \partial_\mu \varphi_j) \approx \delta b^\ell \int_\ell \mathcal{L}(\theta_j, \partial_\mu \theta_j). \quad (\text{A.50})$$

Now focus attention on the second term. Integrating by parts yields

$$\int \left(\delta\phi_j \frac{\partial \mathcal{L}}{\partial \phi_j} + (\partial_\mu \delta\phi_j) \frac{\partial \mathcal{L}}{\partial \partial_\mu \phi_j} \right) = \int \left(\delta\phi_j \frac{\partial \mathcal{L}}{\partial \phi_j} - \delta\phi_j \partial_\mu \frac{\partial \mathcal{L}}{\partial \partial_\mu \phi_j} \right) \quad (\text{A.51})$$

$$+ \int_\ell \delta\phi_j(x^\ell = b^\ell) \frac{\partial \mathcal{L}}{\partial \partial_\ell \phi_j}(x^\ell = b^\ell) \quad (\text{A.52})$$

$$= \int_\ell \delta\phi_j(x^\ell = b^\ell) \frac{\partial \mathcal{L}}{\partial \partial_\ell \phi_j}(x^\ell = b^\ell) \quad (\text{A.53})$$

$$\approx - \int_\ell \partial_\ell \phi_j(x^\ell = b^\ell) \frac{\partial \mathcal{L}}{\partial \partial_\ell \phi_j}(x^\ell = b^\ell) \quad (\text{A.54})$$

where we made use the Euler-Lagrange equations and the fact that the variations on all the boundaries vanished except for the one associated with the x^ℓ direction, and the approxi-

mation

$$\delta\phi_j(b^\ell) = \varphi_j(b^\ell) - \theta_j(b^\ell) = \varphi_j(b^\ell + \delta b^\ell - \delta b^\ell) - \theta_j(b^\ell) \quad (\text{A.55})$$

$$\approx \varphi_j(b^\ell + \delta b^\ell) - \delta b^\ell \partial_\ell \varphi_j(b^\ell + \delta b^\ell) - \theta_j(b^\ell) = -\delta b^\ell \partial_\ell \varphi_j(b^\ell + \delta b^\ell) \quad (\text{A.56})$$

$$\approx -\delta b^\ell \partial_\ell \theta_j(b^\ell). \quad (\text{A.57})$$

Putting the two terms together yields the desired result:

$$\mathcal{F}_{b^\ell + \delta b^\ell}[\varphi_j] - \mathcal{F}_{b^\ell}[\theta_j] \approx \delta b^\ell \int_\ell \left(\mathcal{L} - \partial_\ell \phi_j \frac{\partial \mathcal{L}}{\partial \partial_\ell \phi_j} \right) \quad (\text{A.58})$$

$$= -\delta b^\ell H^\ell(x^\ell = b^\ell), \quad (\text{A.59})$$

where

$$H^\ell \equiv \int_\ell \left(\partial_\ell \phi_j \frac{\partial \mathcal{L}}{\partial \partial_\ell \phi_j} - \mathcal{L} \right). \quad (\text{A.60})$$

The Hamiltonian H^ℓ is potentially a function of x^ℓ along an optimal trajectory since the other directions are integrated out. It is also independent of x^ℓ . To see this calculate

$$-\frac{d}{dx^\ell} \mathcal{H}^\nu = \int_\ell \partial_\ell \left(\mathcal{L} - \partial_\ell \phi_j \frac{\partial \mathcal{L}}{\partial \partial_\nu \phi_j} \right) \quad (\text{A.61})$$

$$= \int_\nu \left(\partial_\ell \phi_j \frac{\partial \mathcal{L}}{\partial \phi_j} + \partial_{\mu\ell} \phi_j \frac{\partial \mathcal{L}}{\partial \partial_\mu \phi_j} - (\partial_{\ell\ell} \phi_j) \frac{\partial \mathcal{L}}{\partial \partial_\ell \phi_j} - (\partial_\ell \phi_j) \partial_\ell \frac{\partial \mathcal{L}}{\partial \partial_\ell \phi_j} \right) \quad (\text{A.62})$$

$$= \int_\ell \left(\partial_\ell \phi_j \left(\frac{\partial \mathcal{L}}{\partial \phi_j} - \partial_\mu \frac{\partial \mathcal{L}}{\partial \partial_\mu \phi_j} \right) \right) + \sum_{\mu \neq \ell} \int_{\mu\ell} \partial_\ell \phi_j \frac{\partial \mathcal{L}}{\partial \partial_\mu \phi_j} \Big|_{x^\mu = a^\mu}^{x^\mu = b^\mu} \quad (\text{A.63})$$

$$= \sum_{\mu \neq \ell} \int_{\mu\ell} \partial_\ell \phi_j \frac{\partial \mathcal{L}}{\partial \partial_\mu \phi_j} \Big|_{x^\mu = a^\mu}^{x^\mu = b^\mu} \quad (\text{A.64})$$

$$= 0 \quad (\text{A.65})$$

There are several reasons why (A.64) may vanish: periodicity, homogeneous Dirichlet boundary conditions, the vanishing of the conjugate momenta on the boundary, and the independence of the fields ϕ_j on the coordinate x^ℓ .

A.2.3 Application to the Optimal Transport System

We shall now apply the methods of the previous sections to the functional associated with optimal transport

$$\mathcal{F}[\vec{u}, \theta, \varphi, p] = \left\langle w\theta - \varphi (\partial_t \theta + \vec{u} \cdot \nabla \theta - \Delta \theta - w) + p(\nabla \cdot \vec{u}) + \frac{\mu}{2}(\text{Pe}^2 - \nabla \vec{u} : \nabla \vec{u}) \right\rangle \quad (\text{A.66})$$

where $\langle \cdot \rangle$ denotes the space-time average,

$$\langle f \rangle = \frac{1}{\tau \Gamma_1 \Gamma_2} \int_0^\tau \int_0^{\Gamma_1} \int_0^{\Gamma_2} \int_0^1 f \, dz \, dy \, dx \, dt, \quad (\text{A.67})$$

τ is “large”, and we have decomposed $\vec{u} = (u, v, w) = (u_1, u_2, u_3)$. The $\nabla \vec{u} : \nabla \vec{u}$ term is $\partial_j u_k \partial_j u_k$, explicitly

$$\nabla \vec{u} : \nabla \vec{u} = (\partial_x u)^2 + (\partial_y u)^2 + (\partial_z u)^2 \quad (\text{A.68})$$

$$+ (\partial_x v)^2 + (\partial_y v)^2 + (\partial_z v)^2 \quad (\text{A.69})$$

$$+ (\partial_x w)^2 + (\partial_y w)^2 + (\partial_z w)^2. \quad (\text{A.70})$$

In order to use the methods of the previous section we rewrite the integrand as a first-order system with a Lagrangian density

$$\mathcal{L} = \mathcal{L}(\vec{u}, \theta, \varphi, \nabla \vec{u}, \nabla \theta, \nabla \varphi, \nabla p, \partial_t \theta) \quad (\text{A.71})$$

$$= w\theta - \nabla \varphi \cdot \nabla \theta - \varphi \partial_t \theta - \varphi \vec{u} \cdot \nabla \theta + \varphi w - \nabla p \cdot \vec{u} + \frac{\mu}{2}(\text{Pe}^2 - \nabla \vec{u} : \nabla \vec{u}). \quad (\text{A.72})$$

All field variables $\vec{u}, \theta, \varphi, p$ are periodic in the horizontal directions $x \in [0, \Gamma_1]$ and $y \in [0, \Gamma_2]$. The field variables θ, φ , and w satisfy homogeneous boundary conditions in the vertical direction z at $z = 0$ and $z = 1$, p has no explicit boundary conditions in the vertical direction, and u and v either have homogeneous boundary conditions (no-slip) or Neumann boundary conditions $\partial_z u = \partial_z v = 0$ at $z = 0, 1$ (stress-free). In time the θ is zero at $t = 0$ and φ is zero at $t = \tau$. The other fields \vec{u} and p do not have any specified boundary conditions in time. We are interested in

1. The “best” possible boundary conditions for the u and v fields on the $z = 0, 1$ boundary.
2. The “best” aspect ratios Γ_1 and Γ_2 in the x and y directions, respectively.
3. The optimal time period \mathcal{T} in the τ for periodic boundary conditions.

With regards to picking out the best boundary conditions for u and v on the $z = 0, 1$ boundary we may use the result from §A.2.1. There we saw that setting the conjugate momenta equal to zero yielded a critical point. In this case we set

$$\frac{\partial \mathcal{L}}{\partial \partial_z u} = 0 \text{ and } \frac{\partial \mathcal{L}}{\partial \partial_z v} = 0, \quad (\text{A.73})$$

at $z = 0$ and $z = 1$ where \mathcal{L} is (A.71). But these imply

$$-\mu \partial_z u(x, y, z = 0, t) = -\mu \partial_z u(x, y, z = 1, t) = 0 \quad (\text{A.74})$$

and

$$-\mu \partial_z v(x, y, z = 0, t) = -\mu \partial_z v(x, y, z = 1, t) = 0 \quad (\text{A.75})$$

respectively, at $z = 0, 1$. These are precisely stress-free boundary conditions.

To pick the “best” aspect ratios Γ_1 and Γ_2 in the x and y direction (or period \mathcal{T} in the t direction) is more subtle. We limit discussion to the x direction and note that the argument for the y direction is precisely the same. Similar results hold in the t direction.

The subtlety comes from the assumption of Dirichlet boundary or periodic conditions for all the field variables, which is precisely not the case for p at the $z = 0, 1$ boundary as well as u and v for stress-free boundary conditions. In particular homogeneity (or periodicity) was used to arrive at (A.52) (which are boundary terms coming from integration by parts). However (A.52) still holds but due to a different reason: the conjugate momenta of p, u and v vanish on the $z = 0$ and $z = 1$ boundary, i.e.

$$\frac{\partial \mathcal{L}}{\partial \partial_z p} = -w \quad (\text{A.76})$$

$$\frac{\partial \mathcal{L}}{\partial \partial_z u} = -\mu \partial_z u \quad (\text{A.77})$$

$$\frac{\partial \mathcal{L}}{\partial \partial_z v} = -\mu \partial_z v \quad (\text{A.78})$$

are all zero at $z = 0$ and $z = 1$.

Furthermore (A.64) also holds so that the Hamiltonian is independent of where it is evaluated. This amounts to checking that the boundary terms from integration by parts goes to zero. For example, in steady and two dimensions (x, z) , letting ϕ denote any of the

field variables u, w, θ, φ or p , we need to check

$$\partial_x \phi \frac{\partial \mathcal{L}}{\partial \partial_z \phi} = 0 \quad (\text{A.79})$$

at $z = 0$ and $z = 1$. For w, θ, φ these are zero due to homogeneous boundary conditions. For no-slip boundary conditions the $\phi = u$ case is zero for the same reason. The $\phi = p$ case is zero because the conjugate momenta (which is w) is zero on the boundary. For stress-free boundary conditions and $\phi = u$ the conjugate momenta is proportional to $\partial_z u$ and this is zero on the boundary.

Derivatives of the functional $\mathcal{F} = \langle \mathcal{L} \rangle$ are then related to the Hamiltonians along a particular direction since all the conditions of §A.2.2. The functional involves averages, hence

$$\frac{\partial}{\partial \Gamma_1} \langle \mathcal{L} \rangle = \frac{\partial}{\partial \Gamma_1} \left(\frac{1}{\tau \Gamma_1 \Gamma_2} \int_0^\tau \int_0^{\Gamma_1} \int_0^{\Gamma_2} \int_0^1 \mathcal{L} dz dy dx dt \right) \quad (\text{A.80})$$

$$= -\frac{\langle \mathcal{L} \rangle}{\Gamma_1} - \frac{1}{\tau \Gamma_1 \Gamma_2} \int_0^\tau \int_0^{\Gamma_2} \int_0^1 \mathcal{H}^x dz dy dt \quad (\text{A.81})$$

where

$$-\mathcal{H}^x = \mathcal{L} - \partial_x u \frac{\partial \mathcal{L}}{\partial \partial_x u} - \partial_x v \frac{\partial \mathcal{L}}{\partial \partial_x v} - \partial_x w \frac{\partial \mathcal{L}}{\partial \partial_x w} \quad (\text{A.82})$$

$$- \partial_x \theta \frac{\partial \mathcal{L}}{\partial \partial_x \theta} - \partial_x \varphi \frac{\partial \mathcal{L}}{\partial \partial_x \varphi} - \partial_x p \frac{\partial \mathcal{L}}{\partial \partial_x p} \quad (\text{A.83})$$

$$= \mathcal{L} + \mu |\partial_x \vec{u}|^2 + 2\partial_x \theta \partial_x \varphi + u \partial_x p + \varphi u \partial_x \theta. \quad (\text{A.84})$$

The spatial Hamiltonian is independent of where it is evaluated, hence we write our optimality condition for the best aspect ratio as

$$0 = \frac{\partial}{\partial \Gamma_1} \langle \mathcal{L} \rangle = -\frac{\langle \mathcal{L} + \mathcal{H}^x \rangle}{\Gamma}. \quad (\text{A.85})$$

In the section that follows we will look at this condition in a scenario where we can calculate everything analytically.

A.2.4 Example: Application to Linearized Optimal Control System

In order to explicitly confirm these results we consider the functional

$$\mathcal{F}[\vec{u}, \theta, \Gamma, \tau] = \frac{1}{\Gamma} \int_0^1 \int_0^\Gamma \left[w\theta - \varphi(-\Delta\theta - w) + p(\nabla \cdot \vec{u}) + \frac{\mu}{2}(\text{Pe}^2 - |\nabla\vec{u}|^2) \right] dz dx \quad (\text{A.86})$$

with stress-free $\partial_z u(x, z=0, 1) = 0$, $w(x, z=0, 1) = 0$ boundary conditions and periodicity in the x direction with period Γ . Here $|\nabla\vec{u}|^2 = \partial_j u_k \partial_j u_k$. This is the same functional as the one in the previous section but without the $\varphi\vec{u} \cdot \nabla\theta$ and $\varphi\partial_t\theta$ terms. Since there is no penalty for integration by parts in the spatial coordinates we will rewrite this functional as the first-order system

$$\mathcal{F}[\vec{u}, \theta, \Gamma, \tau] = \frac{1}{\Gamma} \int_0^1 \int_0^\Gamma \left[w\theta - \nabla\varphi \cdot \nabla\theta + \varphi w - \nabla p \cdot \vec{u} + \frac{\mu}{2}(\text{Pe}^2 - |\nabla\vec{u}|^2) \right] dz dx. \quad (\text{A.87})$$

Here the Lagrangian depends on the fields u, w, θ, φ, p

$$\mathcal{L} = \mathcal{L}(u, w, \theta, \varphi, u_x, w_x, u_z, w_z, \theta_x, \theta_z, \varphi_x, \varphi_z, p_x, p_z), \quad (\text{A.88})$$

and variations of the functional lead to the Euler-Lagrange equations

$$\Delta\theta = w \quad (\text{A.89})$$

$$\Delta\varphi = w \quad (\text{A.90})$$

$$\mu\Delta\vec{u} = \nabla p - (\theta + \varphi)\hat{z} \quad (\text{A.91})$$

$$\nabla \cdot \vec{u} = 0 \quad (\text{A.92})$$

$$\text{Pe}^2 = \frac{1}{\Gamma} \int_0^1 \int_0^\Gamma |\nabla\vec{u}|^2 dx dz. \quad (\text{A.93})$$

A solution is

$$u = -A \frac{m\pi}{k} \cos(m\pi z) \sin(kx) \quad (\text{A.94})$$

$$w = A \sin(m\pi z) \cos(kx) \quad (\text{A.95})$$

$$\theta = \frac{A}{m^2\pi^2 + k^2} \sin(m\pi z) \cos(kx) \quad (\text{A.96})$$

$$\varphi = \theta \quad (\text{A.97})$$

$$p = \frac{2m\pi}{(m^2\pi^2 + k^2)^2} \cos(m\pi z) \cos(kx) \quad (\text{A.98})$$

$$A^2 = \frac{4k^2 \text{Pe}^2}{(m^2\pi^2 + k^2)^2} \quad (\text{A.99})$$

$$\mu = \frac{2k^2}{(m^2\pi^2 + k^2)^3} \quad (\text{A.100})$$

where m is an integer that indexes branches of solutions and $k = 2\pi/\Gamma$. The Nusselt number is

$$\text{Nu} - 1 = \frac{k^2 \text{Pe}^2}{(m^2\pi^2 + k^2)^3}. \quad (\text{A.101})$$

The spatial Hamiltonian density is

$$-\mathcal{H}^x = \mathcal{L} - \partial_x u \frac{\partial \mathcal{L}}{\partial \partial_x u} - \partial_x w \frac{\partial \mathcal{L}}{\partial \partial_x w} - \partial_x \theta \frac{\partial \mathcal{L}}{\partial \partial_x \theta} - \partial_x \varphi \frac{\partial \mathcal{L}}{\partial \partial_x \varphi} - \partial_x p \frac{\partial \mathcal{L}}{\partial \partial_x p} \quad (\text{A.102})$$

$$= \mathcal{L} - \partial_x u (-\mu \partial_x u) - \partial_x w (-\mu \partial_x w) - \partial_x \theta (-\partial_x \varphi) - \partial_x \varphi (\partial_x \theta) - \partial_x p (-u) \quad (\text{A.103})$$

$$= w\theta + \partial_x \theta \partial_x \varphi - \partial_z \theta \partial_z \varphi + w\varphi - \partial_z p w \quad (\text{A.104})$$

$$+ \frac{\mu}{2} (\text{Pe}^2 + (\partial_x u)^2 + (\partial_x w)^2 - (\partial_z u)^2 - (\partial_z w)^2) \quad (\text{A.105})$$

and spatial Hamiltonian is

$$-H^x = - \int_{z=0}^{z=1} \mathcal{H}^x dz = \frac{k^2 \text{Pe}^2 (5k^2 - m^2\pi^2)}{(k^2 + m^2\pi^2)^4}. \quad (\text{A.106})$$

The optimal aspect ratio satisfies

$$0 = \frac{\delta \mathcal{F}}{\delta \Gamma} = (-\langle \mathcal{L} \rangle - \langle \mathcal{H}^x \rangle) / \Gamma \quad (\text{A.107})$$

$$= - \frac{2k^2 \text{Pe}^2 (2k^2 - m^2\pi^2)}{(k^2 + m^2\pi^2)^4} \frac{k}{2\pi} \quad (\text{A.108})$$

which is the same we would have deduced by differentiating the Nusselt number with respect to Γ (we can use $d\Gamma = d\frac{2\pi}{k} = -2\pi/k^2 dk$) and set this equal to zero. Each branch of solutions (indexed by m) yields a distinct optimal aspect ratio (hence the assumption that trajectories were nearby).

APPENDIX B

Compact Sets in Hilbert Spaces

In this appendix we discuss sufficient condition for weak convergence to imply strong convergence in the Hilbert space ℓ^2 . We look at this to better understand the Rellich-Kondrachov theorem as well as to understand what kind of sets are compact in infinitely many dimensions.

Let λ_n where $n \in \mathbb{N}$ be a sequence of numbers such that for each constant $c \in (0, \infty)$ the cardinality of the set $\{|\lambda_n| \leq c\}$ is finite, but there exists an N such that for each $c \in (0, \infty)$ we have $|\lambda_N| \geq c$. Said succinctly, for each $c \in \mathbb{N}$ the sequence λ_n satisfies $|\{\lambda_n : |\lambda_n| \leq c\}| < \infty$ and $|\{\lambda_n : |\lambda_n| > c\}| = \infty$. We will also assume that the set has a minimal (not necessarily unique) element that is non-zero, i.e. $|\lambda_n| > 0$ for all $n \in \mathbb{N}$. For example, the set of integers satisfy this property as does the set of eigenvalues of the Laplacian in a “nice” domain with Dirichlet boundary conditions. We call sequences that satisfy this criteria “guard sequences”.

Let

$$\|f\|_\lambda = \sqrt{\sum_{n=1}^{\infty} (\lambda_n)^2 (f_n)^2} \quad (\text{B.1})$$

and

$$(f, g)_\lambda = \sum_{n=1}^{\infty} (\lambda_n)^2 f_n g_n. \quad (\text{B.2})$$

where f_n, g_n are the components of $f, g \in \ell^2$, respectively. The way that we defined the λ_n means that $\|\cdot\|_\lambda$ is a norm and $(f, g)_\lambda$ is an inner product.

We prove the following theorem about a sufficient condition for weak convergence to imply strong convergence.

Theorem. *Suppose that a sequence f^m for $m \in \mathbb{N}$ converges weakly to zero in ℓ^2 and*

choose any sequence λ_n that is a guard sequence. If the sequence of elements f^m satisfy

$$\|f^m\|_\lambda \leq \alpha \quad (\text{B.3})$$

for each $m \in \mathbb{N}$ and a fixed positive number α , then f^m converges strongly in ℓ^2 to zero.

Proof. Fix $\epsilon > 0$ and let $G_\epsilon = \{n \in \mathbb{N} : |\lambda_n| \geq \alpha \sqrt{\frac{2}{\epsilon}}\}$ and denote that the cardinality of the complement (which is finite by definition) by N . Since

$$\alpha^2 \frac{2}{\epsilon} \sum_{n \in G_\epsilon} (f_n^m)^2 \leq \sum_{n \in G_\epsilon} (\lambda_n)^2 (f_n^m)^2 \leq \sum_{n \in G_\epsilon} (\lambda_n)^2 (f_n^m)^2 + \sum_{n \notin G_\epsilon} (\lambda_n)^2 (f_n^m)^2 \quad (\text{B.4})$$

$$= \sum_{n=1}^{\infty} (\lambda_n)^2 (f_n^m)^2 = \|f^m\|_\lambda^2 \leq \alpha^2 \quad (\text{B.5})$$

for each m , we have

$$\sum_{n \in G_\epsilon} (f_n^m)^2 < \frac{\epsilon}{2} \quad (\text{B.6})$$

for each m . If $N = 0$ we are done, otherwise we proceed as follows. The sequence converging weakly to zero in ℓ^2 means that for each $g \in \ell^2$ there exists an M_g (dependent on the $g \in \ell^2$) such that for all $m > M_g$

$$\left| \sum_{n=1}^{\infty} f_n^m g_n \right| < \sqrt{\frac{\epsilon}{2N}}, \quad (\text{B.7})$$

where N is the cardinality of the complement of G_ϵ . Consider the finite collection of basis elements $\{e_j : j \notin G_\epsilon\}$. For each e_j we can find a corresponding M_j such that for all $m > M_j$ we have $|f_j^m| < \sqrt{\frac{\epsilon}{2N}}$. Now choose $M = \max\{M_j : j \notin G_\epsilon\}$. Then we have that

$$\sum_{n \notin G_\epsilon} (f_n^m)^2 < \frac{\epsilon}{2} \quad (\text{B.8})$$

for each $m > M$. Putting the two together yields

$$\sum_{n=1}^{\infty} (f_n^m)^2 < \epsilon. \quad (\text{B.9})$$

Thus our norm in ℓ^2 converges to zero. Since we have weak convergence in ℓ^2 and convergence of the norm, we have strong convergence. \square

This is a sufficient condition to prove strong convergence in the ℓ^2 space of concern. In particular this shows that a function who has a Fourier series representation that converges weakly in $H^{0+\epsilon}[\Omega]$ (unrelated ϵ) will converge strongly in $L^2[\Omega]$, where Ω is a nice domain that allows for a Fourier series representation, i.e. a periodic domain with finite period. This also shows that the set $\{f \in \ell^2 : \|f\|_\lambda \leq 1\}$ is compact in ℓ^2 .

APPENDIX C

Double Lorenz Properties

C.1 Coefficients and Parameters

The constants in the Double Lorenz equations are as follows

$$\text{Ra} = \text{The Rayleigh number} \quad (\text{C.1})$$

$$\text{Nu} = \text{The Nusselt number} \quad (\text{C.2})$$

$$\sigma = \text{Prandtl number} \quad (\text{C.3})$$

$$A = \text{Aspect Ratio} \quad (\text{C.4})$$

$$k = 2/A \quad (\text{C.5})$$

$$\rho_1 = \frac{(1 + k^2)^3}{k^2} \quad (\text{C.6})$$

$$\rho_2 = \frac{(4 + k^2)^3}{k^2} \quad (\text{C.7})$$

$$c_1 = \frac{(3 + k^2)(4 + k^2)}{2(1 + k^2)^2} \quad (\text{C.8})$$

$$d_1 = \frac{(4 + k^2)(k^2 - 5)}{2(1 + k^2)^2} \quad (\text{C.9})$$

$$c_2 = \frac{2k^2(1 + k^2)^2}{(4 + k^2)^3} \quad (\text{C.10})$$

$$d_2 = \frac{2(1 + k^2)^2(k^2 - 8)}{(4 + k^2)^3} \quad (\text{C.11})$$

$$a = \frac{4 + k^2}{1 + k^2} \quad (\text{C.12})$$

$$b_1 = \frac{4}{1 + k^2} \quad (\text{C.13})$$

$$b_2 = \frac{16}{4 + k^2} \quad (\text{C.14})$$

$$r_1 = \frac{\text{Ra}}{\rho_1} \quad (\text{C.15})$$

$$r_2 = \frac{\text{Ra}}{\rho_2} \quad (\text{C.16})$$

$$r_3 = \frac{k^2 b_1}{16} \text{Ra} \quad (\text{C.17})$$

$$r_4 = \frac{k^2 b_1}{128} \text{Ra}. \quad (\text{C.18})$$

We use the relations

$$\frac{2\rho_1}{b_1} c_1 - \frac{2\rho_2}{b_2} c_2 - \frac{3}{4} a \rho_1 = 0 \quad (\text{C.19})$$

$$-\frac{2\rho_1}{b_1} d_1 + \frac{2\rho_2}{b_2} d_2 + \frac{3}{4} a \rho_1 = 0 \quad (\text{C.20})$$

to derive (2.63) for the truncated system.

C.2 Bounds

Consider the energy function

$$E(y_1, z_1, y_2, z_2) = \frac{1}{2} \left(y_1^2 + (z_1 - 1)^2 + \frac{1}{4} [y_2^2 + (z_2 - 1)^2] \right). \quad (\text{C.21})$$

Taking the time derivative and making use of the temperature variable equations (2.67), (2.68), (2.70), and (2.71) yields

$$\dot{E}(y_1, z_1, y_2, z_2) = -y_1^2 - b_1 z_1^2 + b_1 z_1 + \frac{a}{4} (-y_2^2 - b_2 z_2^2 + b_2 z_2). \quad (\text{C.22})$$

Adding zero in the form $2\alpha(E - E)$ where $\alpha \in (0, \min\{1, b_1\})$ to the right hand side of (C.22) results in the following differential inequality,

$$\begin{aligned} \dot{E}(y_1, z_1, y_2, z_2) &= -2\alpha E + \frac{5}{4}\alpha + (\alpha - 1)y_1^2 + (\alpha - b_1)z_1^2 + (b_1 - 2\alpha)z_1 \\ &\quad + \frac{1}{4} [(\alpha - a)y_2^2 + (\alpha - ab_2)z_2^2 + (ab_2 - 2\alpha)z_2] \end{aligned} \quad (\text{C.23})$$

$$\begin{aligned} &= -2\alpha E + \frac{5}{4}\alpha + \frac{(b_1 - 2\alpha)^2}{4(b_1 - \alpha)} + \frac{(ab_2 - 2\alpha)^2}{16(ab_2 - \alpha)} \\ &\quad + (\alpha - 1)y_1 + (\alpha - b_1) \left(z_1 + \frac{b_1 - 2\alpha}{2(\alpha - b_1)} \right)^2 \\ &\quad + \frac{\alpha - a}{4}y_2 + \frac{\alpha - ab_2}{4} \left(z_2 + \frac{ab_2 - 2\alpha}{2(\alpha - ab_2)} \right)^2 \end{aligned} \quad (\text{C.24})$$

$$\leq -2\alpha E + \frac{b_1^2}{4(b_1 - \alpha)} + \frac{b_1^2}{(4b_1 - \alpha)}. \quad (\text{C.25})$$

The differential inequality may be solved to yield

$$\begin{aligned} E(t) &\leq e^{-2\alpha t} \left(E_0 - \frac{1}{2\alpha} \left[\frac{b_1^2}{4(b_1 - \alpha)} + \frac{b_1^2}{(4b_1 - \alpha)} \right] \right) \\ &\quad + \frac{1}{2\alpha} \left[\frac{b_1^2}{4(b_1 - \alpha)} + \frac{b_1^2}{(4b_1 - \alpha)} \right] \end{aligned} \quad (\text{C.26})$$

where E_0 is the initial value of the energy (C.22). The $\alpha \in (0, \min\{1, b_1\})$ that minimizes the steady state of (C.26) is not terribly illuminating (it is the root of a cubic), thus we will instead pick the simpler but suboptimal $\alpha = b_1/2$ for $b_1 \in (0, 2]$ and $\alpha = 1$ for $b_1 \in (2, \infty)$ to explicitly display the time-asymptotic bounds

$$\limsup_{t \rightarrow \infty} E(y_1, z_1, y_2, z_2) \leq \begin{cases} \frac{9}{14} & \text{for } b_1 \in (0, 2) \\ \frac{1}{2} \left[\frac{b_1^2}{4(b_1-1)} + \frac{b_1^2}{(4b_1-1)} \right] & \text{for } b_1 \in [2, \infty) \end{cases} \quad (\text{C.27})$$

on the temperature variables.

C.3 Deriving the Background

To obtain a bound for when $Ra \geq \sqrt{\frac{(1+k^2)^3(4+k^2)^3}{k^4}}$ we demand that the determinants of each matrix

$$\begin{bmatrix} \frac{1}{r_1}(1-\alpha) & \alpha(1-z_1^0) \\ \alpha(1-z_1^0) & -\alpha \end{bmatrix} \text{ and } \begin{bmatrix} \frac{1}{r_2}(1-\alpha) & \alpha(1-z_2^0) \\ \alpha(1-z_2^0) & -\alpha \end{bmatrix} \quad (\text{C.28})$$

be zero. Based off of intuition from the Lorenz system we make the following choice for α

$$\alpha = \frac{z_1^0 + z_2^0}{(z_1^0)^2 + (z_2^0)^2}. \quad (\text{C.29})$$

If $z_1^0, z_2^0 \in [0, 1]$ then

$$z_1^0 + z_2^0 \geq (z_1^0)^2 + (z_2^0)^2 \Leftrightarrow \alpha \geq 1, \quad (\text{C.30})$$

as required. This leads to the system of equations

$$-\frac{1}{r_1}(1-\alpha) = \alpha(1-z_1^0)^2 \quad (\text{C.31})$$

$$-\frac{1}{r_2}(1-\alpha) = \alpha(1-z_2^0)^2. \quad (\text{C.32})$$

Dividing the first equation by the second yields

$$\frac{r_2}{r_1} = \left(\frac{1-z_1^0}{1-z_2^0} \right)^2 \Leftrightarrow z_2^0 = \gamma(z_1^0 - 1) + 1 \quad (\text{C.33})$$

where $\gamma = \sqrt{r_1/r_2} = a^{3/2} \in (1, 8)$. We can eliminate z_2^0 in favor of z_1^0 , use definition of α and the equation $-\frac{1}{r_1}(1-\alpha) = \alpha(1-z_1^0)^2$ to get

$$\alpha(1 - (1 - z_1^0)^2) = 1 \quad (\text{C.34})$$

\Leftrightarrow

$$(z_1^0 + \gamma(z_1^0 - 1) + 1)(1 - r_1(1 - z_1^0)^2) = (z_1^0)^2 + (\gamma(z_1^0 - 1) + 1)^2 \quad (\text{C.35})$$

Note that $z_1^0 = 1$ is a root and that if $z_1^0 > 1$ the left hand side is negative while the right hand side is positive. We still need to check that z_1^0 is positive. Solving for the other two

roots yields

$$z_1^0 = \frac{-1 + 2r_1\gamma - \gamma^2 \pm \sqrt{(\gamma^2 + 1)^2 + 4r_1(r_1 - 2\gamma)}}{2(r_1 + r_1\gamma)}. \quad (\text{C.36})$$

We will take the positive root¹. We need a few observations about z_1^0 as a function of r_1 . First note that $\text{Ra} \geq \sqrt{\frac{(1+k^2)^3(4+k^2)^3}{k^4}} \Leftrightarrow r_1 \geq \gamma$. When $r_1 = \gamma$ we have

$$z_1^0 = \frac{\gamma^2 - 1}{\gamma + \gamma^2} = 1 - \frac{1}{\gamma} \quad (\text{C.37})$$

which is the minimum value of the discriminant. From $r_1 \geq \gamma$ onwards the z_1^0 is strictly increasing. To see this we can calculate the derivative to be

$$\frac{\partial}{\partial r_1} z_1^0 = \frac{4r_1\gamma + (1 + \gamma^2) \left(-1 - \gamma^2 + \sqrt{4r_1^2 - 8r_1\gamma + (1 + \gamma^2)^2} \right)}{2r_1^2(1 + \gamma)\sqrt{4r_1^2 - 8r_1\gamma + (1 + \gamma^2)^2}}. \quad (\text{C.38})$$

Note that the denominator is always positive so we can concentrate on the positiveness of the numerator. When $r_1 = \gamma$ we have that the numerator is $2(-1 + \gamma^2)$ which is positive. From this point onwards the numerator is an increasing function of r_1 since the derivative of the numerator is

$$4\gamma + \frac{(8r_1 - 8\gamma)(1 + \gamma^2)}{2\sqrt{4r_1^2 - 8r_1\gamma + (1 + \gamma^2)^2}} \quad (\text{C.39})$$

which is positive for $r_1 \geq \gamma$. Thus we have that z_1^0 is a monotonic function of r_1 for $r_1 \geq \gamma$ that starts at $1 - 1/\gamma$. Note that in the limit as $\text{Ra} \rightarrow \infty$ we have that $z_1^0 \rightarrow 1$ (going back to the original expression). From what we observed earlier $z_1^0 \leq 1$ as well. Hence the z_1^0 conditions that we needed for the α term are satisfied. Now let us check the z_2^0 term. With the relation

$$z_2^0 = \gamma(z_1^0 - 1) + 1 \quad (\text{C.40})$$

¹If we choose the other root it seems to be the case that z_2^0 will always be negative.

we observe that since z_1 is strictly increasing so is z_2^0 . The quantity z_2^0 starts at zero and asymptotes to one. Hence we have the upper bound

$$\langle x_1 y_1 \rangle + \frac{a}{4} \langle x_2 y_2 \rangle \leq b_1 z_1^0 + \frac{a}{4} b_2 z_2^0 \quad (\text{C.41})$$

$$\begin{aligned} & \Leftrightarrow \\ \text{Nu} & \leq 1 + 2(1 + \gamma) \left(\frac{-1 + 2r_1\gamma - \gamma^2 + \sqrt{(\gamma^2 + 1)^2 + 4r_1(r_1 - 2\gamma)}}{2(r_1 + r_1\gamma)} \right) \\ & \quad + 2(1 - \gamma) \end{aligned} \quad (\text{C.42})$$

$$\begin{aligned} & \Leftrightarrow \\ \text{Nu} & \leq 1 + 2 \left(1 - \frac{1}{r_1} \right) + \frac{1}{r_1} \left(1 - \gamma^2 + \sqrt{(\gamma^2 + 1)^2 + 4r_1(r_1 - 2\gamma)} \right) \end{aligned} \quad (\text{C.43})$$

$$\text{for Ra} \geq \sqrt{\frac{(1+k^2)^3(4+k^2)^3}{k^4}}.$$

APPENDIX D

Background Bound Details

Here we will show

$$2\langle w\theta\tau' \rangle \geq -\frac{\delta}{2} \left\langle \frac{c}{4} |\nabla \vec{u}|^2 + \frac{1}{c} |\nabla \theta|^2 \right\rangle, \quad (\text{D.1})$$

where $|\nabla \vec{u}|^2 = \nabla \vec{u} : \nabla \vec{u} = \partial_j u_k \partial_j u_k$ and $2\langle w\theta\tau' \rangle$ is

$$2\langle w\theta\tau' \rangle = \limsup_{T \rightarrow \infty} \frac{2}{T\Gamma_1\Gamma_2} \int_0^T dt \int_0^{\Gamma_1} dx \int_0^{\Gamma_2} dy \left(\int_0^1 dz \tau' w \theta \right) \quad (\text{D.2})$$

$$= \limsup_{T \rightarrow \infty} -\frac{1}{\delta T\Gamma_1\Gamma_2} \int_0^T dt \int_0^{\Gamma_1} dx \left(\int_0^{\Gamma_2} dy \left(\int_0^\delta dz w \theta + \int_{1-\delta}^1 dz w \theta \right) \right). \quad (\text{D.3})$$

We will do this by making use of a few observations. The first observation is that for $0 \leq z \leq \frac{1}{2}$

$$|w(x, y, z, t)| = \left| \int_0^z d\zeta \frac{\partial w}{\partial \zeta}(x, y, \zeta, t) \right| \leq \int_0^z d\zeta \left| \frac{\partial w}{\partial \zeta}(x, y, \zeta, t) \right| \quad (\text{D.4})$$

$$\leq \sqrt{z} \sqrt{\int_0^z d\zeta \left| \frac{\partial w}{\partial \zeta}(x, y, \zeta, t) \right|^2} \leq \sqrt{z} \sqrt{\int_0^1 d\zeta \left| \frac{\partial w}{\partial \zeta}(x, y, \zeta, t) \right|^2}. \quad (\text{D.5})$$

We used the fundamental theorem of calculus, the homogeneous boundary condition, and Cauchy-Schwarz on 1 and $\partial_z w$. The θ term has a similar pointwise inequality

$$|\theta(x, y, z, t)| \leq \sqrt{z} \sqrt{\int_0^1 d\zeta \left| \frac{\partial \theta}{\partial \zeta}(x, y, \zeta, t) \right|^2} \quad (\text{D.6})$$

and for $\frac{1}{2} \leq z \leq 1$ we have similar bounds

$$|w(x, y, z, t)| \leq \sqrt{1-z} \sqrt{\int_0^1 d\zeta \left| \frac{\partial w}{\partial \zeta}(x, y, \zeta, t) \right|^2} \quad (\text{D.7})$$

$$|\theta(x, y, z, t)| \leq \sqrt{1-z} \sqrt{\int_0^1 d\zeta \left| \frac{\partial \theta}{\partial \zeta}(x, y, \zeta, t) \right|^2}. \quad (\text{D.8})$$

Let $0 \leq a = \sqrt{\int_0^1 d\zeta \left| \frac{\partial w}{\partial \zeta}(x, y, \zeta, t) \right|^2}$ and $0 \leq b = \sqrt{\int_0^1 d\zeta \left| \frac{\partial \theta}{\partial \zeta}(x, y, \zeta, t) \right|^2}$, thus

$$|\theta w| \leq \min\{z, 1-z\} ab \quad (\text{D.9})$$

$$\leq \frac{\min\{z, 1-z\}}{2} \left(ca^2 + \frac{1}{c} b^2 \right) \quad (\text{D.10})$$

$$= \frac{\min\{z, 1-z\}}{2} \left(c \int_0^1 d\zeta \left| \frac{\partial w}{\partial \zeta}(x, y, \zeta, t) \right|^2 + \frac{1}{c} \int_0^1 d\zeta \left| \frac{\partial \theta}{\partial \zeta}(x, y, \zeta, t) \right|^2 \right) \quad (\text{D.11})$$

with c to be chosen later. We need two more inequalities. One is

$$\int_0^1 d\zeta \left[\frac{\partial \theta}{\partial \zeta}(x, y, \zeta, t) \right]^2 \leq \int_0^1 d\zeta |\nabla \theta|^2. \quad (\text{D.12})$$

The other inequality that we need will be the only place incompressibility will be used. Incompressibility implies

$$2 \left\langle \left(\frac{\partial w}{\partial z} \right)^2 \right\rangle = -2 \left\langle \frac{\partial u}{\partial x} \frac{\partial w}{\partial z} + \frac{\partial v}{\partial y} \frac{\partial w}{\partial z} \right\rangle \quad (\text{D.13})$$

$$= -2 \left\langle \frac{\partial u}{\partial z} \frac{\partial w}{\partial x} + \frac{\partial v}{\partial z} \frac{\partial w}{\partial y} \right\rangle \quad (\text{D.14})$$

and

$$\left\langle \left(\frac{\partial w}{\partial z} \right)^2 + \left(\frac{\partial w}{\partial z} \right)^2 \right\rangle = \left\langle \left(\frac{\partial w}{\partial z} \right)^2 + \left(\frac{\partial u}{\partial x} + \frac{\partial v}{\partial y} \right)^2 \right\rangle \quad (\text{D.15})$$

$$= \left\langle \left(\frac{\partial w}{\partial z} \right)^2 + \left(\frac{\partial u}{\partial x} \right)^2 + \left(\frac{\partial v}{\partial y} \right)^2 + 2 \frac{\partial u}{\partial x} \frac{\partial v}{\partial y} \right\rangle \quad (\text{D.16})$$

$$= \left\langle \left(\frac{\partial w}{\partial z} \right)^2 + \left(\frac{\partial u}{\partial x} \right)^2 + \left(\frac{\partial v}{\partial y} \right)^2 + 2 \frac{\partial u}{\partial y} \frac{\partial v}{\partial x} \right\rangle. \quad (\text{D.17})$$

Adding (D.13) and (D.15), adding zero in the form $\langle |\nabla \vec{u}|^2 - |\nabla \vec{u}|^2 \rangle$ to the right hand side,

and grouping terms by color yields

$$4 \left\langle \left(\frac{\partial w}{\partial z} \right)^2 \right\rangle = \langle |\nabla \vec{u}|^2 \rangle - \left\langle \left(\frac{\partial w}{\partial x} \right)^2 + \left(\frac{\partial w}{\partial y} \right)^2 + \left(\frac{\partial u}{\partial y} \right)^2 + \left(\frac{\partial u}{\partial z} \right)^2 \right\rangle \quad (\text{D.18})$$

$$+ \left\langle \left(\frac{\partial v}{\partial x} \right)^2 + \left(\frac{\partial v}{\partial z} \right)^2 - 2 \frac{\partial u}{\partial z} \frac{\partial w}{\partial x} + 2 \frac{\partial v}{\partial z} \frac{\partial w}{\partial y} - 2 \frac{\partial u}{\partial y} \frac{\partial v}{\partial x} \right\rangle \quad (\text{D.19})$$

$$= \langle |\nabla \vec{u}|^2 \rangle - \left\langle \left(\frac{\partial u}{\partial y} - \frac{\partial v}{\partial x} \right)^2 + \left(\frac{\partial u}{\partial z} + \frac{\partial w}{\partial x} \right)^2 \right\rangle$$

$$+ \left\langle \left(\frac{\partial v}{\partial z} + \frac{\partial w}{\partial y} \right)^2 \right\rangle \quad (\text{D.20})$$

$$\leq \langle |\nabla \vec{u}|^2 \rangle \quad (\text{D.21})$$

which means

$$-\frac{1}{4} \langle |\nabla \vec{u}|^2 \rangle \leq - \left\langle \left(\frac{\partial w}{\partial z} \right)^2 \right\rangle. \quad (\text{D.22})$$

The spatial integral of the background decomposition yields

$$\int_0^1 dz \tau' w \theta = -\frac{1}{2\delta} \left(\int_0^\delta dz w \theta + \int_{1-\delta}^1 dz w \theta \right). \quad (\text{D.23})$$

We will concentrate on the \int_0^δ integral, noting that calculations for $\int_{1-\delta}^1$ will be identical. This will result in a factor of 2 to account for in the end. The calculation goes as follows

$$-\frac{1}{2\delta} \int_0^\delta dz w \theta \geq -\frac{c}{2\delta} \int_0^\delta dz \left[\frac{\min\{z, 1-z\}}{2} \left(\int_0^1 d\zeta \left| \frac{\partial w}{\partial \zeta}(x, y, \zeta, t) \right|^2 \right) \right] \quad (\text{D.24})$$

$$- \frac{1}{2c\delta} \int_0^\delta dz \left[\frac{\min\{z, 1-z\}}{2} \left(\int_0^1 d\zeta \left| \frac{\partial \theta}{\partial \zeta}(x, y, \zeta, t) \right|^2 \right) \right] \quad (\text{D.25})$$

$$= -\frac{\delta}{8} \int_0^1 d\zeta \left[\left(c \left| \frac{\partial w}{\partial \zeta}(x, y, \zeta, t) \right|^2 + \frac{1}{c} \left| \frac{\partial \theta}{\partial \zeta}(x, y, \zeta, t) \right|^2 \right) \right]. \quad (\text{D.26})$$

Using (D.12) and (D.22) yields,

$$-\frac{1}{2\delta\Gamma_1\Gamma_2} \int_0^{\Gamma_1} dx \int_0^{\Gamma_2} dy \int_0^\delta dz w \theta \geq -\frac{\delta}{4} \left\langle \frac{c}{4} |\nabla \vec{u}|^2 + \frac{1}{c} |\nabla \theta|^2 \right\rangle. \quad (\text{D.27})$$

In total we have the lower bound

$$2\langle w\theta\tau'\rangle \geq -\frac{\delta}{2} \left\langle \frac{c}{4} |\nabla \vec{u}|^2 + \frac{1}{c} |\nabla \theta|^2 \right\rangle. \quad (\text{D.28})$$

BIBLIOGRAPHY

- [1] Pétrélis, F. and Pétrélis, N., “Bounds on the dissipation in the Lorenz system,” *Physics Letters A*, Vol. 326, 2004, pp. 85–92.
- [2] Wen, B., Chini, G. P., Kerswell, R. R., and Doering, C. R., “Aspect-Ratio-Dependent Upper Bounds for Two-Dimensional Rayleigh–Bénard Convection between Stress-Free Isothermal Boundaries,” *Physical Review E*, Vol. 85, 2015.
- [3] Whitehead, J. P. and Doering, C. R., “Ultimate state of two-dimensional Rayleigh–Bénard convection between free-slip fixed-temperature boundaries,” *Physical Review Letters*, Vol. 106, 2011, pp. 244501.
- [4] Doering, C. R. and Constantin, P., “Variational bounds on energy dissipation in incompressible flows. III. Convection,” *Physical Review E*, Vol. 53, 1996, pp. 5957–5981.
- [5] Parrilo, P. A., “Semidefinite programming relaxations for semialgebraic problems,” *Math. Program.*, Vol. 96, No. 2, 2003, pp. 293–320.
- [6] Goulart, P. J. and Chernyshenko, S., “Global stability analysis of fluid flows using sum-of-squares,” *Physica D: Nonlinear Phenomena*, Vol. 241, No. 6, 2012, pp. 692 – 704.
- [7] Thiffeault, J. and Horton, W., “Energy-conserving truncations for convection with shear flow,” *Physics of Fluids*, 1996, pp. 1715–1719.
- [8] Lorenz, E. N., “Deterministic nonperiodic flow,” *Journal of the Atmospheric Sciences*, Vol. 20, 1963, pp. 130–141.
- [9] Gluhovsky, A., Tong, C., and Agee, E., “Selection of Modes in Convective Low-Order Models,” *Journal of the Atmospheric Sciences*, Vol. 59, 2002, pp. 1383–1393.
- [10] Tucker, W., “A Rigorous ODE Solver and Smale’s 14th Problem,” *Foundations of Computational Mathematics*, Vol. 2, 2002, pp. 53–117.
- [11] Luzzatto1, S., Melbourne, I., and Paccaut, F., “The Lorenz Attractor is Mixing,” *Communications in Mathematical Physics*, Vol. 260, 2005, pp. 393–401.
- [12] Treve, Y. M. and Manley, O. P., “Energy conserving Galerkin approximations for 2-D hydrodynamic and MHD Bénard convection,” *Physica D*, Vol. 4, 1982, pp. 319–342.

- [13] Dullin, H. R., Schmidt, S., Richter, P. H., and Grossmann, S. K., “Extended phase diagram of the Lorenz model,” *International Journal of Bifurcation and Chaos*, Vol. 17, 2007, pp. 3013–3033.
- [14] Illing, L., Fordyce, R. F., Saunders, A. M., and Ormond, R., “Experiments with a Malkus-Lorenz water wheel: Chaos and Synchronization,” *American Journal of Physics*, Vol. 80, 2012, pp. 192–202.
- [15] Souza, A. N. and Doering, C. R., “Maximal transport in the Lorenz equations,” *Physics Letters A*, Vol. 379, 2015, pp. 518–523.
- [16] Souza, A. N. and Doering, C. R., “Transport bounds for a truncated model of Rayleigh-Bénard convection,” *Physica D: Nonlinear Phenomena*, Vol. 308, 2015, pp. 26 – 33.
- [17] Lord Rayleigh, “On convection currents in a horizontal layer of fluid, when the higher temperature is on the under side,” *Philosophical Magazine*, Vol. 32, 1916, pp. 529–546.
- [18] Malkus, W. V. R., “Non-periodic convection at high and low Prandtl number,” *Mémoires de la Société Royale des Sciences de Liège Series 6*, Vol. 4, 1972, pp. 125–128.
- [19] Knobloch, E., “On the Statistical Dynamics of the Lorenz Model,” *Journal of Statistical Physics*, Vol. 20, 1979, pp. 695–709.
- [20] Foias, C., Jolly, M., Kukavica, I., and Titi, E., “The Lorenz equations as a metaphor for the Navier-Stokes equations,” *Discrete and Continuous Dynamical Systems*, Vol. 7, 2001, pp. 403–429.
- [21] Sparrow, C. T., “The Lorenz Equations: Bifurcations, Chaos, and Strange Attractors,” *Springer Series in Applied Mathematical Sciences*, Vol. 41, 1982, pp. 1–269.
- [22] Reitmann, V. and Leonov, G. A., “Attraktoreingranzung fuer nichtlineare Systeme,” *Springer Teubner-Texte zur Mathematik*, Vol. 97, 1987, pp. 1–196.
- [23] Doering, C. R. and Gibbon, J. D., “On the shape and dimension of the Lorenz attractor,” *Dynamics & Stability of Systems*, Vol. 10, 1995, pp. 255–268.
- [24] Swinnerton-Dyer, P., “Bounds for trajectories of the Lorenz equations: an illustration of how to choose Liapunov functions,” *Physics Letters A*, Vol. 281, 2001, pp. 161–167.
- [25] Suzuki, M., Sakamoto, N., and Yasukochi, T., “A butterfly-shaped localization set for the Lorenz attractor,” *Physics Letters A*, Vol. 372, 2008, pp. 2614–2617.
- [26] Leonov, G., Pogromsky, A. Y., and Starkov, K., “The dimension formula for the Lorenz attractor,” *Physics Letters A*, Vol. 375, 2011, pp. 1179–1182.

- [27] Goluskin, D., “Zonal flow driven by convection and convection driven by internal heating,” *Columbia University Doctoral Thesis*, 2012, pp. 46–66.
- [28] Folland, G. B., *Real Analysis: Modern Techniques and Their Applications*, Wiley, 2nd ed., 1999.
- [29] Evans, L. C., *Partial Differential Equations*, American Mathematical Society, 2002.
- [30] Boyer, F. and Fabrie, P., *Mathematical Tools for the Study of the Incompressible Navier–Stokes Equations and Related Models*, Springer, 1st ed., 2009.
- [31] Kerswell, R. R., “New Results in the variational approach to turbulent Boussinesq Convection,” *Physics of Fluids*, Vol. 13, 2001, pp. 192–209.
- [32] Hassanzadeh, P., Chini, G. P., and Doering, C. R., “Wall to wall optimal transport,” *Journal of Fluid Mechanics*, Vol. 751, 2014, pp. 627–662.
- [33] Hassanzadeh, P., Chini, G. P., and Doering, C. R., “Wall to wall optimal transport,” *Journal of Fluid Mechanics*, Vol. 751, 2014, pp. 627–662.
- [34] Boyd, J., *Chebyshev and Fourier Spectral Methods*, Dover, 2nd ed., 2001.
- [35] Trefethen, L. N., *Spectral Methods in MATLAB*, SIAM, 1st ed., 2001.
- [36] Qian, N., “On the momentum term in gradient descent learning algorithms,” *Neural Networks*, Vol. 12, No. 1, 1999, pp. 145 – 151.
- [37] Viswanath, D. and Tobiasco, I., “Navier-Stokes solver using Greens functions I: Channel flow and plane Couette flow,” *Journal of Computational Physics*, Vol. 251, 2013, pp. 414 – 431.
- [38] Viswanath, D., “Spectral integration of linear boundary value problems,” *Journal of Computational and Applied Mathematics*, Vol. 290, 2015, pp. 159 – 173.
- [39] Kleiser, L. and Schumann, U., “Treatment of incompressibility and boundary conditions in 3-D numerical spectral simulations of plane channel flows,” *3rd Conference on Numerical Methods in Fluid Mechanics*, edited by E. H. Hirschel, 1980, pp. 165–173.
- [40] Feynman, R. P. and Hibbs, A. R., *Quantum Mechanics and Path Integrals*, McGraw-Hill Companies, 1st ed., 1965.